Department of Neurology

Medical School Hannover

Center for Systems Neuroscience

University of Veterinary Medicine Hannover

Characterization of toxin induced de- and remyelination in the central nervous system and role of the chemokine receptor CXCR2

THESIS

Submitted in partial fulfilment of the requirements for the degree

DOCTOR OF PHILOSOPHY (PhD)

At the University of Veterinary Medicine Hannover

by

Maren Lindner

Berlin

Hannover 2007

Supervisor:	Prof. Dr. Martin Stangel
Advisory Committee:	Prof. Dr. Martin Stangel Prof. Dr. Wolfgang Baumgärtner Prof. Dr. Rita Gerardy-Schahn
External Evaluation:	Prof. Dr. Edgar Meinl Department for Neuroimmunology Max-Planck Institute of Neurobiology Martiensried
Date of oral exam:	November 2nd 2007

Publications contained in the thesis:

Lindner M, Heine S, Haastert K, Garde N, Fokuhl J, Linsmeier F, Grothe C, Baumgaertner W, Stangel M. Sequential myelin protein expression during remyelination reveals fast and efficient repair after central nervous system demyelination.
Neuropathol Appl Neurobiol *in press*

Lindner M, Trebst C, Heine S, Koutsoudaki PN, Stangel M. The chemokine receptor CXCR2 is expressed on oligodendrocyte precursor cells in vivo but is not required for successful remyelination after cuprizone-induced demyelination
In preparation

Lindner M, Fokuhl J, Linsmeier F, Trebst C, Stangel M. Extensive remyelination after chronic toxic demyelination in the central nervous system
In preparation

Lindner M*, Skripuletz T*, Kotsiari A, Garde N, Fokuhl J, Linsmeier F, Trebst C, Stangel M. Cortical demyelination can be induced in mice using the cuprizone model and is strain dependent
In preparation
*equal contributions as first authors

Hoffman K, **Lindner M**, Groeticke I, Stangel M, Loescher W. Epileptic seizures and hippocampal damage after cuprizone-induced demyelination in mice.
Exp Neurol *submitted*

Contents

1 Introduction **5**
References Introduction **10**
2 Aims **15**
3 Results **16**
Chapter I: Sequential protein expression reveals fast and efficient repair after central nervous system demyelination **16**
Abstract **17**
Introduction **17**
Materials and Methods **18**
Results **19**
Discussion **23**
Chapter II: The chemokine receptor CXCR2 is expressed on oligodendrocyte precursor cells *in vivo* but is not required for successful remyelination after cuprizone-induced demyelination **27**
Abstract **28**
Introduction **29**
Materials and Methods **31**
Results **34**
Discussion **38**
Chapter III: Extensive remyelination after chronic toxic demyelination in the central nervous system **52**
Abstract **53**
Introduction **54**
Materials and Methods **55**
Results **57**
Discussion **60**
Chapter IV: Cortical demyelination can be induced in mice using the cuprizone model and is strain dependent **71**
Abstract **72**
Introduction **73**
Materials and Methods **75**
Results **78**
Discussion **81**
Chapter V: Epileptic seizures and hippocampal damage after cuprizone-induced demyelination in mice **94**
Abstract **95**
Introduction **96**
Materials and Methods **98**
Results **103**
Discussion **108**
4 Discussion **132**
References Discussion **136**
5 Summary **138**
6 Zusammenfassung **141**
Curriculum Vitae **143**
List of publications **144**
Acknowledgements **146**

1 Introduction

Multiple sclerosis (MS) is an inflammatory disease of the central nervous system that affects more than two million people worldwide. Although descriptions date back as far as the Middle Ages, MS was first recognized as a distinct disease in the nineteenth century with the first published pathologic report in 1868 by Jean-Martin Charcot (Charcot, 1868). He examined the brain of a young woman and documented characteristic scars, which he described as “la sclérose en plaques”.

The average age of disease onset is between 20 to 40 years, whereas women are more often affected than men (2:1) with a higher prevalence (60 – 200/100,000) in Northern Europe and North America compared to 6-20/100,000 in low risk areas such as Japan (Pugliatti et al., 2006; Sospedra and Martin, 2005).

The majority (~85%) of MS patients initially have a relapsing-remitting disease (RRMS) course characterized by clearly defined alternating episodes of relapses and recovery (Weinshenker, 1996; Noseworthy et al., 2000). Relapses result from inflammation and demyelination, whereas recovery is accompanied by restoration of nerve conduction, resolution of inflammation and remyelination (Trapp et al., 1999; Waxman, 1998). Within a period of about 25 years, ~90% of patients with RRMS exhibit a secondary-progressive disease (SPMS) course characterized by steadily increasing permanent neurologic disability (Noseworthy et al., 2000; Weinshenker et al., 1989). About 10% of MS patients experience primary-progressive MS (PPMS) which is marked by a steady decline in neurologic function from disease onset without recovery. The fourth clinical disease course, called progressive-relapsing MS (PRMS), can be observed in ~5% of MS patients and is characterized by steady progressive neurologic decline punctuated by well-demarcated acute attacks with or without recovery (Dutta and Trapp, 2007).

Even though considerable efforts were undertaken in the MS research field during the last decades, the exact cause of multiple sclerosis is still unknown and the therapeutic treatments are limited. It is generally accepted that MS is an autoimmune disease with a so far unrecognised environmental risk factor (Weinshenker, 1996; Cepok et al., 2005; Lipton et al., 2007; Fleming and Fabry, 2007) and multiple genetic loci (Haines et al., 1996; Ebers et al., 1996; Lincoln et al., 2005; Reich et al., 2005; Sawcer et al., 2005; Sawcer et al., 2004) contributing to the susceptibility to the disease.

The pathologic hallmarks of MS lesions include breakdown of the blood-brain barrier (BBB), multifocal inflammation, demyelination, oligodendrocyte (the cells that produce myelin) loss, reactive gliosis, and axon degeneration(Noseworthy et al., 2000; Raine, 1994; Ferguson et al., 1997; Trapp et al., 1998). Although the immune-mediated destruction of CNS myelin and oligodendrocytes is considered the primary pathology in MS, the major cause of permanent neurologic disability is axonal loss (Bjartmar et al., 2003; Bruck and Stadelmann, 2003). Thus, the protection of axons by enhancing remyelination is a major focus in current MS research.

The pathological heterogeneity between MS patients was investigated by Lucchinetti and colleagues. They analysed biopsies and autopsies of MS patients and described four distinct patterns of demyelination, defined on the basis of myelin protein loss, the geography and extension of plaques, the pattern of oligodendrocyte destruction, and the immunopathological evidence of complement activation. Pattern I is predominated by T cells and macrophages, and candidate effector molecules include TNF-α, INF-γ, and radical species. In pattern II antibody and complement deposition predominates. Patterns III and IV are highly suggestive of a primary oligodendrocyte dystrophy, reminiscent of virus- or toxin-induced demyelination rather than autoimmunity (Lucchinetti et al., 2000). Interestingly, the pattern of demyelination was heterogeneous between patients, but homogeneous within multiple active lesions from the same patient.

Demyelination is not always permanent in multiple sclerosis. Reappearance of oligodendrocytes within active lesions associated with early stages of remyelination are frequently seen in patients with acute or early multiple sclerosis (Prineas et al., 1984a; Prineas et al., 1984b; Raine and Wu, 1993; Lucchinetti et al., 1999). Recent studies could demonstrate that remyelination is more extensive than previously thought in a subset of MS patients (Patrikios et al., 2006; Patani et al., 2007). However, most chronic lesions of multiple sclerosis are not remyelinated. Despite the presence of oligodendrocyte progenitor cells (OPC) in the MS plaque that are in principle capable to remyelinate axons repair processes fail (Scolding et al., 1998; Chang et al., 2000; Maeda et al., 2001). Why remyelination fails in MS is still an enigma. It is not clear whether a lack of signals or inhibitory signals may account for the remyelination failure (Stangel and Trebst, 2006).

Remyelination in the CNS is mediated by OPC that have to proliferate, migrate and differentiate into mature oligodendrocytes in order to myelinate several axons at the same time (Stangel and Trebst, 2006; Zhao et al., 2005). A large variety of factors, including growth factors and cytokines are known to modulate the complex process of remyelination (Heine et al., 2006; Arnett et al., 2001; Plant et al., 2005; Armstrong et al., 2002; Kumar et al., 2007). Previous studies described the expression of the chemokine receptor CXCR2 on OPC (Nguyen & Stangel 2001; Tsai et al. 2002). In addition, CXCR2 is expressed on astrocytes (Danik et al., 2003; Flynn et al., 2003) and on microglial cells (Flynn et al., 2003; Filipovic et al., 2003). Recently, CXCR2 expression was found on proliferating oligodendrocytes in association with CXCL1 positive astrocytes at the edge of MS lesions, postulating a role for CXCR2 and its ligand CXCL1 in the recruitment of OPC into the MS lesion (Omari et al., 2006; Omari et al., 2005). However, the exact role of the chemokine receptor CXCR2 and its ligand during remyelination is not known.

Besides characteristic white matter lesions in the CNS, involvement of the cortex was long not recognised. Recent neuropathological studies revealed numerous lesions within the cerebral cortex in MS patients when applying immunohistochemistry for myelin proteins to autopsy brain tissue (Bo et al., 2003b; Kidd et al., 1999; Peterson et al., 2001). Moreover cortical lesions have been suggested to contribute to disease progression in MS (Kutzelnigg et al., 2005). Interestingly, cortical lesions were found to be less inflammatory than white matter lesions (Bo et al., 2003a). A direct comparison of the extent of remyelination in white matter and cortical lesions of the same patients revealed that remyelination of cortical lesions was consistently more extensive (Albert et al., 2007). Therefore, the potential for remyelination is high in cortical MS lesions.

To study the pathophysiological mechanisms of remyelination the cuprizone model is a reliable and widely used model (Hiremath et al., 1998; Matsushima and Morell, 2001). Feeding of the copper chelator cuprizone (bis-cyclohexanone oxaldihydrazone) to young adult mice leads to a toxic induced, reproducible demyelination of the corpus callosum after 6 weeks, followed by a spontaneous and fast remyelination process after withdrawal from the cuprizone diet (Lindner et al., 2007). The cuprizone model as a model to study remyelination within the CNS is known since decades (Ludwin, 1978; Blakemore, 1981). Whereas earlier studies investigated mainly the superior cerebellar peduncle, recent studies focus on the corpus callosum (Dupree et al., 2005; Arnett et al., 2004; Emery et al., 2006). The extent of de- and remyelination is strongly dependent on the cuprizone dose, the age of mice and strain used (Matsushima and Morell, 2001; Ludwin, 1980; Armstrong et al., 2002; Blakemore, 1972). The exact mechanisms why cuprizone primarily affects oligodendroglia are not yet known. However, it is assumed that disturbance of energy metabolism in oligodendrocytes is the major cause of demyelination (Matsushima and Morell, 2001). Besides the cuprizone model, induction of a focal lesion by injecting lysolecithin or ethidium bromide into the

rodent CNS serves as another commonly used toxic demyelination model (Woodruff and Franklin, 1999; Chari et al., 2006).

Other MS models which reflect the inflammatory compound of the disease are the intensively studied model of experimental autoimmune encephalomyelitis (EAE) and virus induced demyelination (Theiler virus) model. Both models are characterized by scattered lesions; break down of the blood-brain barrier and severe inflammation with infiltrating T cells.

Using the cuprizone model has the advantage of the reproducibility regarding the amount and site of demyelination. Furthermore, the blood-brain barrier is sustained (Bakker and Ludwin, 1987) and the remyelination can be examined without infiltration of T cells implying a reduction in the complexity of the system.

References Introduction

1. Albert M, Antel J, Bruck W, Stadelmann C (2007) Extensive cortical remyelination in patients with chronic multiple sclerosis. Brain Pathol 17: 129-138.

2. Armstrong RC, Le TQ, Frost EE, Borke RC, Vana AC (2002) Absence of fibroblast growth factor 2 promotes oligodendroglial repopulation of demyelinated white matter. J Neurosci 22: 8574-8585.

3. Arnett HA, Fancy SP, Alberta JA, Zhao C, Plant SR, Kaing S, Raine CS, Rowitch DH, Franklin RJ, Stiles CD (2004) bHLH transcription factor Olig1 is required to repair demyelinated lesions in the CNS. Science 306: 2111-2115.

4. Arnett HA, Mason J, Marino M, Suzuki K, Matsushima GK, Ting JP (2001) TNF alpha promotes proliferation of oligodendrocyte progenitors and remyelination. Nat Neurosci 4: 1116-1122.

5. Bakker DA, Ludwin SK (1987) Blood-brain barrier permeability during Cuprizone-induced demyelination. Implications for the pathogenesis of immune-mediated demyelinating diseases. J Neurol Sci 78: 125-137.

6. Bjartmar C, Wujek JR, Trapp BD (2003) Axonal loss in the pathology of MS: consequences for understanding the progressive phase of the disease. J Neurol Sci 206: 165-171.

7. Blakemore WF (1972) Observations on oligodendrocyte degeneration, the resolution of status spongiosus and remyelination in cuprizone intoxication in mice. J Neurocytol 1: 413-426.

8. Blakemore WF (1981) Remyelination in the CNS. Prog Clin Biol Res 59A:105-9.: 105-109.

9. Bo L, Vedeler CA, Nyland H, Trapp BD, Mork SJ (2003a) Intracortical multiple sclerosis lesions are not associated with increased lymphocyte infiltration. Mult Scler 9: 323-331.

10. Bo L, Vedeler CA, Nyland HI, Trapp BD, Mork SJ (2003b) Subpial demyelination in the cerebral cortex of multiple sclerosis patients. J Neuropathol Exp Neurol 62: 723-732.

11. Bruck W, Stadelmann C (2003) Inflammation and degeneration in multiple sclerosis. Neurol Sci 24 Suppl 5:S265-7.: S265-S267.

12. Cepok S, Zhou D, Srivastava R, Nessler S, Stei S, Bussow K, Sommer N, Hemmer B (2005) Identification of Epstein-Barr virus proteins as putative targets of the immune response in multiple sclerosis. J Clin Invest 115: 1352-1360.

13. Chang A, Nishiyama A, Peterson J, Prineas J, Trapp BD (2000) NG2-positive oligodendrocyte progenitor cells in adult human brain and multiple sclerosis lesions. J Neurosci 20: 6404-6412.

14. Charcot M (1868) Histologie de la slerose en plaques. Gaz Hosp 554-558.

15. Chari DM, Zhao C, Kotter MR, Blakemore WF, Franklin RJ (2006) Corticosteroids delay remyelination of experimental demyelination in the rodent central nervous system. J Neurosci Res 83: 594-605.

16. Danik M, Puma C, Quirion R, Williams S (2003) Widely expressed transcripts for chemokine receptor CXCR1 in identified glutamatergic, gamma-aminobutyric acidergic, and cholinergic neurons and astrocytes of the rat brain: a single-cell reverse transcription-multiplex polymerase chain reaction study. J Neurosci Res 74: 286-295.

17. Dupree JL, Mason JL, Marcus JR, Stull M, Levinson R, Matsushima GK, Popko B (2005) Oligodendrocytes assist in the maintenance of sodium channel clusters independent of the myelin sheath. Neuron Glia Biol 1:1-14.: 1-14.

18. Dutta R, Trapp BD (2007) Pathogenesis of axonal and neuronal damage in multiple sclerosis. Neurology 68: S22-S31.

19. Ebers GC, Kukay K, Bulman DE, Sadovnick AD, Rice G, Anderson C, Armstrong H, Cousin K, Bell RB, Hader W, Paty DW, Hashimoto S, Oger J, Duquette P, Warren S, Gray T, O'connor P, Nath A, Auty A, Metz L, Francis G, Paulseth JE, Murray TJ, Pryse-Phillips W, Nelson R, Freedman M, Brunet D, Bouchard JP, Hinds D, Risch N (1996) A full genome search in multiple sclerosis. Nat Genet 13: 472-476.

20. Emery B, Cate HS, Marriott M, Merson T, Binder MD, Snell C, Soo PY, Murray S, Croker B, Zhang JG, Alexander WS, Cooper H, Butzkueven H, Kilpatrick TJ (2006) Suppressor of cytokine signaling 3 limits protection of leukemia inhibitory factor receptor signaling against central demyelination. Proc Natl Acad Sci U S A 103: 7859-7864.

21. Ferguson B, Matyszak MK, Esiri MM, Perry VH (1997) Axonal damage in acute multiple sclerosis lesions. Brain 120: 393-399.

22. Filipovic R, Jakovcevski I, Zecevic N (2003) GRO-alpha and CXCR2 in the human fetal brain and multiple sclerosis lesions. Dev Neurosci 25: 279-290.

23. Fleming J, Fabry Z (2007) The hygiene hypothesis and multiple sclerosis. Ann Neurol 61: 85-89.

24. Flynn G, Maru S, Loughlin J, Romero IA, Male D (2003) Regulation of chemokine receptor expression in human microglia and astrocytes. J Neuroimmunol 136: 84-93.

25. Haines JL, Ter Minassian M, Bazyk A, Gusella JF, Kim DJ, Terwedow H, Pericak-Vance MA, Rimmler JB, Haynes CS, Roses AD, Lee A, Shaner B, Menold M, Seboun E, Fitoussi RP, Gartioux C, Reyes C, Ribierre F, Gyapay G, Weissenbach J, Hauser SL, Goodkin DE, Lincoln R, Usuku K, Oksenberg JR, . (1996) A complete genomic screen for multiple sclerosis underscores a role for the major histocompatability complex. The Multiple Sclerosis Genetics Group. Nat Genet 13: 469-471.

26. Heine S, Ebnet J, Maysami S, Stangel M (2006) Effects of interferon-beta on oligodendroglial cells. J Neuroimmunol 177: 173-180.

27. Hiremath MM, Saito Y, Knapp GW, Ting JP, Suzuki K, Matsushima GK (1998) Microglial/macrophage accumulation during cuprizone-induced demyelination in C57BL/6 mice. J Neuroimmunol 92: 38-49.

28. Kidd D, Barkhof F, McConnell R, Algra PR, Allen IV, Revesz T (1999) Cortical lesions in multiple sclerosis. Brain 122: 17-26.

29. Kumar S, Biancotti JC, Yamaguchi M, de Vellis J (2007) Combination of growth factors enhances remyelination in a cuprizone-induced demyelination mouse model. Neurochem Res 32: 783-797.

30. Kutzelnigg A, Lucchinetti CF, Stadelmann C, Bruck W, Rauschka H, Bergmann M, Schmidbauer M, Parisi JE, Lassmann H (2005) Cortical demyelination and diffuse white matter injury in multiple sclerosis. Brain 128: 2705-2712.

31. Lincoln MR, Montpetit A, Cader MZ, Saarela J, Dyment DA, Tiislar M, Ferretti V, Tienari PJ, Sadovnick AD, Peltonen L, Ebers GC, Hudson TJ (2005) A predominant role for the HLA class II region in the association of the MHC region with multiple sclerosis. Nat Genet 37: 1108-1112.

32. Lindner M, Heine S, Haastert K, Garde N, Fokuhl J, Linsmeier F, Grothe C, Baumgaertner W, Stangel M (2007) Sequential myelin protein expression during remyelination reveals fast and efficient repair after central nervous system demyelination. Neuropathol Appl Neurobiol in press

33. Lipton HL, Liang Z, Hertzler S, Son KN (2007) A specific viral cause of multiple sclerosis: One virus, one disease. Ann Neurol 61:514-523

34. Lucchinetti C, Bruck W, Parisi J, Scheithauer B, Rodriguez M, Lassmann H (1999) A quantitative analysis of oligodendrocytes in multiple sclerosis lesions. A study of 113 cases. Brain 122: 2279-2295.

35. Lucchinetti C, Bruck W, Parisi J, Scheithauer B, Rodriguez M, Lassmann H (2000) Heterogeneity of multiple sclerosis lesions: implications for the pathogenesis of demyelination. Ann Neurol 47: 707-717.

36. Ludwin SK (1978) Central nervous system demyelination and remyelination in the mouse: an ultrastructural study of cuprizone toxicity. Lab Invest 39: 597-612.

37. Ludwin SK (1980) Chronic demyelination inhibits remyelination in the central nervous system. An analysis of contributing factors. Lab Invest 43: 382-387.

38. Maeda Y, Solanky M, Menonna J, Chapin J, Li W, Dowling P (2001) Platelet-derived growth factor-alpha receptor-positive oligodendroglia are frequent in multiple sclerosis lesions. Ann Neurol 49: 776-785.

39. Matsushima GK, Morell P (2001) The neurotoxicant, cuprizone, as a model to study demyelination and remyelination in the central nervous system. Brain Pathol 11: 107-116.

40. Noseworthy JH, Lucchinetti C, Rodriguez M, Weinshenker BG (2000) Multiple sclerosis. N Engl J Med 343: 938-952.

41. Omari KM, John G, Lango R, Raine CS (2006) Role for CXCR2 and CXCL1 on glia in multiple sclerosis. Glia 53: 24-31.

42. Omari KM, John GR, Sealfon SC, Raine CS (2005) CXC chemokine receptors on human oligodendrocytes: implications for multiple sclerosis. Brain 128: 1003-1015.

43. Patani R, Balaratnam M, Vora A, Reynolds R (2007) Remyelination can be extensive in multiple sclerosis despite a long disease course. Neuropathol Appl Neurobiol 33: 277-287.

44. Patrikios P, Stadelmann C, Kutzelnigg A, Rauschka H, Schmidbauer M, Laursen H, Sorensen PS, Bruck W, Lucchinetti C, Lassmann H (2006) Remyelination is extensive in a subset of multiple sclerosis patients. Brain 129: 3165-3172.

45. Peterson JW, Bo L, Mork S, Chang A, Trapp BD (2001) Transected neurites, apoptotic neurons, and reduced inflammation in cortical multiple sclerosis lesions. Ann Neurol 50: 389-400.

46. Plant SR, Arnett HA, Ting JP (2005) Astroglial-derived lymphotoxin-alpha exacerbates inflammation and demyelination, but not remyelination. Glia 49: 1-14.

47. Prineas JW, Kwon EE, Cho ES, Sharer LR (1984a) Continual breakdown and regeneration of myelin in progressive multiple sclerosis plaques. Ann N Y Acad Sci 436:11-32.: 11-32.

48. Prineas JW, Kwon EE, Sternberger NH, Lennon VA (1984b) The distribution of myelin-associated glycoprotein and myelin basic protein in actively demyelinating multiple sclerosis lesions. J Neuroimmunol 6: 251-264.

49. Pugliatti M, Rosati G, Carton H, Riise T, Drulovic J, Vecsei L, Milanov I (2006) The epidemiology of multiple sclerosis in Europe. Eur J Neurol 13: 700-722.

50. Raine CS (1994) Multiple sclerosis: immune system molecule expression in the central nervous system. J Neuropathol Exp Neurol 53: 328-337.

51. Raine CS, Wu E (1993) Multiple sclerosis: remyelination in acute lesions. J Neuropathol Exp Neurol 52: 199-204.

52. Reich D, Patterson N, De Jager PL, McDonald GJ, Waliszewska A, Tandon A, Lincoln RR, DeLoa C, Fruhan SA, Cabre P, Bera O, Semana G, Kelly MA, Francis DA, Ardlie K, Khan O, Cree BA, Hauser SL, Oksenberg JR, Hafler DA (2005) A whole-genome admixture scan finds a candidate locus for multiple sclerosis susceptibility. Nat Genet 37: 1113-1118.

53. Sawcer S, Ban M, Maranian M, Yeo TW, Compston A, Kirby A, Daly MJ, De Jager PL, Walsh E, Lander ES, Rioux JD, Hafler DA, Ivinson A, Rimmler J, Gregory SG, Schmidt S, Pericak-Vance MA, Akesson E, Hillert J, Datta P, Oturai A, Ryder LP, Harbo HF, Spurkland A, Myhr KM, Laaksonen M, Booth D, Heard R, Stewart G, Lincoln R, Barcellos LF, Hauser SL, Oksenberg JR, Kenealy SJ, Haines JL (2005) A high-density screen for linkage in multiple sclerosis. Am J Hum Genet 77: 454-467.

54. Sawcer SJ, Maranian M, Singlehurst S, Yeo T, Compston A, Daly MJ, De Jager PL, Gabriel S, Hafler DA, Ivinson AJ, Lander ES, Rioux JD, Walsh E, Gregory SG, Schmidt S, Pericak-Vance MA, Barcellos L, Hauser SL, Oksenberg JR, Kenealy SJ, Haines JL (2004) Enhancing linkage analysis of complex disorders: an evaluation of high-density genotyping. Hum Mol Genet 13: 1943-1949.

55. Scolding N, Franklin R, Stevens S, Heldin CH, Compston A, Newcombe J (1998) Oligodendrocyte progenitors are present in the normal adult human CNS and in the lesions of multiple sclerosis. Brain 121: 2221-2228.

56. Sospedra M, Martin R (2005) Immunology of multiple sclerosis. Annu Rev Immunol 23:683-747.: 683-747.

57. Stangel M, Trebst C (2006) Remyelination strategies: new advancements toward a regenerative treatment in multiple sclerosis. Curr Neurol Neurosci Rep 6: 229-235.

58. Trapp BD, Peterson J, Ransohoff RM, Rudick R, Mork S, Bo L (1998) Axonal transection in the lesions of multiple sclerosis. N Engl J Med 338: 278-285.

59. Trapp BD, Ransohoff R, Rudick R (1999) Axonal pathology in multiple sclerosis: relationship to neurologic disability. Curr Opin Neurol 12: 295-302.

60. Waxman SG (1998) Demyelinating diseases--new pathological insights, new therapeutic targets. N Engl J Med 338: 323-325.

61. Weinshenker BG (1996) Epidemiology of multiple sclerosis. Neurol Clin 14: 291-308.

62. Weinshenker BG, Bass B, Rice GP, Noseworthy J, Carriere W, Baskerville J, Ebers GC (1989) The natural history of multiple sclerosis: a geographically based study. I. Clinical course and disability. Brain 112: 133-146.

63. Woodruff RH, Franklin RJ (1999) The expression of myelin protein mRNAs during remyelination of lysolecithin-induced demyelination. Neuropathol Appl Neurobiol 25: 226-235.

64. Zhao C, Fancy SP, Kotter MR, Li WW, Franklin RJ (2005) Mechanisms of CNS remyelination--the key to therapeutic advances. J Neurol Sci 233: 87-91.

2 Aims

The main goal of this study was to investigate the process of remyelination by using the cuprizone model, a toxic demyelination model. Exploring the factors that may influence remyelination requires a method to quantify de- and remyelination. Hence, the first step implied the establishment of a fast, but also reliable quantification method.

The remyelination process strongly depends on the recruitment of oligodendrocyte precursor cells (OPC), which proliferate, migrate and finally differentiate into myelinating oligodendrocytes. The chemokine receptor CXCR2 is supposed to influence the behaviour of OPC. Therefore, we first elucidated the role of CXCR2 during de- and remyelination. Secondly, CXCR2 deficient mice were studied regarding physiological myelination as well as de- and remyelination in the cuprizone model.

The impact of chronic demyelination on remyelination was studied to evaluate the influence of OPC depletion. An insufficient repopulation of OPC may impair remyelination leading eventually to degeneration of axons and possibly also neurons. Therefore, we investigated axonal and neuronal damage during chronic demyelination and compared these results with acute demyelination.

Chapter I

Sequential myelin protein expression during remyelination reveals fast and efficient repair after central nervous system demyelination

Maren Lindner[1,4], Sandra Heine[1], Kirsten Haastert[2], Niklas Garde[1], Jantje Fokuhl[1], Franziska Linsmeier[1], Claudia Grothe[2,4], Wolfgang Baumgärtner[3,4], Martin Stangel[1,4*]

[1]Department of Neurology, Medical School Hannover, [2]Department of Neuroanatomy, Medical School Hannover, [3]Department of Pathology, University of Veterinary Medicine, Hannover, [4]Center for Systems Neuroscience, Hannover, Germany

Neuropathology and Applied Neurobiology *in press*

Neuropathology and Applied Neurobiology (2007), 33, ••–••

doi: 10.1111/j.1365-2990.2007.00879.x

Sequential myelin protein expression during remyelination reveals fast and efficient repair after central nervous system demyelination

M. Lindner*†, S. Heine*, K. Haastert‡, N. Garde*, J. Fokuhl*, F. Linsmeier*, C. Grothe†‡, W. Baumgärtner§† and M. Stangel*†

*Departments of *Neurology and ‡Neuroanatomy, Medical School Hannover, §Department of Pathology, University of Veterinary Medicine, Hannover, and †Center for Systems Neuroscience, Hannover, Germany*

M. Lindner, S. Heine, K. Haastert, N. Garde, J. Fokuhl, F. Linsmeier, C. Grothe, W. Baumgärtner and M. Stangel (2007) *Neuropathology and Applied Neurobiology* 33, 000–000

Sequential myelin protein expression during remyelination reveals fast and efficient repair after central nervous system demyelination

To understand the mechanisms of remyelination and the reasons for regeneration, failure is one of the major challenges in multiple sclerosis research. This requires a good knowledge and reliable analysis of experimental models. This work was undertaken to characterize the pattern of myelin protein expression during experimental remyelination. Acute demyelination of the corpus callosum was induced by feeding of 0.3% cuprizone for 6 weeks, followed by a 10-week remyelination period. We used a combination of Luxol fast blue (LFB) myelin staining, electron microscopy (EM) and immunohistochemistry for the myelin proteins 2′,3′-cyclic nucleotide 3′ phosphodiesterase (CNPase), myelin basic protein (MBP), proteolipid protein (PLP) and myelin oligodendrocyte glycoprotein (MOG). Early remyelination was detected by the re-expression of CNPase, MBP and PLP as early as 4 days. MOG, as a marker for late differentiation of oligodendrocytes, was not detectable until 2 weeks of remyelination. EM data correlated well with the LFB myelin staining and myelin protein expression, with 50% of the axons being rapidly remyelinated within 2 weeks. While particularly MBP but also PLP and CNPase are re-expressed very early before significant remyelination is observed by EM, the late marker MOG shows a lag behind the remyelination detected by EM. The presented data indicate that immunohistochemistry for various myelin proteins expressed early and late during myelin formation is a suitable and reliable method to follow remyelination in the cuprizone model. Furthermore, investigation of early remyelination confirms that the intrinsic repair programme is very fast and switched on within days.

Keywords: myelin proteins, myelin, remyelination

Introduction

The question why remyelination fails in multiple sclerosis has received wide attention during the past few years [1]. The reasons are manifold and mostly not clear due to the fact that the exact molecular mechanisms of how remyelination is accomplished are not yet understood. The maturation process of oligodendrocyte precursor cells with the capacity to remyelinate nude axons follows a complex and timed pattern of several factors [2,3].

One explanation of remyelination failure is the inability of immature precursor cells of the oligodendrocyte lineage to differentiate into myelin-forming oligodendrocytes [4–6]. Whether inhibitory signals or just a lack of, for example axonal signals might be the reason is still not clear and is the subject of intense research with the

Correspondence: Maren Stangel, Department of Neurology, Medical School Hannover, Carl-Neuberg-Str. 1, 30625 Hannover, Germany. Tel: +49 511532 6677; Fax: +49 511532 3115; E-mail: stangel.martin@mh-hannover.de

© 2007 Blackwell Publishing Ltd

UNCORRECTED PROOF

ultimate goal of developing new treatment strategies for multiple sclerosis patients [7]. Thus, studying the remyelination process in detail to identify components that contribute to the repair process is of special interest.

The cuprizone model is a well-characterized and reliable animal model to study de- and remyelination processes in the central nervous system (CNS) [8,9]. In this model, young adult mice are fed the copper chelator cuprizone (bis-cyclohexanone oxaldihydrazone), resulting in a reproducible demyelination of the corpus callosum within weeks [10]. After withdrawal of the toxin, spontaneous remyelination can be observed [11], which makes this model ideal to study the remyelination process. The extent of de- and remyelination is largely dependent on the cuprizone dose, the age of mice and strain used [8,11–15].

Studying remyelination in detail requires a simple, but at the same time reliable, quantification method. The most-accepted method and regarded as gold standard, but also the most tedious and time consuming, uses electron microscopy (EM) to differentiate between myelinated, unmyelinated, and remyelinated axons. Myelin sheaths of remyelinated axons are thinner and can be identified by a higher G-ratio [16–18]. On the other hand, Luxol fast blue (LFB) represents a simple and rapid method to quantify the degree of myelination [19]. However, it is believed that this technique is slightly less accurate compared with EM [17]. Recent studies used the gene expression of myelin basic protein (MBP) [20] or myelin structural components [21] to quantify the de- and remyelination process. Finally, immunohistochemical studies have also been used to visualize de- and remyelination [22,23].

In this study we have characterized the sequence of myelin protein re-expression during remyelination in the cuprizone model. Beside new insights into the early and late phase of remyelination, the comparison of different approaches to quantify the extent of myelin formation and the correlation between LFB staining and EM revealed that immunohistochemistry presents a reliable and rapid quantification method.

Materials and methods

Cuprizone treatment and tissue processing

C57BL/6 mice were obtained from Charles River (Sulzfeld, Germany). All experiments were performed according to the national animal laws and approved by the local government authority.

Eight-week-old male mice were fed *ad libitum* 0.3% (w/w) cuprizone (bis-cyclohexanone oxaldihydrazone, Sigma-Aldrich Inc., St Louis, MO, USA) mixed into a ground standard rodent chow. In some preliminary experiments, 0.2% cuprizone was also fed as indicated. Cuprizone diet was maintained for 6 weeks; thereafter mice were put on a normal chow for another 10 weeks. At different time points (0, 2, 4, 6, 6.5, 7, 8, 9, 10, 11, 12 and 16 weeks), animals were perfused with 4% paraformaldehyde (PFA) in phosphate buffer via the left cardiac ventricle. Brains were removed and post-fixed in 4% PFA and paraffin or epon embedded. Seven-micrometer serial paraffin sections were cut and dried at 37°C overnight.

For epon, embedding brains were cut in 1-mm sections (bregma −0.94 according to mouse atlas by Paxinos and Franklin [24]) including the corpus callosum. Trimmed sections were post-fixed in 2.5% glutaraldehyde, further processed in 1% osmium tetroxide, dehydrated and embedded in epon. Semi-thin sections were cut and stained with toluidine blue. For each block, semi-thin sections were analysed to select the region of interest. After that, blocks were trimmed, and ultra-thin sections were cut and analysed with a Zeiss EM10C (Xx, Xx). Animals for EM were treated simultaneously with the animals for histochemical analysis, and brains were removed at the same time.

Histology and immunohistochemistry

Serial paraffin sections (bregma −0.94 according to mouse atlas by Paxinos and Franklin [24]) were stained for myelin with LFB. Selected slides were counterstained with periodic acid-Schiff base.

For immunohistochemistry, paraffin-embedded sections were de-waxed, rehydrated and microwaved for 5 min in 10 mM citrate buffer (pH 6.0). Sections were quenched with H_2O_2, blocked for 1 h in PBS containing 3% normal goat serum, 0.1% Triton X-100, and then incubated overnight with primary antibody against various myelin proteins: proteolipid protein (PLP, 1:500 Serotec, Düsseldorf, Germany), MBP (1:1000 Sternberger Monoclonals Inc., Berkeley, CA, USA), cyclic nucleotide 3′ phosphodiesterase (CNPase, 1:100 Chemicon, Hampshire, UK) and myelin oligodendrocyte glycoprotein (MOG, 1:2 hybridoma supernatant, generous gift by C. Linington).

After washing, sections were further incubated with biotinylated secondary antibody (Vector Laboratories, Burlingame, UK) for 1 h, followed by peroxidase-coupled

© 2007 Blackwell Publishing Ltd,

UNCORRECTED PROOF

avidin-biotin complex (ABC Kit, Vector Laboratories). Reactivity was visualized with diamino-3,3′benzidine (DAB, Dako Cytomation, Hamburg, Germany), and sections were dehydrated and mounted with Eukitt.

Morphometric analysis

Luxol fast blue- or myelin protein-stained sections from six animals for each time point were scored in a blinded manner by three observers (M.L., J.F., F.L.) and graded on a scale from 0 (complete myelination) to 3 (complete demyelination).

Myelin protein-stained sections were also measured morphometrically using AnalySIS software (Soft Imaging System, Münster, Germany). Each section was photographed (magnification: 20×) using a Zeiss axiophot microscope (Carl Zeiss), and five regions of interest in the middle of the corpus callosum were chosen for morphometrical analysis. For each section, positive pixels were defined and sections for each myelin protein were analysed in the same session.

For EM, at least 300 fibres per animal ($n = 3$) at selected time points (0, 6, 6.5, 8 and 16 weeks) were analysed. G-ratio (axon diameter divided by fibre diameter) and percentage of myelinated axons were measured.

Electron microscopy (EM) results were compared with controls using the unpaired Student's *t*-test. A *P*-value of <0.05 was considered statistically significant. Correlation of EM data and immunohistochemistry was calculated by Pearson product moment correlation.

Statistical analysis

The degree of myelination between different time points was compared using Mann–Whitney rank test for scoring results. Morphometrical measurements using AnalySIS software and percentage of myelinated fibres in EM were compared with the unpaired *t*-test. A *P*-value of <0.05 was considered statistically significant.

Results

Comparison of cuprizone concentrations for complete demyelination of the corpus callosum

The cuprizone model has been used in the past in different mouse strains at various concentrations. In recent years, mainly C57BL/6 have been utilized and characterized [8,9]. Most studies used a concentration of 0.2–0.3% cuprizone for 4–6 weeks to induce demyelination [12,25,26]. There is a controversy over whether the maximum demyelination is accomplished by 5 weeks of cuprizone treatment, with some remyelination occurring until week 6. Although this is true for the treatment with 0.2% cuprizone [8,23], most investigators allow the demyelination and cuprizone feeding for 6 weeks [27–29]. To ascertain that there is complete demyelination without a beginning of remyelination, we have compared 0.2% and 0.3% of cuprizone treatments for 6 weeks. Using 0.2% cuprizone there was some re-expression of myelin protein at week 6 compared with week 4 while the animals were still fed cuprizone (Figure 1). This was most obvious for MBP, as described previously [23]. In contrast, demyelination was complete at week 6 using 0.3% cuprizone (Figure 1). We have therefore used this concentration for all further experiments.

Luxol fast blue staining

Luxol fast blue staining revealed a complete demyelination of the corpus callosum after 6 weeks of cuprizone treatment (Figures 1 and 2). This was followed by a fast remyelination process that was already observed 4 days after cuprizone withdrawal, the earliest time point studied (Figures 2 and 3). Remyelination then continued steadily, with approximately two-thirds of the myelin being restored within 2 weeks (Figure 3, week 8), and nearly complete remyelination at the end of the observation period (Figures 2 and 3). However, myelin in remyelinated sections appeared less structured and organized compared with control animals.

Myelin protein expression during remyelination

A complete demyelination after 6 weeks of cuprizone treatment as seen in LFB-stained sections could also be observed in immunohistochemically stained sections for the myelin proteins PLP, MBP, CNPase and MOG (Figure 2). However, the re-expression of these myelin proteins showed a different temporal pattern. Rapid reoccurrence of PLP, MBP and CNPase was seen within 4 days during the remyelination phase and was nearly complete after 2 weeks (Figure 4A). In contrast, re-expression of MOG was considerably delayed and was first detected after 2 weeks of remyelination. Although the amount of MOG continuously increased thereafter, it never reached

© 2007 Blackwell Publishing Ltd,

UNCORRECTED PROOF

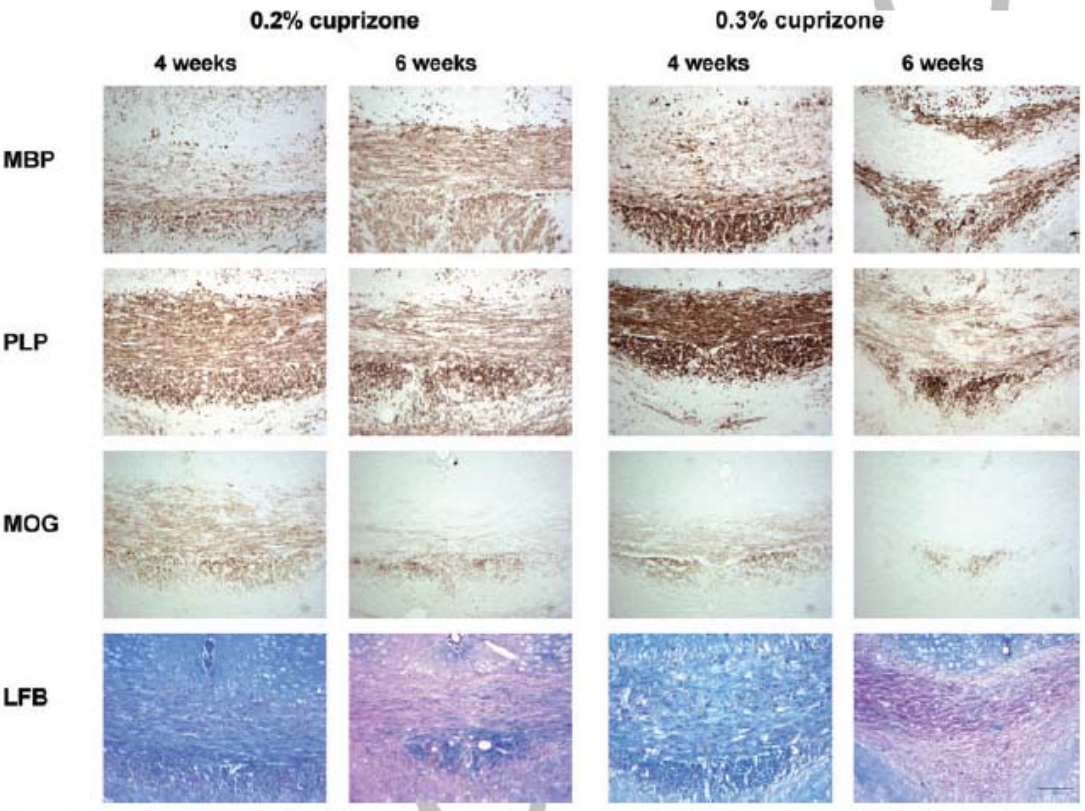

Figure 1. Comparison of demyelination of the corpus callosum induced by 0.2% and 0.3% cuprizone in C57BL/6 mice. After 4 weeks of treatment, demyelination is incomplete as visualized by LFB, MBP, PLP and MOG staining for both concentrations. After 6 weeks, the amount of MBP increases compared with 4 weeks in the 0.2% group while demyelination progresses in the 0.3% group. This is less evident for the other myelin proteins. Note that myelin staining is completely absent for all proteins stained in the middle of the corpus callosum after 6 weeks of a 0.3% cuprizone diet. Bar: 100 µm. LFB, Luxol fast blue; MBP, myelin basic protein; MOG, myelin oligodendrocyte glycoprotein; PLP, proteolipid protein.

control levels during the observation period of 10 weeks after withdrawal of cuprizone.

Besides the visual analysis by a blinded scorer, the same sections were also analysed morphometrically with the AnalySIS software (Figure 4B). Similar to the scoring system, complete demyelination was seen after 6 weeks of cuprizone feeding. PLP, MBP and CNPase were detected 4 days after withdrawal of cuprizone (degree of myelination increased by 40% compared with maximum demyelination at week 6), reaching control levels at week 8 (6 + 2 weeks) for MBP and CNPase. MOG re-expression was much slower, showing a myelin increase of 15% after 2 weeks on a normal diet and remained low until the end of the experiment at week 16 (6 + 10 weeks).

Overall, both methods show the same pattern of rapid re-expression of myelin proteins MBP, PLP, and CNPase and a delayed reoccurrence of MOG. Comparison of both methods showed a very good correlation (correlation coefficient of $R > 0.9$) for all proteins. However, for the minor myelin protein MOG, the AnalySIS software seemed to underestimate the degree of myelination (Figure 4A,B).

Before usage of the software-based system for analysis of stained sections, we validated the method by measuring a taken picture from a PLP-stained section at five different days by the same person (data nor shown). Due to the fact that for every slide a new cut-off has to be defined, we tested whether this would influence the measured data. For three measured control sections, standard deviations

© 2007 Blackwell Publishing Ltd,

UNCORRECTED PROOF

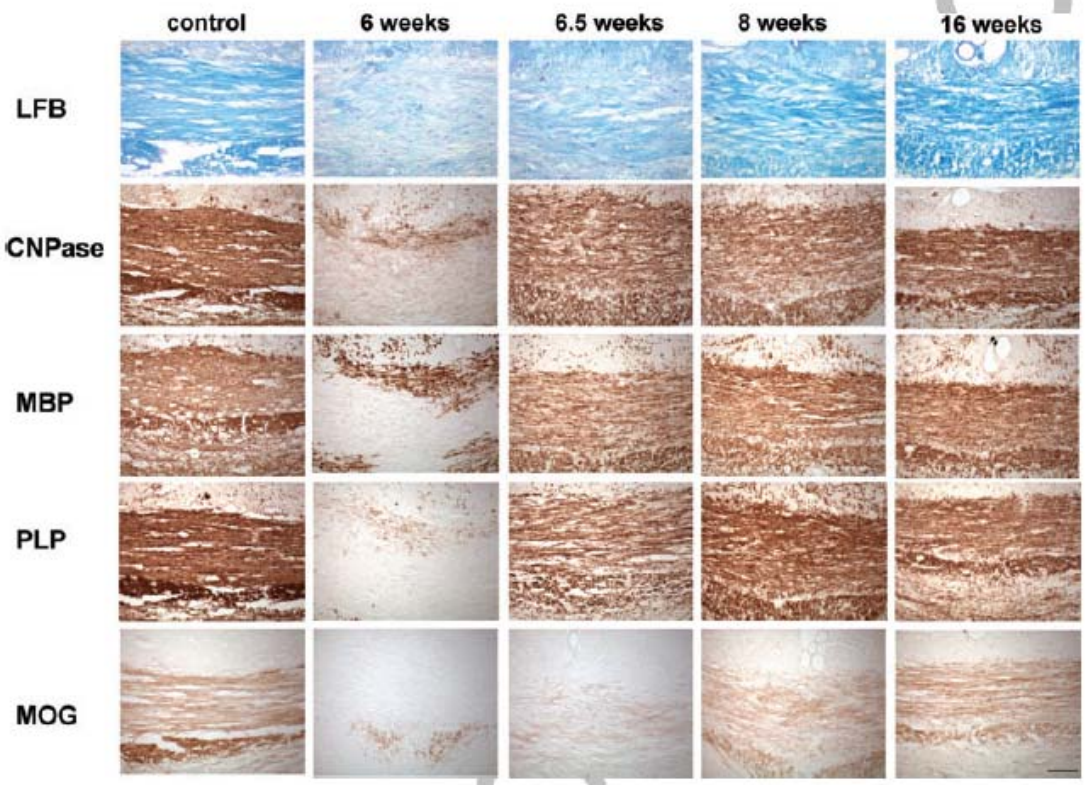

COLOUR

Figure 2. LFB-PAS and myelin protein-stained sections of the corpus callosum. Sections were photographed (20×) using a Zeiss axiophot microscope (Carl Zeiss) or a Leica DMLB microscope showing the middle of the corpus callosum. Demyelination can be seen in all stainings after 6 weeks of cuprizone treatment. This was followed by a recovery phase on normal diet for 10 weeks (weeks 6.5–16). Note that PLP, MBP and CNPase are re-expressed after 4 days of remyelination, while MOG expression is considerably delayed. Bar represents 50 µm. LFB, Luxol fast blue; MBP, myelin basic protein; MOG, myelin oligodendrocyte glycoprotein; PLP, proteolipid protein.

were between 2.1% and 3.3%, whereas for a demyelinated PLP-stained section (week 6, $n = 3$), standard deviations were between 1.2% and 11.8%. Thus, for a demyelinated section, where less myelin is detectable, the variance of measured myelin is higher. This could explain the difference between the visual scoring and computer-based analysis for MOG (Figure 4A,B). Apparently a weak staining signal is more difficult to analyse for a computerized system than for the human eye.

Electron microscopy

Electron micrographs (Figure 5) confirmed the marked demyelination at weeks 4 and 6. Furthermore, macrophages and myelin debris were most prominent at weeks 6 and 6.5, and were cleared completely at week 8 (data not shown). Swollen dystrophic axons as described by Stidworthy *et al.* [16] could be seen at weeks 4, 6 and 6.5, and very rarely at week 8 (data not shown), whereas at week 16 the axons and myelin sheaths appeared as in control mice.

To quantify remyelination, G-ratios and the percentage of myelinated axons were measured. The results are summarized in Table 1. The degree of demyelination reached its maximum at week 6 when the G-ratio was highest, corresponding to the thinnest myelin sheath. Within the first 4 days of remyelination, there is no major change regarding the G-ratio, but within the next week and a half, the G-ratio decreased about 0.1, with nearly no further decrease during the next 8 weeks. The number of myelinated axons increased in a similar pattern (Table 1). There was a slight statistically significant ($P = 0.0221$) increase at week 6 in comparison with week 4, despite a

© 2007 Blackwell Publishing Ltd.

UNCORRECTED PROOF

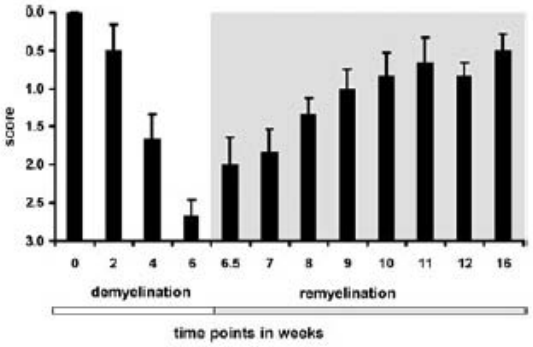

Figure 3. Course of de- and remyelination as judged by scoring of LFB-PAS stained sections. $n = 6$, error bars represent SEM. Score of 0: complete myelination, score of 3: complete demyelination. Sections were scored blinded to the time point by three independent raters. During remyelination the scores were significantly lower from week 7 onwards as compared with week 6 (week 7: $P = 0.026$; week 8: $P = 0.002$; from week 9: $P < 0.001$).

higher G-ratio, probably due to coexistence of de- and remyelination. The increase was highest between week 6.5 and week 8, and this was also statistically significant ($P = 0.032$). Two weeks after withdrawal of cuprizone, approximately 50% of axons were wrapped by new myelin sheaths ($P < 0.001$ compared with maximal demyelination at week 6), whereas the increase of myelinated axons in the following 8 weeks (week 16) was only approximately 10% (Table 1). This suggests that the first 2 weeks after cuprizone withdrawal are the most important for remyelination.

Comparison of evaluation methods

In order to optimize the quantification of the remyelination process, we correlated the per cent of myelinated axons measured by EM and the scores for LFB and myelin proteins (Table 2). Complete demyelination at week 6 was reliably detected by all methods. Analysis for the whole process of de- and remyelination showed the best correlation of EM with LFB scores. LFB staining showed also a good correlation with EM during the remyelination phase, where staining for the early myelin proteins MBP, CNPase and PLP was less well correlated (Table 2). This seems to be mainly due to the prominent expression of these proteins after 4 days of remyelination (week 6.5, Figure 6), when there is only little remyelination as measured by EM. Conversely, 2 weeks after withdrawal of cuprizone, when considerable remyelination was seen in EM sections, there

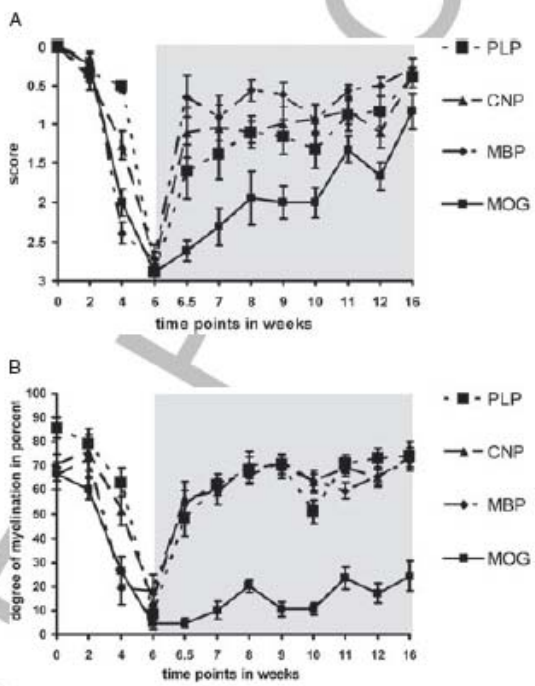

Figure 4. (A) Scoring of myelin protein stained sections. $n = 6$, error bars represent SEM. Score of 0: complete myelination, score of 3: complete demyelination. Sections were score in a blinded manner by three independent observers. The scores of all myelin proteins were significantly lower at week 6.5 as compared with week 6 (PLP: $P = 0.015$; MBP: $P = 0.002$; CNP and MOG: $P < 0.001$), demonstrating the early re-expression of myelin proteins after withdrawal of cuprizone. (B) Degree of myelination of myelin protein stained section ($n = 6$) measured morphometrically with AnalySIS software. Error bars represent SEM. There was a statistically significant difference between week 6.5 and week 6 for PLP ($P < 0.001$), MBP ($P = 0.003$) and CNP ($P < 0.001$). For MOG the difference was significant at week 8 ($P = 0.002$) and from week 11 ($P = 0.007$) onward as compared with maximal demyelination at week 6. LFB, Luxol fast blue; MBP, myelin basic protein; MOG, myelin oligodendrocyte glycoprotein; PLP, proteolipid protein.

was only little MOG protein detectable. Thus, MBP, CNPase, and to a lesser degree PLP, seem to be good markers for early myelin formation, even before the myelin sheath has formed several wraps around the axon to be detectable by EM. MOG, which is known to be expressed late during oligodendrocyte differentiation, was detected even after the newly formed myelin was seen on EM. MOG thus represents a marker for the late phase of remyelination that correlated best with EM data during this phase (Table 2).

© 2007 Blackwell Publishing Ltd,

UNCORRECTED PROOF

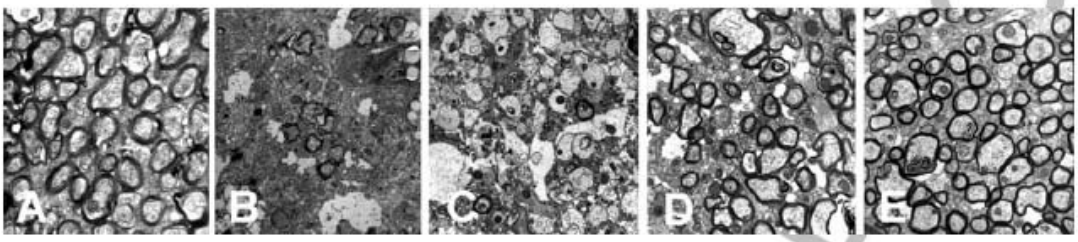

Figure 5. Electron micrographs of cuprizone-treated animals showing axons of the corpus callosum in a control animal (A), after 6 weeks of cuprizone treatment (B), and during recovery for 4 days (C), 2 weeks (D) and 10 weeks (E).

	Demyelination			*Remyelination*		
	Control	*4 weeks*	*6 weeks*	*6.5 weeks*	*8 weeks*	*16 weeks*
G-ratio	0.802 ± 0.014	0.926 ± 0.063*	0.964 ± 0.004***	0.944 ± 0.065*	0.846 ± 0.006**	0.833 ± 0.014
Per cent of myelinated axons	93.27 ± 1.19	13.79 ± 2.88***	18.44 ± 1.43***	23.14 ± 13.24**	67.67 ± 3.99**	76.04 ± 4.35*
		$P = 0.0221$	n.s.	$P = 0.032$	n.s	
			$P < 0.001$			
			$P < 0.001$			

In total, 300 fibres per animal ($n = 3$) were analysed, data are represented as means with standard deviation, and toxic demyelination was induced by feeding cuprizone for 6 week, followed by a recovery phase on normal diet for another 10 weeks (week 16).
*$P < 0.05$, **$P < 0.01$, ***$P < 0.001$ vs. control. Statistical analysis of percentage of myelinated axons between time points is given at the bottom.
EM, electron microscopy; n.s., not significant.

Table 2. Correlation of EM data (per cent myelinated axons) with LFB, PLP, CNPase, MBP and MOG staining (coefficient *R*-values, Pearson test) for the whole de- and remyelination process and for remyelination only

	Correlation of EM data De- and remyelination (weeks 0–16)		*Remyelination (weeks 6–16)*	
	R-*value*	P-*value*	R-*value*	P-*value*
LFB	0.9	0.015	0.936	0.064
PLP	0.635	0.176	0.879	0.121
CNP	0.766	0.076	0.752	0.248
MBP	0.828	0.042	0.702	0.298
MOG	0.874	0.023	0.917	0.083

EM, electron microscopy; LFB, Luxol fast blue; MBP, myelin basic protein; MOG, myelin oligodendrocyte glycoprotein; PLP, proteolipid protein.

Discussion

Here we demonstrate that remyelination is a fast process occurring within days after withdrawal of the demyelinating agent. Although other reports have suggest rapid CNS remyelination within weeks [30–32], early time points shorter than 1 week, as in our study, have not been investigated. In particular, the myelin proteins MBP, CNPase and PLP were already detected after 4 days of remyelination, and the majority of remyelination was achieved within 2 weeks. In contrast, the re-expression of MOG was considerably delayed and could not be detected within

© 2007 Blackwell Publishing Ltd,

UNCORRECTED PROOF

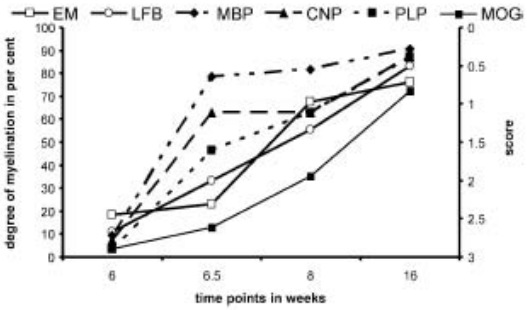

Figure 6. Comparison of EM results with LFB, PLP, MBP, CNPase and MOG scoring during remyelination. EM data represent per cent myelinated axons. EM, electron microscopy; LFB, Luxol fast blue; MBP, myelin basic protein; MOG, myelin oligodendrocyte glycoprotein; PLP, proteolipid protein.

these first 2 weeks. MOG thus seems to be an excellent marker for late remyelination. This is comparable to developmental studies [2] and other experimental models [32]. Birgbauer and co-worker [33] demonstrated that, after toxic demyelination in cerebellar slice cultures, CNPase and MBP appear faster than MOG, which did not return to control levels even after 11 days in culture. The reoccurrence of MOG during remyelination lags behind the presence of remyelinated axons detectable on EM. This suggests that although axons are already being surrounded by thin myelin sheaths, the myelin may not have its full functional properties. The precise function of MOG is still not known. It is not required for myelinogenesis during development [34], and activation of MOG transcription depends, besides an intrinsic oligodendroglial maturation programme, also on a neuronal signal [35]. Therefore, MOG seems to be an important marker during regeneration and might represent better the functionality of the newly built axon-glial myelin unit adding valuable information to EM data.

Histological LFB staining is commonly used for myelin detection both in experimental demyelination like the cuprizone model [9] and in multiple sclerosis lesions [36]. Due to its simple handling, this method is well suited to screen large numbers of samples, but there are limitations due to false-positive signals from lipid debris of degraded myelin, and thus leading to an overestimation of organized myelin [8]. However, in contrast to the study of Mason *et al.* [17], we find a very good correlation between LFB results and EM data. This may be explained by the slightly higher concentration of 0.3% cuprizone used in our study as compared with 0.2% [17]. We have used this concentration to ascertain that there is peak demyelination after 6 weeks of cuprizone treatment (Figure 1). Furthermore, we investigated a more caudal region (bregma −0.94) of the corpus callosum, and it was shown previously that de- and remyelination may slightly differ in the various regions of the corpus callosum in the cuprizone model [16]. To overcome the inaccuracies of LFB staining, immunohistochemical staining of myelin proteins, for example MBP [37,38] or PLP [36], seems a promising approach. This method has the advantage of being simple to perform and less time consuming than EM; however, our data demonstrate that the results depend on the myelin protein investigated. The findings have to be interpreted with the knowledge of when these proteins are re-expressed. While MBP is expressed very early in the remyelination process, there is a considerable overestimation when compared with myelin sheaths detected by EM. Thus, although MBP staining seems to be an excellent marker to demonstrate early remyelination processes, it should not be used as the only method to quantify remyelination. In contrast, MOG staining will not pick up the early processes of remyelination but is a good marker for myelin formation during the late phase. Thus, a combination of MBP and MOG immunohistochemistry seems a suitable and simple method to quantify remyelination, providing valuable information on both early and late phases of remyelination.

Quantification of immunohistochemical staining is commonly performed by a scoring system. This has the disadvantage of depending, at least partially, on the subjective impression of the rater in contrast to more objective methods such as mRNA quantification [20] or biochemical assays [39]. However, such a subjective impression may also have advantages; for example, in our study investigators could always differentiate between remyelinated structures and controls in a direct comparison due to the less-structured appearance of remyelinated lesions. In order to have a more objective readout of the immunohistochemical staining, we compared the visual scoring of sections with a computer-based morphometrical method. Although the results of the scoring system and the computer-assisted method revealed similar results for myelin proteins PLP, MBP and CNPase, the computer program always underestimated the amount of MOG due to its weaker staining. In addition, due to the necessity to digitalize the regions of interest and to define the cut-off for positive pixel for each section, the computer-assisted method was more time consuming than the visual

© 2007 Blackwell Publishing Ltd,

UNCORRECTED PROOF

scoring. Thus, despite some disadvantages, the immunohistochemistry for MBP or PLP and MOG analysed by blinded scorer seems to be the best and most effective quantification method to follow remyelination in the cuprizone model.

The cuprizone model has been used very successfully in the past years to delineate basic mechanisms of remyelination, including the characterization of crucial transcription factors [27], the role of cytokines [23,28,29,40], or growth factors [12,41], to mention but a few.

Our findings also have implications on the understanding of repair processes and the design of regenerative therapies. Obviously, the termination of the demyelinating cause has to be accomplished as fast as possible to allow for remyelination. The microenvironment in the CNS during remyelination is sufficient to allow for a fast repair process. The cellular programmes for remyelination are activated within a few days and seem to be highly efficient. Thus, inhibitory signals in pathological situations have to be identified and eliminated.

Finally, the knowledge of the expression pattern of myelin proteins during remyelination is required for the interpretation of neuropathological data. Recent studies have demonstrated that in a subset of multiple sclerosis patients, there is extensive remyelination as judged by PLP staining [36]. However, our data suggest that this may reflect only the early phase of remyelination. We therefore propose that a combination of an early and late myelin protein like PLP (or MBP) and MOG respectively, should be used to follow remyelination to achieve better information on the quality of the newly built myelin.

Acknowledgements

We thank Ilona Cierpka-Leja for excellent technical assistance and Kerstin Rohn for invaluable help with EM. This work was supported by internal funds of the MHH (HiLF) and the DFG (SFB 566).

References

1 Franklin RJ. Why does remyelination fail in multiple sclerosis? *Nat Rev Neurosci* 2002; 3: 705–14
2 Baumann N, Pham-Dinh D. Biology of oligodendrocyte and myelin in the mammalian central nervous system. *Physiol Rev* 2001; 81: 871–927
3 Stangel M, Hartung HP. Remyelinating strategies for the treatment of multiple sclerosis. *Prog Neurobiol* 2002; 68: 361–76
4 Wolswijk G. Chronic stage multiple sclerosis lesions contain a relatively quiescent population of oligodendrocyte precursor cells. *J Neurosci* 1998; 18: 601–9
5 Chang A, Tourtellotte WW, Rudick R, Trapp BD. Premyelinating oligodendrocytes in chronic lesions of multiple sclerosis. *N Engl J Med* 2002; 346: 165–73
6 Chang A, Nishiyama A, Peterson J, Prineas J, Trapp BD. NG2-positive oligodendrocyte progenitor cells in adult human brain and multiple sclerosis lesions. *J Neurosci* 2000; 20: 6404–12
7 Stangel M, Trebst C. Remyelination strategies: new advancements toward a regenerative treatment in multiple sclerosis. *Curr Neurol Neurosci Rep* 2006; 6: 229–35
8 Matsushima GK, Morell P. The neurotoxicant, cuprizone, as a model to study demyelination and remyelination in the central nervous system. *Brain Pathol* 2001; 11: 107–16
9 Hiremath MM, Saito Y, Knapp GW, Ting JP, Suzuki K, Matsushima GK. Microglial/macrophage accumulation during cuprizone-induced demyelination in C57BL/6 mice. *J Neuroimmunol* 1998; 92: 38–49
10 Arnett HA, Hellendall RP, Matsushima GK, Suzuki K, Laubach VE, Sherman P, Ting JP. The protective role of nitric oxide in a neurotoxicant-induced demyelinating model. *J Immunol* 2002; 168: 427–33
11 Ludwin SK. Chronic demyelination inhibits remyelination in the central nervous system. An analysis of contributing factors. *Lab Invest* 1980; 43: 382–7
12 Armstrong RC, Le TQ, Frost EE, Borke RC, Vana AC. Absence of fibroblast growth factor 2 promotes oligodendroglial repopulation of demyelinated white matter. *J Neurosci* 2002; 22: 8574–85
13 Blakemore WF. Observations on oligodendrocyte degeneration, the resolution of status spongiosus and remyelination in cuprizone intoxication in mice. *J Neurocytol* 1972; 1: 413–26
14 Blakemore WF. Remyelination of the superior cerebellar peduncle in old mice following demyelination induced by cuprizone. *J Neurol Sci* 1974; 22: 121–6
15 Ludwin SK. Central nervous system demyelination and remyelination in the mouse: an ultrastructural study of cuprizone toxicity. *Lab Invest* 1978; 39: 597–612
16 Stidworthy MF, Genoud S, Suter U, Mantei N, Franklin RJ. Quantifying the early stages of remyelination following cuprizone-induced demyelination. *Brain Pathol* 2003; 13: 329–39
17 Mason JL, Langaman C, Morell P, Suzuki K, Matsushima GK. Episodic demyelination and subsequent remyelination within the murine central nervous system: changes in axonal calibre. *Neuropathol Appl Neurobiol* 2001; 27: 50–8
18 Blakemore WF. Demyelination of the superior cerebellar peduncle in the mouse induced by cuprizone. *J Neurol Sci* 1973; 20: 63–72
19 Scholtz CL. Quantitative histochemistry of myelin using Luxol Fast Blue MBS. *Histochem J* 1977; 9: 759–65

© 2007 Blackwell Publishing Ltd,

UNCORRECTED PROOF

20 Morell P, Barrett CV, Mason JL, Toews AD, Hostettler JD, Knapp GW, Matsushima GK. Gene expression in brain during cuprizone-induced demyelination and remyelination. *Mol Cell Neurosci* 1998; 12: 220–7

21 Jurevics H, Largent C, Hostettler J, Sammond DW, Matsushima GK, Kleindienst A, Toews AD, Morell P. Alterations in metabolism and gene expression in brain regions during cuprizone-induced demyelination and remyelination. *J Neurochem* 2002; 82: 126–36

22 Ludwin SK, Sternberger NH. An immunohistochemical study of myelin proteins during remyelination in the central nervous system. *Acta Neuropathol (Berl)* 1984; 63: 240–8

23 Gao X, Gillig TA, Ye P, D'Ercole AJ, Matsushima GK, Popko B. Interferon-gamma protects against cuprizone-induced demyelination. *Mol Cell Neurosci* 2000; 16: 338–49

5 24 Paxinos G, Franklin KBJ.*The Mouse Brain in Stereotaxic Coordinates*.XX: XXX, 2001

25 Emery B, Cate HS, Marriott M, Merson T, Binder MD, Snell C, Soo PY, Murray S, Croker B, Zhang JG, Alexander WS, Cooper H, Butzkueven H, Kilpatrick TJ. Suppressor of cytokine signaling 3 limits protection of leukemia inhibitory factor receptor signaling against central demyelination. *Proc Natl Acad Sci USA* 2006; 103: 7859–64

26 Stidworthy MF, Genoud S, Li WW, Leone DP, Mantei N, Suter U, Franklin RJ. Notch1 and Jagged1 are expressed after CNS demyelination, but are not a major rate-determining factor during remyelination. *Brain* 2004; 127: 1928–41

27 Arnett HA, Fancy SP, Alberta JA, Zhao C, Plant SR, Kaing S, Raine CS, Rowitch DH, Franklin RJ, Stiles CD. bHLH transcription factor Olig1 is required to repair demyelinated lesions in the CNS. *Science* 2004; 306: 2111–15

28 Mason JL, Suzuki K, Chaplin DD, Matsushima GK. Interleukin-1beta promotes repair of the CNS. *J Neurosci* 2001; 21: 7046–52

29 Lin W, Kemper A, Dupree JL, Harding HP, Ron D, Popko B. Interferon-gamma inhibits central nervous system remyelination through a process modulated by endoplasmic reticulum stress. *Brain* 2006; 129: 1306–18

30 Merkler D, Ernsting T, Kerschensteiner M, Bruck W, Stadelmann C. A new focal EAE model of cortical demyelination: multiple sclerosis-like lesions with rapid resolution of inflammation and extensive remyelination. *Brain* 2006; 129: 1972–83

31 Miller DJ, Asakura K, Rodriguez M. Central nervous system remyelination clinical application of basic neuroscience principles. *Brain Pathol* 1996; 6: 331–44

32 Woodruff RH, Franklin RJ. The expression of myelin protein mRNAs during remyelination of lysolecithin-induced demyelination. *Neuropathol Appl Neurobiol* 1999; 25: 226–35

33 Birgbauer E, Rao TS, Webb M. Lysolecithin induces demyelination in vitro in a cerebellar slice culture system. *J Neurosci Res* 2004; 78: 157–66

34 Delarasse C, Daubas P, Mars LT, Vizler C, Litzenburger T, Iglesias A, Bauer J, Della GB, Schubart A, Decker L, Dimitri D, Roussel G, Dierich A, Amor S, Dautigny A, Liblau R, Pham-Dinh D. Myelin/oligodendrocyte glycoprotein-deficient (MOG-deficient) mice reveal lack of immune tolerance to MOG in wild-type mice. *J Clin Invest* 2003; 112: 544–53

35 Solly SK, Thomas JL, Monge M, Demerens C, Lubetzki C, Gardinier MV, Matthieu JM, Zalc B. Myelin/oligodendrocyte glycoprotein (MOG) expression is associated with myelin deposition. *Glia* 1996; 18: 39–48

36 Patrikios P, Stadelmann C, Kutzelnigg A, Rauschka H, Schmidbauer M, Laursen H, Sorensen PS, Bruck W, Lucchinetti C, Lassmann H. Remyelination is extensive in a subset of multiple sclerosis patients. *Brain* 2006; 129: 3165–72

37 Tanaka S, Mito T, Takashima S. Progress of myelination in the human fetal spinal nerve roots, spinal cord and brainstem with myelin basic protein immunohistochemistry. *Early Hum Dev* 1995; 41: 49–59

38 Bodhireddy SR, Lyman WD, Rashbaum WK, Weidenheim KM. Immunohistochemical detection of myelin basic protein is a sensitive marker of myelination in second trimester human fetal spinal cord. *J Neuropathol Exp Neurol* 1994; 53: 144–9

39 Jurevics H, Hostettler J, Muse ED, Sammond DW, Matsushima GK, Toews AD, Morell P. Cerebroside synthesis as a measure of the rate of remyelination following cuprizone-induced demyelination in brain. *J Neurochem* 2001; 77: 1067–76

40 Arnett HA, Mason J, Marino M, Suzuki K, Matsushima GK, Ting JP. TNF alpha promotes proliferation of oligodendrocyte progenitors and remyelination. *Nat Neurosci* 2001; 4: 1116–22

41 Mason JL, Jones JJ, Taniike M, Morell P, Suzuki K, Matsushima GK. Mature oligodendrocyte apoptosis precedes IGF-1 production and oligodendrocyte progenitor accumulation and differentiation during demyelination/remyelination. *J Neurosci Res* 2000; 61: 251–62

Received 11 May 2007
Accepted after revision 20 May 2007

© 2007 Blackwell Publishing Ltd, *Neuropathology and Applied Neurobiology*, 33, ••–••

UNCORRECTED PROOF

Chapter II

The chemokine receptor CXCR2 is expressed on oligodendrocyte precursor cells *in vivo* but is not required for successful remyelination after cuprizone-induced demyelination

Maren Lindner[1,2], Corinna Trebst[1], Sandra Heine[1], Paraskevi N. Koutsoudaki[1,2], Martin Stangel[1,2*]

[1]Department of Neurology, Medical School Hannover, and [2]Center for Systems Neuroscience, Hannover, Germany

in preparation

Abstract

Unravelling the factors that can positively influence remyelination is one of the major challenges in multiple sclerosis research. Expression of the chemokine receptor CXCR2 on oligodendrocytes both *in vitro* and in MS lesions has suggested a possible role for CXCR2 in the recruitment of oligodendrocyte precursor cells (OPC). In order to investigate the function of CXCR2 during remyelination *in vivo* we studied this receptor in cuprizone-induced demyelination and the subsequent remyelination. We found that CXCR2 is constitutively expressed on OPC, whereas on monocytes/microglia CXCR2 is upregulated upon activation during demyelination. Hence, the expression of CXCR2 is differentially regulated in oligodendrocytes and monocytes/microglia. Studies in CXCR2-/- mice revealed no differences during physiological myelination in the brain. Furthermore, we subjected CXCR2-/- mice to the cuprizone model demonstrating that remyelination as assessed by LFB, MOG and PLP scoring, was not altered in comparison to wildtype controls. In addition, the number of OPC and the amount of microglial accumulation was similar in both CXCR2-/- and wildtype animals during the whole de- and remyelination process.

These results suggest that despite expression on OPC and microglia CXCR2 plays a minor role during remyelination and its functions can be compensated by other molecules.

Introduction

Destruction of myelin in the central nervous system is one of the neuropathological hallmarks in multiple sclerosis (MS). Although extensive remyelination may occur in some 20% of MS cases (Patrikios et al., 2006; Patani et al., 2007) repair processes fail frequently despite the presence of oligodendrocyte progenitor cells (OPC) in the MS plaque that are in principle capable to remyelinate axons (Scolding et al., 1998; Chang et al., 2000; Maeda et al., 2001). The reasons for this remyelination failure may be manifold (Franklin, 2002; Stangel and Trebst, 2006) and the knowledge of the molecular mechanisms responsible for remyelination is only limited. A large number of factors are known to influence the complex process of remyelination including cytokines (Heine et al., 2006; Arnett et al., 2001; Butzkueven et al., 2006; Plant et al., 2005; Zhang et al., 2006) and growth factors (Armstrong et al., 2002; Kumar et al., 2007; Lee et al., 2007; Zhou et al., 2006). In recent years the expression of the chemokine receptor CXCR2 has been described on OPC (Nguyen and Stangel, 2001; Tsai et al., 2002) and the presence in MS lesions suggested a role of this receptor for remyelination (Omari et al., 2006; Omari et al., 2005; Filipovic et al., 2003).

CXCR2 is a seven transmembrane G protein-coupled receptor that belongs to the family of chemokine receptors that are subdivided according to the relative position of cysteine residues, namely CC, CXC, CX3C, and C. Most receptors can bind more than one chemokine, and most chemokines are ligands for several receptors, indicating a redundancy for the chemokine/chemokine receptor system (Baggiolini, 1998; Mantovani, 1999). In the CNS the chemokine receptor CXCR2 is expressed on subsets of neurons (Coughlan et al., 2000; Danik et al., 2003; Horuk et al., 1997), astrocytes (Danik et al., 2003; Flynn et al., 2003), microglia (Flynn et al., 2003; Filipovic et al., 2003), and OPC (Nguyen and Stangel, 2001). In addition, its ligand CXCL1 (GRO-α) has been demonstrated in rodents to act synergistically with platelet-derived growth factor (PDGF-α) to induce proliferation of primary OPC (Robinson et al., 1998) and to arrest their migration *in vitro* and *in vivo* (Tsai et al., 2002). Furthermore it

was shown (Kadi et al., 2006) that CXCL1 is able to stimulate myelin basic protein synthesis in a dose-dependent manner in primary myelinating cultures thereby enhancing myelin formation. Recently, CXCR2 expression was also shown on proliferating oligodendrocytes in association with CXCL1 positive astrocytes at the edge of MS lesions, postulating a role of CXCR2 and its ligand CXCL1 on the recruitment of OPC toward the MS lesion (Omari et al., 2006; Omari et al., 2005).

In order to study the role of CXCR2 during remyelination we used cuprizone-induced de- and remyelination, a well characterized and reliable animal model of toxic demyelination with spontaneous remyelination in the CNS (Matsushima and Morell, 2001; Hiremath et al., 1998; Lindner et al., 2007).

Materials and Methods

Animals

All experiments were performed according to the national animal laws and approved by the local government authority. C57BL/6 mice were obtained from Charles River (Sulzfeld, Germany). Heterozygous CXCR2 deficient mice (C.129S2(B6)-*IL8rb*$^{tm1/Mwm}$/J) were purchased from Jackson Labs (Bar Harbor, ME, USA). CXCR2-/- mice and matched balb/cJ wildtype animals were bred under the same conditions. Genotyping was performed by PCR using the primers oIMR0013 (5'-CTTGGGTGGAGAGGCTATTC-3') and oIMR0014 (5'-AGGTGAGATGACAGGAGATC-3') for neomycin and the primers oIMR0453 (5'-GGTCGTACTGCGTATCCTGCCTCAG -3') and oIMR0454 (5'-TAGCCATGATCTTGAGAAGTCCATG -3') for the CXCR2 receptor. The amplification cycle consisted of 2 min at 94°C followed by 30 cycles at 94°C for 30 s, 57°C for 30 s, and 72°C for 1.30 min. Chain elongation at 72°C was continued for 10 min after the last cycle. PCR products were separated on a 1.5% agarose gel. Wildtype animals had a single band at 360 bp while the homozygous knock-out mice had a single band at 280 bp.

Cuprizone treatment and tissue processing

Male C57BL/6 mice (8 weeks old) were fed *ad libitum* with 0.3% (w/w) cuprizone (bis-cyclohexanone oxaldihydrazone, Sigma-Aldrich Inc., St.Louis, MO) mixed into a ground standard rodent chow. Cuprizone diet was maintained for 6 weeks, thereafter mice were put on a normal chow for another 10 weeks. Animals (n = 6) were perfused with 4% paraformaldehyde (PFA) in phosphate buffer via the left cardiac ventricle. Brains were removed and postfixed in 4% PFA and paraffin embedded.

CXCR2-/- and wildtype balb/cJ control male mice (8 weeks old) were maintained for 6 weeks on a 0.2% (w/w) cuprizone diet, followed by a recovery phase of 6 weeks. Although the extent of demyelination at the corpus callosum was less compared to C57BL/6, the dosage of

0.2% cuprizone was determined as the highest tolerable dosage in the balb/c background. Animals (n = 5 per group) were sacrificed and processed as described above.

Histology and Immunohistochemistry

7 µm serial paraffin sections between bregma -0.94 and bregma -1.8 (according to mouse atlas by Paxinos and Franklin (Paxinos and Franklin, 2001)) were analysed. Sections were stained for myelin with Luxol-fast blue periodic acid-Schiff base (LFB-PAS).

For immunohistochemistry, paraffin embedded sections were de-waxed, rehydrated and microwaved for 5 min in 10 mM citrate buffer (pH 6.0). Sections were quenched with H_2O_2, blocked for 1 h in PBS containing 3% normal goat serum, 0.1% Triton X-100, and then incubated overnight with primary antibody. The following primary antibodies were used: for myelin proteins PLP (mouse IgG, 1:500 Serotec, Düsseldorf, Germany) and MOG (mouse IgG, 1:2 hybridoma supernatant, generous gift from C. Linington), for the chemokine receptor CXCR2 (rabbit polyclonal, 1:200, Santa Cruz Biotechnology, Santa Cruz, California, USA), for astrocytes GFAP (mouse IgG, 1:200, Chemicon, Hamphire, UK), for microglia Mac-3 (rat IgG, 1:50, BD Pharmingen, Heidelberg, Germany), for OPC NG2 (rabbit polyclonal, 1:200, Chemicon, Hamphire, UK), and Olig2 (mouse IgG, 1:200, hybridoma supernatant, generous gift by T. Magnus and M.S. Rao). After washing, sections were further incubated with biotinylated secondary antibody (Vector Laboratories, Burlingame, UK) for one h, followed by peroxidase-coupled avidin-biotin complex (ABC Kit, Vector Laboratories). Reactivity was visualized with diamino-3,3'benzidine (DAB, Dako Cytomation, Hamburg, Germany).

For double stainings the following fluorescently labelled secondary antibodies were used: Cy3-goat anti-mouse, Cy3-goat anti-rat or FITC-goat anti-rabbit (Dianova, Hamburg, Germany). Sections were analysed by conventional fluorescent microscopy (Leica DMLB, Wetzlar, Germany) and confocal microscopy (Leica DMIRE2, Wetzlar, Germany).

Quantification of de- and remyelination

Luxol-fast blue and myelin protein (PLP, MOG) stained section were scored by three blinded observers using a scale from 0 (normal myelin) to 3 (complete demyelination) as described previously (Lindner et al., 2007).

Quantification of cells

Quantification of cells was done right and left from the midline within the corpus callosum in an area of at least 0.125 mm² using a magnification of 40x (Leica DMLB, Wetzlar, Germany).

Physiological myelination studies

To investigate the physiological myelination, brains from wildtype (n = 4) and CXCR2-/- mice (n = 4) at postnatal day P0, P7, P21 and P56 were removed and processed as described above. Paraffin sections were stained for the myelin proteins PLP and MOG and additionally for CNPase (mouse IgG, 1:100, Chemicon, Hamphire, UK) and MBP (mouse IgG, 1:1000 Sternberger Monoclonals Inc., Berkeley, USA). For OPC the sections were stained with NG2 (rabbit polyclonal, 1:200, Chemicon, Hamphire, UK). NG2 positive cells were counted as described above. MBP positive cells were counted within an area of at least 0.5 mm² along the corpus callosum using a magnification of 20x (Leica DMLB).

Statistical Analysis

Data were analysed with SigmaStat using the unpaired student's t-test and Mann-Whitney rank - sum test to compare wildtype and CXCR2-/- animals. A p value <0.05 was considered as statistically significant.

Results

OPC identified by Olig2 and NG2 respond to cuprizone-induced demyelination

As described previously (Lindner et al., 2007), 6 weeks of cuprizone treatment in C57BL/6 mice lead to a complete demyelination of the corpus callosum. Upon removal of cuprizone there was a rapid remyelination within the first two weeks. During cuprizone feeding the NG2+ cells increased in the corpus callosum (Fig. 1I) in accordance with other reports (Hiremath et al., 1998; Matsushima and Morell, 2001), as well as in the thalamus (Fig. 1G), and in the hypothalamus (Fig. 1H). Olig2+ progenitors could be observed in control animals in the corpus callosum and to some extent also in the striatum (Fig. 1A, B). During demyelination the number of Olig2+ cells increased in the corpus callosum until week 7 and remained at the same high level during remyelination (data not shown).

Astrogliosis and microglial accumulation during demyelination

Astrocytes, identified by GFAP staining, peaked in numbers from week 4 to week 6 (data not shown) during the demyelination phase. An increase in astrogliosis which was associated with hypertrophied astrocytes with thick processes was first seen at week 4 and persisted until week 10 (Fig. 1C, D). Microglia identified by Mac-3 staining, massively accumulated in the corpus callosum at week 4 (1707 ± 66 cells/mm²) and week 6 (1825 ± 86 cells/mm²) of demyelination (data not shown). The number of microglia decreased rapidly as soon as remyelination started (week 6.5: 229 ± 89 cells/mm²). In addition to the corpus callosum (Fig. 1E) monocytes/microglia were also present in the striatum (Fig. 1F) from week 6 to week 9. Both astroglial and microglial changes were similar to previously published reports (Hiremath et al., 1998).

CXCR2 is expressed during de- and remyelination

Since CXCR2 is expressed on OPC (Nguyen and Stangel, 2001) and was suggested to play a role during the remyelination of MS lesions (Omari et al., 2006; Omari et al., 2005) we investigated the expression of CXCR2 in the cuprizone model. Quantification of CXCR2 positive cells (Fig. 1I) showed an increase between week 2 (293 ± 43 cells/mm²) and week 4 (579 ± 37 cells/mm²) (Fig. 2). During the peak of demyelination (week 6) and early remyelination (week 6 to week 8) the number of CXCR2 positive cells remained at the same high level (Fig. 2). Furthermore, CXCR2 positive cells were seen in the thalamus and in the striatum (Fig. 1L, M).

CXCR2 is constitutively expressed by OPC and upregulated on monocytes/microglia during de- and remyelination

The morphology and co-localization of CXCR2 positive cells with NG2 suggested that these cells were OPC (compare Fig. 2I with 2K and Fig. 2G with 2L). However, the total number of CXCR2+ cells exceeded the number of NG2+ cells observed (e.g. at week 4 579 ± 37 cells/mm² versus 331 ± 74 cells/mm² CXCR2 and NG2, respectively). We therefore performed double stainings to identify the source of CXCR2 expression. Because double staining of CXCR2 with NG2 was not possible due to both antibodies being raised in the same species, we used Olig2 as an OPC marker and CNPase as a marker for a more differentiated oligodendrocyte cell. CXCR2 expression was co-localized with both Olig2 (Fig. 3A-A'') and CNPase (Fig. 3B-B''). In addition to the cells of the oligodendroglial lineage, monocytes/microglia showed CXCR2 expression (Fig. 3C-C'') in particular at time points when they peaked in numbers (week 4 and 6). Astrocytes were never seen to express CXCR2 at any of the investigated time point (Fig. 3D-D'').

We quantified double stainings at selected time points in the corpus callosum to investigate the distribution of CXCR2 expression (Tab. 1). Most OPC expressed constitutively CXCR2, which is only slightly increased during de- and remyelination. In contrast, CXCR2 was not

expressed on microglia in control mice, but was upregulated during demyelination to be expressed in up to 50% of all present microglia, representing 70% of all CXCR2 positive cells at peak demyelination. During remyelination, CXCR2 expression is downregulated again on microglia to reach control levels at the end of remyelination (Tab. 1). Thus, there seems to be only little if any regulation for CXCR2 expression in OPC, while CXCR2 is upregulated on activated monocytes/microglia.

CXCR2 deficient mice have a normal myelination pattern in the CNS

Since it has been described that the pattern of oligodendrocyte recruitment is modified in CXCR2-/- mice in the spinal cord at P7 (Tsai et al., 2002), we evaluated the number and distribution of NG2 positive cells during physiological myelination in the corpus callosum (data not shown). We found no significant difference in the number of NG2+ progenitors in CXCR2-/- animals compared to wildtype controls (n = 4) for all investigated time points. Furthermore, we investigated the myelination pattern as judged by Luxol fast blue, PLP, MBP, CNPase and MOG stainings. Again, wildtype and CXCR2-/- mice displayed the same degree of myelin protein expression at all investigated time points. In addition, the number of MBP positive cells at P7 did not differ significantly between wildtype and CXCR2-/- mice (10.5 cells/mm² and 9.5 cells/mm², respectively, $p = 0.52$).

Taken together, there was no significant difference in the physiological myelination in CXCR2-/- mice compared to wildtype controls in the corpus callosum.

CXCR2 is not required for successful remyelination

To analyse the role of CXCR2 during de- and remyelination, we subjected CXCR2-/- mice to the cuprizone model. CXCR2 and wildtype balb/cJ mice were fed a 0.2% cuprizone diet for 6 weeks. Preliminary experiments determined 0.2% cuprizone as the highest tolerable dosage in

the balb/c background, and the extent of demyelination in the corpus callosum was less compared to C57BL/6.

The extent of de- and remyelination was quantified as mentioned above. LFB stained sections (n = 5) (data not shown) showed only a small and non-significantly reduction in demyelination in CXCR2-/- mice compared to wildtype controls. Similar results were seen for the re-expression of the myelin proteins PLP and MOG (Fig. 4A and B). Thus, the course of de- and remyelination was not altered in CXCR2-/- mice compared to wildtype animals.

Numbers of OPC, accumulation of microglia, and amount of astrogliosis were not altered in CXCR2-/- mice during de- and remyelination

During cuprizone treatment the number of NG2+ progenitors increased at week 3 and declined after removal of cuprizone from the diet (Fig. 5A). There was no difference between wildtype and CXCR2-/- animals (n = 5). Accumulation of monocytes/microglia was monitored by mac-3 staining. The number of monocytes/microglia in the middle of the corpus callosum increased at week 3, peaked at week 6, and remained at this level until week 8 (Fig. 5B). Again, there was no difference between wildtype and CXCR2 deficient animals. Finally, the number of astrocytes (data not shown) did not change during the course of de- and remyelination. The amount of astrogliosis that persisted from week 6 to week 12 was not different in CXCR2-/- mice as compared to wildtype controls.

These data suggest that neither migration or differentiation of OPC nor monocyte/microglia recruitment or astrogliosis were altered after cuprizone-induced demyelination in the absence of CXCR2.

Discussion

In order to remyelinate a lesion, oligodendrocyte progenitors have to proliferate, migrate and differentiate in a quite complex pattern influenced by several factors. Recent studies suggested a role for the chemokine receptor CXCR2 and its ligand CXCL1 during remyelination (Omari et al., 2006; Omari et al., 2005; Filipovic et al., 2003). Filipovic and co-worker (Filipovic et al., 2003) found CXCR2/CXCL1 expression predominantly on OPC in the subventricular zone in normal human brain tissue, while there was a complete absence of CXCL1/CXCR2 on OPC in demyelinated multiple sclerosis lesions. They suggested a role for CXCR2 in oligodendrocyte progenitor recruitment and an absence of this signal may explain the failure of remyelination in multiple sclerosis. Another study (Omari et al., 2006; Omari et al., 2005) found CXCR2 constitutively expressed on oligodendrocytes and upregulated in multiple sclerosis lesion, in concert with an upregulation of CXCL1 in astrocytes at the edges of an active MS lesion. We therefore investigated the role of CXCR2 in a toxic de- and remyelination model to elucidate the role of this chemokine receptor during remyelination.

We show here that CXCR2 is constitutively expressed on NG2+ OPC and expression was not altered during both de- and remyelination. Double staining demonstrated that both early Olig2+ oligodendrocyte progenitors as well as CNPase+ mature oligodendrocytes express CXCR2. In contrast, CXCR2 is absent on resting monocytes/microglia and is upregulated upon activation of these cells during demyelination. Such a differential regulation of CXCR2 on monocytes/microglia has also been observed in experimental stroke (Popivanova et al., 2003) and CNS injury (Valles et al., 2006). Thus, upregulation of CXCR2 on microglia in the CNS seems to be a rather unspecific consequence of microglial activation after various stimuli, including toxic demyelination.

The physiological myelination pattern in the brain of CXCR2-/- mice was not modified compared to wildtype animals. Although an altered migration of OPC has been described at

P7 in the spinal cord of CXCR2-/- mice (Tsai et al., 2002), there were no differences at other time points. Therefore it can be concluded that CXCR2 has only a minor role during physiological myelination of the CNS and its function is obviously compensated by other factors. However, there may be strain differences as suggested by a recent study where CXCR2-/- mice were backcrossed into a C57BL/6 background (Padovani-Claudio et al., 2006). This led to premature death and an increase in the density of mature oligodendrocytes in the corpus callosum. Taking into account that body weight and brain size were significantly altered in these animals compared to CXCR2-/- mice with balb/c background, conclusions for our study should be made with caution.

The different observations in the spinal cord and the corpus callosum may result from the fact that spinal cord derived oligodendrocyte progenitors differ from brain derived progenitors as suggested by *in vitro* studies (Bjartmar, 1998; Devon, 1987). This may also account for the different results described for the effect of CXCL1 on OPC derived from spinal cord (Robinson et al., 1998) and brain hemispheres (Kadi et al., 2006). Possibly spinal cord OPC are more sensitive to chemokines than brain derived OPC, which may be explained by the heterogeneity of the oligodendroglial cell population (Nishiyama, 2007; Liu and Rao, 2004).

Our studies in the cuprizone model with CXCR2-/- mice showed no impairment of remyelination as assessed by Luxol-fast blue, PLP, and MOG stained sections. The recruitment of OPC was not disrupted, neither was the accumulation of microglia altered. Thus, the expression of CXCR2 is not a major requirement for successful remyelination. Its function is obviously compensated *in vivo*, presumably by other chemokine receptors, e.g. CXCR4 (Maysami et al., 2006; Dziembowska et al., 2005). This would again underline the complexity and redundancy of the chemokine system.

The impact of CXCR2 signalling in MS can not be answered definitely, but our study suggests that CXCR2 is not a major requirement for the recruitment of oligodendrocyte progenitors and remyelination. Certainly, the isolated lack of CXCR2 is unlikely to be the only factor responsible for the failure of remyelination in MS. Similarly, Jagged-1 signalling via Notch1 receptors on OPC has been suggested as reason for remyelination failure in MS (John et al., 2002), but ablation of Notch1 did not alter experimental remyelination (Stidworthy et al., 2004). These findings, similar to ours, demonstrate that impairment of a single molecular mechanism does not necessarily disrupt the complex process of remyelination. Apparently many mechanisms described to influence oligodendrocyte functions can be compensated in vivo. This implies for the development of therapeutic strategies to enhance remyelination that possibly several molecular mechanisms have to be targeted at the same time.

Acknowledgements

We thank Ilona Cierpka-Leja for excellent technical assistance. Dr. M.S. Rao and Dr. T. Magnus generously provided the Olig2 antibody. This work was supported by the DFG (SFB 566/A11).

Tables

Tab. 1

Distribution of CXCR2 expression during de-and remyelination

	Percentage from total number of CXCR2+ cells		Percentage of CXCR2+ cells from total number of	
time points	**Olig2+ cells**	**Mac-3+ cells**	**Olig2+ cells**	**Mac3+ cells**
control	75 ± 5	0	15±5	0
4 weeks	20 ± 10	65 ± 5	30±10	30±10
6 weeks	30 ± 5	70 ± 5	25±5	50±20
6.5 weeks	50 ± 10	45 ± 10	30±10	30±5
8 weeks	70 ± 15	30 ± 5	35±30	25±15
16 weeks	90 ± 5	0	20±10	0

Quantification of double stainings of at least three animals per investigated time point, cells were counted in the middle of the corpus callosum using a magnification of 40x (Leica DMLB). Results are represented in percent with standard error of the mean.

Fig. 1

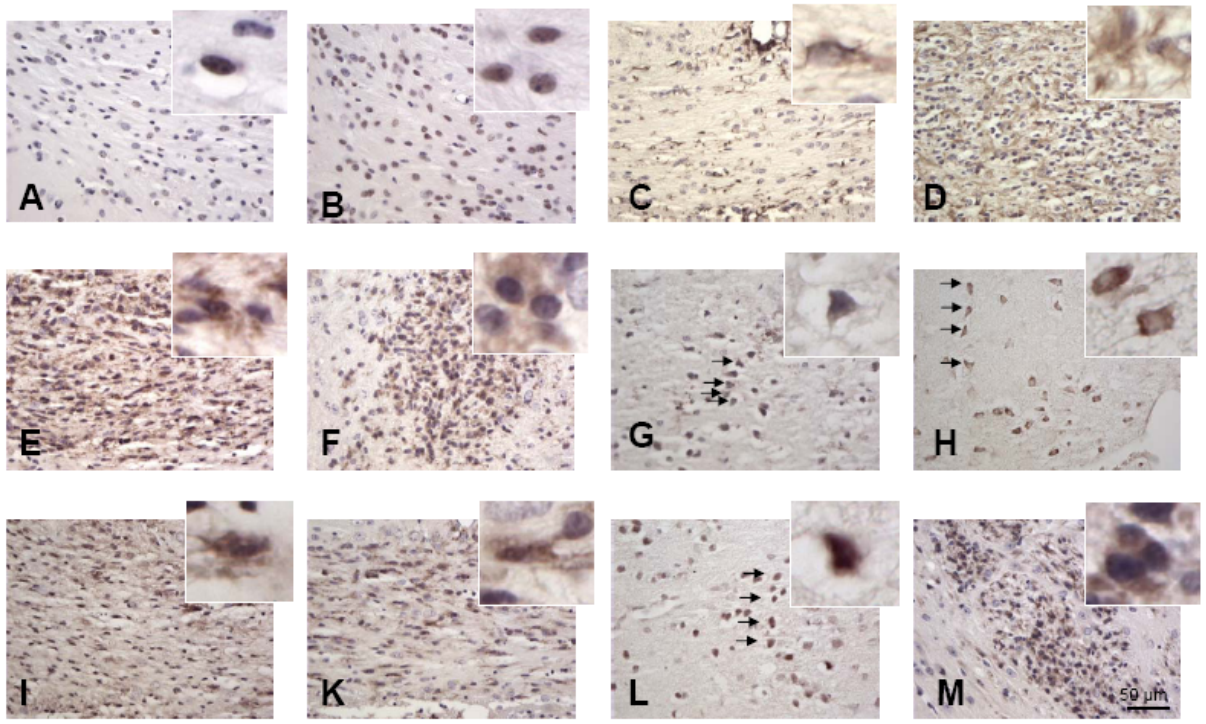

Fig. 1:

Immunohistochemistry for glial cells and CXCR2 expression during cuprizone induced de- and remyelination. Olig2 positive oligodendrocyte precursor cells in the corpus callosum at week 6 (**A**) and in the striatum at week 7 (**B**), accumulation of astrocytes (GFAP staining) in the corpus callosum at week 6 (**D**) in comparison to a control animal (**C**). Microglia (mac-3 staining) accumulation peaked at week 4 in the corpus callosum (**E**) and was also observed in the striatum at week 6 (**F**). NG2 positive oligodendrocyte progenitor cells were seen in the thalamus (**G**) and hypothalamus (**H**) at week 6 and also in the corpus callosum at week 4 (**I**). The morphology of CXCR2 positive cells resembled NG2 positive cells in the corpus callosum (**K**) and the thalamus (**L**) at week 4, whereas CXCR2 positive cells in the striatum at week 4 (**M**) resembled the morphology of microglia. Note the similar appearance of stained cells in (**M**) and (**F**)

Fig. 2

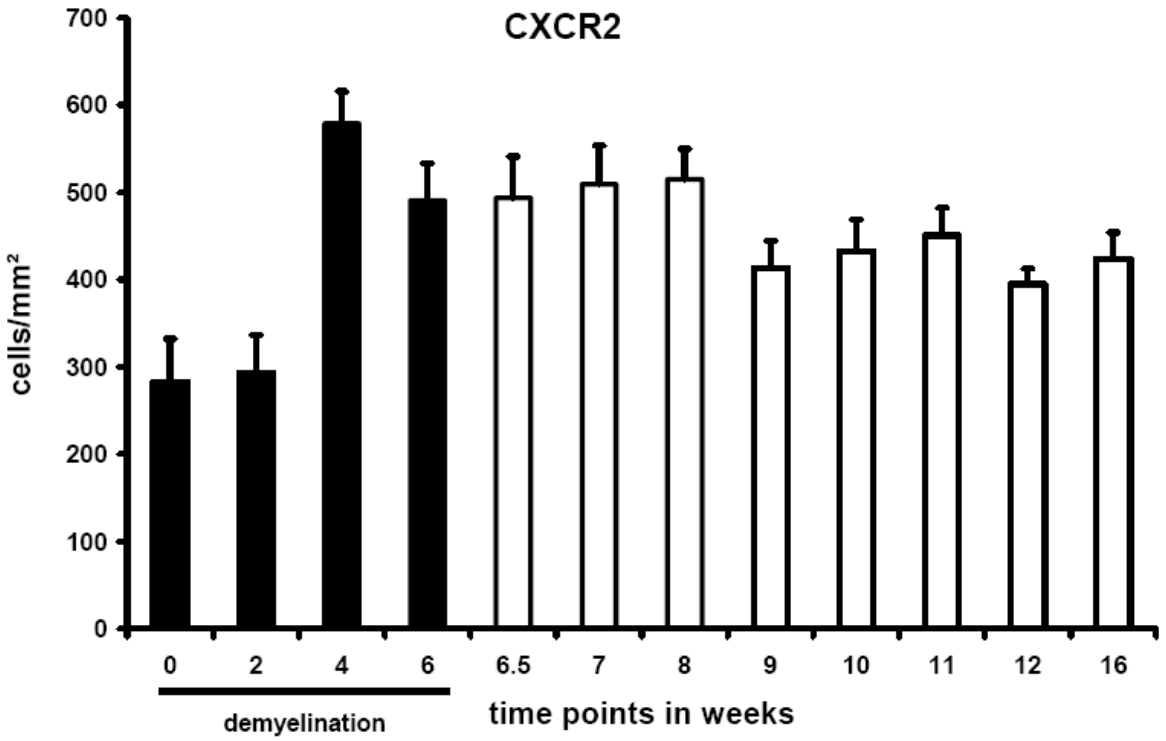

Fig. 2:

Quantification of CXCR2 positive cells during demyelination (week 0 – 6) and remyelination (week 6.5 – 16). Positive cells were counted in hematoxilin counterstained sections within an area of at least 0.125 mm² in the middle of the corpus callosum using a magnification of 40x (Leica DMLB). n = 6, error bars represent SEM.

Fig. 3

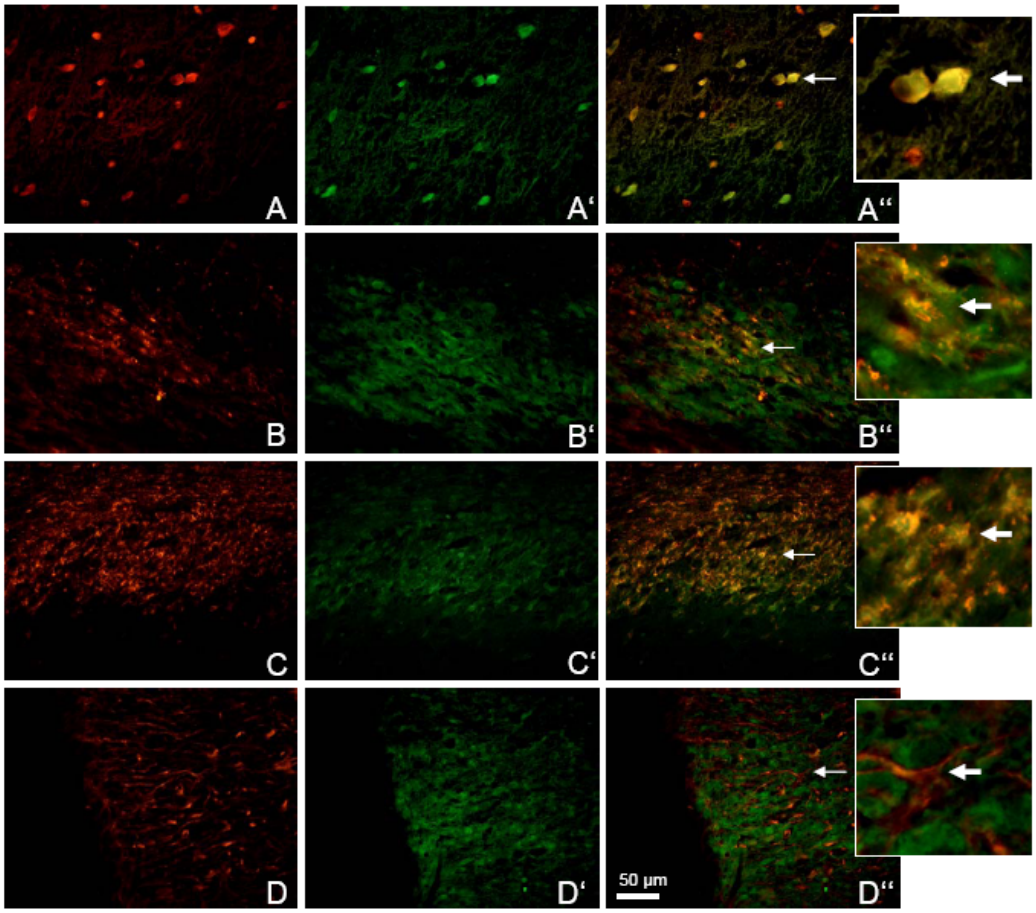

Fig. 3:

Identification of the cellular source of CXCR2 expression by double immunofluorescence stainings. Presented scheme as follows: **A** Olig2 (OPC marker), **A'** CXCR2, **A''** Olig2/CXCR2 overlay. CXCR2 co-localized with Olig2 positive OPC (**A-A''**), CNPase positive oligodendrocytes (**B-B''**), and mac-3 positive monocytes/microglia (**C-C''**), while GFAP positive astrocytes were always negative for CXCR2 staining (**D-D''**).

Fig. 4A

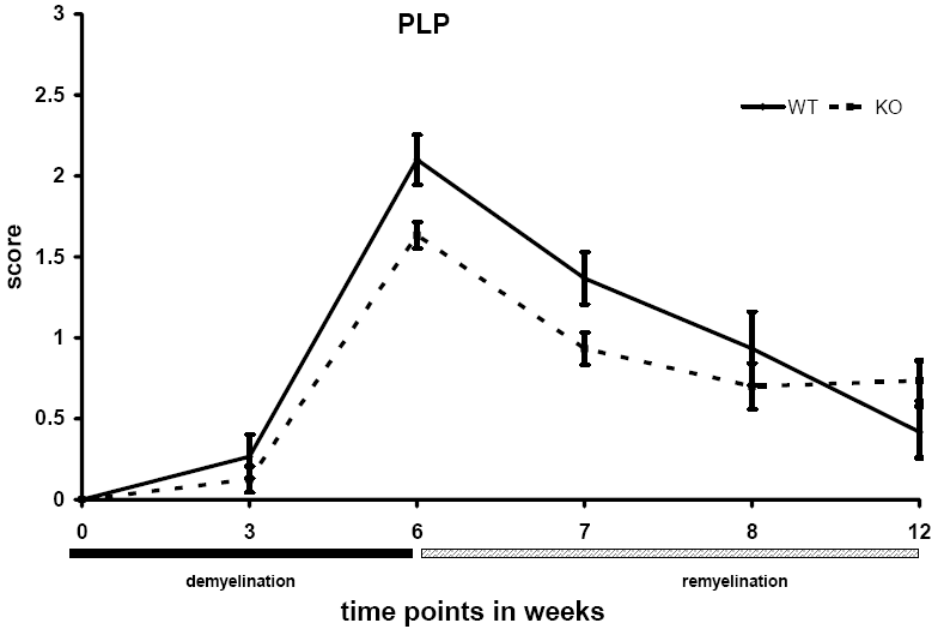

Fig. 4B

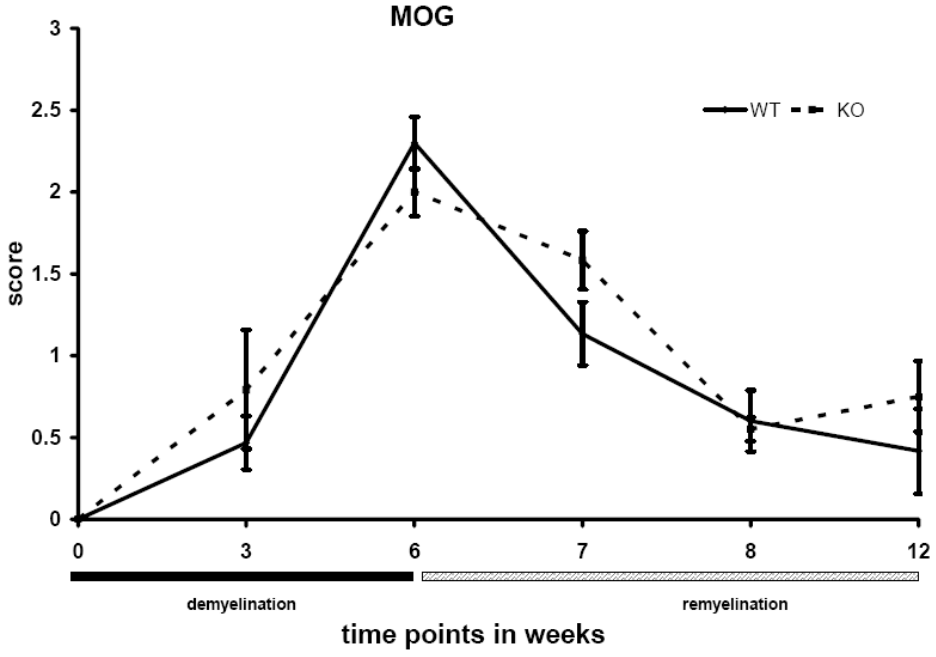

Fig. 4:

Course of de- and remyelination of wildtype and CXCR2-/- mice as judged by scoring of **A:** PLP and **B:** MOG stained sections. n = 5, error bars represent SEM. Score of 0: complete myelination, score of 3: complete demyelination. Sections were scored in a blinded manner by three independent observers.

Fig. 5A

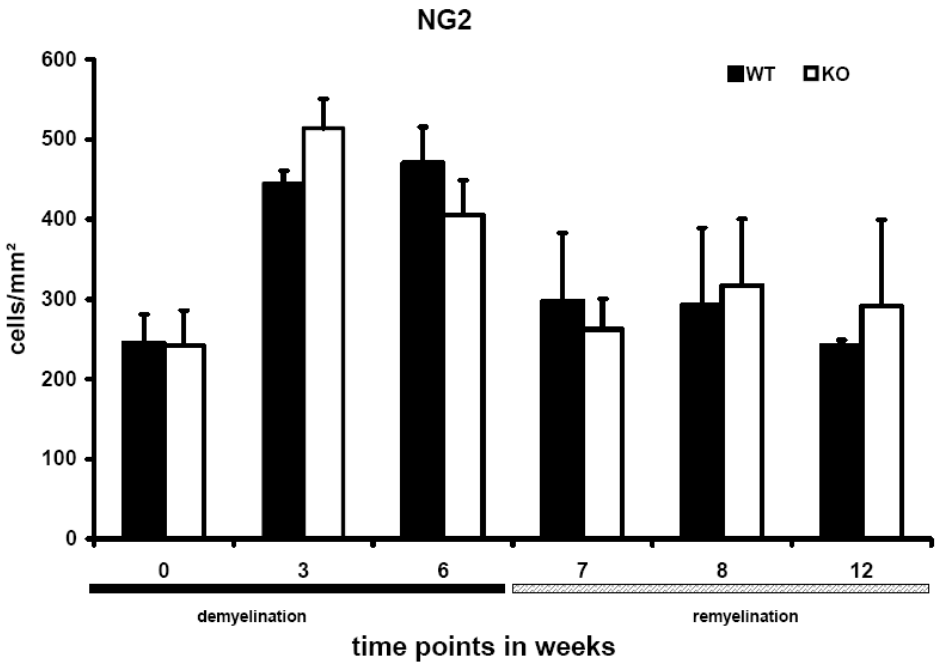

Fig. 5B

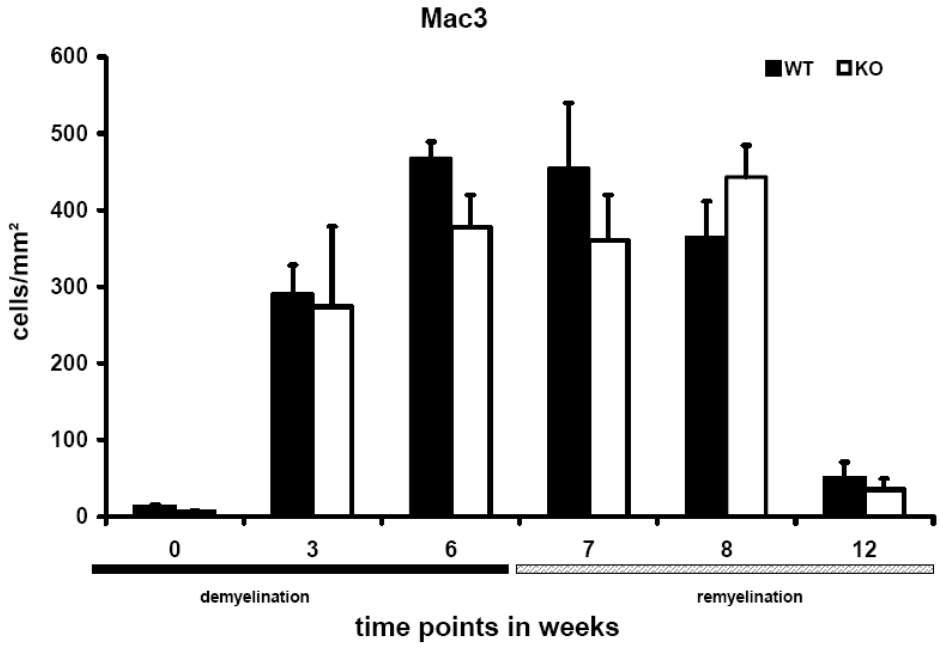

Fig. 5:

Quantification of **A**: OPC (NG2), **B**: monocytes/microglia (Mac-3), during de- and remyelination in wildtype and CXCR2-/- animals. Positive cells were counted in hematoxilin counterstained sections within an area of at least 0.125 mm² in the middle of the corpus callosum using a magnification of 40x (Leica DMLB). n = 5, error bars represents SEM.

References

1. Armstrong RC, Le TQ, Frost EE, Borke RC, Vana AC (2002) Absence of fibroblast growth factor 2 promotes oligodendroglial repopulation of demyelinated white matter. J Neurosci 22: 8574-8585.

2. Arnett HA, Mason J, Marino M, Suzuki K, Matsushima GK, Ting JP (2001) TNF alpha promotes proliferation of oligodendrocyte progenitors and remyelination. Nat Neurosci 4: 1116-1122.

3. Baggiolini M (1998) Chemokines and leukocyte traffic. Nature 392: 565-568.

4. Bjartmar C (1998) Morphological heterogeneity of cultured spinal and cerebral rat oligodendrocytes. Neurosci Lett 247: 91-94.

5. Butzkueven H, Emery B, Cipriani T, Marriott MP, Kilpatrick TJ (2006) Endogenous leukemia inhibitory factor production limits autoimmune demyelination and oligodendrocyte loss. Glia 53: 696-703.

6. Chang A, Nishiyama A, Peterson J, Prineas J, Trapp BD (2000) NG2-positive oligodendrocyte progenitor cells in adult human brain and multiple sclerosis lesions. J Neurosci 20: 6404-6412.

7. Coughlan CM, McManus CM, Sharron M, Gao Z, Murphy D, Jaffer S, Choe W, Chen W, Hesselgesser J, Gaylord H, Kalyuzhny A, Lee VM, Wolf B, Doms RW, Kolson DL (2000) Expression of multiple functional chemokine receptors and monocyte chemoattractant protein-1 in human neurons. Neuroscience 97: 591-600.

8. Danik M, Puma C, Quirion R, Williams S (2003) Widely expressed transcripts for chemokine receptor CXCR1 in identified glutamatergic, gamma-aminobutyric acidergic, and cholinergic neurons and astrocytes of the rat brain: a single-cell reverse transcription-multiplex polymerase chain reaction study. J Neurosci Res 74: 286-295.

9. Devon RM (1987) Comparison of oligodendrocytes grown in neocortex and spinal cord aggregate cultures. Brain Res 429: 289-294.

10. Dziembowska M, Tham TN, Lau P, Vitry S, Lazarini F, Dubois-Dalcq M (2005) A role for CXCR4 signaling in survival and migration of neural and oligodendrocyte precursors. Glia 50: 258-269.

11. Filipovic R, Jakovcevski I, Zecevic N (2003) GRO-alpha and CXCR2 in the human fetal brain and multiple sclerosis lesions. Dev Neurosci 25: 279-290.

12. Flynn G, Maru S, Loughlin J, Romero IA, Male D (2003) Regulation of chemokine receptor expression in human microglia and astrocytes. J Neuroimmunol 136: 84-93.

13. Franklin RJ (2002) Why does remyelination fail in multiple sclerosis? Nat Rev Neurosci 3: 705-714.

14. Heine S, Ebnet J, Maysami S, Stangel M (2006) Effects of interferon-beta on oligodendroglial cells. J Neuroimmunol 177: 173-180.

15. Hiremath MM, Saito Y, Knapp GW, Ting JP, Suzuki K, Matsushima GK (1998) Microglial/macrophage accumulation during cuprizone-induced demyelination in C57BL/6 mice. J Neuroimmunol 92: 38-49.

16. Horuk R, Martin AW, Wang Z, Schweitzer L, Gerassimides A, Guo H, Lu Z, Hesselgesser J, Perez HD, Kim J, Parker J, Hadley TJ, Peiper SC (1997) Expression of chemokine receptors by subsets of neurons in the central nervous system. J Immunol 158: 2882-2890.

17. John GR, Shankar SL, Shafit-Zagardo B, Massimi A, Lee SC, Raine CS, Brosnan CF (2002) Multiple sclerosis: re-expression of a developmental pathway that restricts oligodendrocyte maturation. Nat Med 8: 1115-1121.

18. Kadi L, Selvaraju R, de Lys P, Proudfoot AE, Wells TN, Boschert U (2006) Differential effects of chemokines on oligodendrocyte precursor proliferation and myelin formation in vitro. J Neuroimmunol 174: 133-146.

19. Kumar S, Biancotti JC, Yamaguchi M, de Vellis J (2007) Combination of growth factors enhances remyelination in a cuprizone-induced demyelination mouse model. Neurochem Res 32: 783-797.

20. Lee X, Yang Z, Shao Z, Rosenberg SS, Levesque M, Pepinsky RB, Qiu M, Miller RH, Chan JR, Mi S (2007) NGF regulates the expression of axonal LINGO-1 to inhibit oligodendrocyte differentiation and myelination. J Neurosci 27: 220-225.

21. Lindner M, Heine S, Haastert K, Garde N, Fokuhl J, Linsmeier F, Grothe C, Baumgaertner W, Stangel M (2007) Sequential myelin protein expression during remyelination reveals fast and efficient repair after central nervous system demyelination. Neuropathol Appl Neurobiol in press

22. Liu Y, Rao MS (2004) Glial progenitors in the CNS and possible lineage relationships among them. Biol Cell 96: 279-290.

23. Maeda Y, Solanky M, Menonna J, Chapin J, Li W, Dowling P (2001) Platelet-derived growth factor-alpha receptor-positive oligodendroglia are frequent in multiple sclerosis lesions. Ann Neurol 49: 776-785.

24. Mantovani A (1999) The chemokine system: redundancy for robust outputs. Immunol Today 20: 254-257.

25. Matsushima GK, Morell P (2001) The neurotoxicant, cuprizone, as a model to study demyelination and remyelination in the central nervous system. Brain Pathol 11: 107-116.

26. Maysami S, Nguyen D, Zobel F, Pitz C, Heine S, Hopfner M, Stangel M (2006) Modulation of rat oligodendrocyte precursor cells by the chemokine CXCL12. Neuroreport 17: 1187-1190.

27. Nguyen D, Stangel M (2001) Expression of the chemokine receptors CXCR1 and CXCR2 in rat oligodendroglial cells. Brain Res Dev Brain Res 128: 77-81.

28. Nishiyama A (2007) Polydendrocytes: NG2 cells with many roles in development and repair of the CNS. Neuroscientist 13: 62-76.

29. Omari KM, John G, Lango R, Raine CS (2006) Role for CXCR2 and CXCL1 on glia in multiple sclerosis. Glia 53: 24-31.

30. Omari KM, John GR, Sealfon SC, Raine CS (2005) CXC chemokine receptors on human oligodendrocytes: implications for multiple sclerosis. Brain 128: 1003-1015.

31. Padovani-Claudio DA, Liu L, Ransohoff RM, Miller RH (2006) Alterations in the oligodendrocyte lineage, myelin, and white matter in adult mice lacking the chemokine receptor CXCR2. Glia 54:471-483

32. Patani R, Balaratnam M, Vora A, Reynolds R (2007) Remyelination can be extensive in multiple sclerosis despite a long disease course. Neuropathol Appl Neurobiol 33: 277-287.

33. Patrikios P, Stadelmann C, Kutzelnigg A, Rauschka H, Schmidbauer M, Laursen H, Sorensen PS, Bruck W, Lucchinetti C, Lassmann H (2006) Remyelination is extensive in a subset of multiple sclerosis patients. Brain 129: 3165-3172.

34. Paxinos G, Franklin KBJ (2001) The Mouse Brain in Stereotaxic Coordinates. Academic Press, New York.

35. Plant SR, Arnett HA, Ting JP (2005) Astroglial-derived lymphotoxin-alpha exacerbates inflammation and demyelination, but not remyelination. Glia 49: 1-14.

36. Popivanova BK, Koike K, Tonchev AB, Ishida Y, Kondo T, Ogawa S, Mukaida N, Inoue M, Yamashima T (2003) Accumulation of microglial cells expressing ELR motif-positive CXC chemokines and their receptor CXCR2 in monkey hippocampus after ischemia-reperfusion. Brain Res 970: 195-204.

37. Robinson S, Tani M, Strieter RM, Ransohoff RM, Miller RH (1998) The chemokine growth-regulated oncogene-alpha promotes spinal cord oligodendrocyte precursor proliferation. J Neurosci 18: 10457-10463.

38. Scolding N, Franklin R, Stevens S, Heldin CH, Compston A, Newcombe J (1998) Oligodendrocyte progenitors are present in the normal adult human CNS and in the lesions of multiple sclerosis. Brain 121: 2221-2228.

39. Stangel M, Trebst C (2006) Remyelination strategies: new advancements toward a regenerative treatment in multiple sclerosis. Curr Neurol Neurosci Rep 6: 229-235.

40. Stidworthy MF, Genoud S, Li WW, Leone DP, Mantei N, Suter U, Franklin RJ (2004) Notch1 and Jagged1 are expressed after CNS demyelination, but are not a major rate-determining factor during remyelination. Brain 127: 1928-1941.

41. Tsai HH, Frost E, To V, Robinson S, Ffrench-Constant C, Geertman R, Ransohoff RM, Miller RH (2002) The chemokine receptor CXCR2 controls positioning of oligodendrocyte precursors in developing spinal cord by arresting their migration. Cell 110: 373-383.

42. Valles A, Grijpink-Ongering L, de Bree FM, Tuinstra T, Ronken E (2006) Differential regulation of the CXCR2 chemokine network in rat brain trauma: implications for neuroimmune interactions and neuronal survival. Neurobiol Dis 22: 312-322.

43. Zhang Y, Taveggia C, Melendez-Vasquez C, Einheber S, Raine CS, Salzer JL, Brosnan CF, John GR (2006) Interleukin-11 potentiates oligodendrocyte survival and maturation, and myelin formation. J Neurosci 26: 12174-12185.

44. Zhou YX, Flint NC, Murtie JC, Le TQ, Armstrong RC (2006) Retroviral lineage analysis of fibroblast growth factor receptor signaling in FGF2 inhibition of oligodendrocyte progenitor differentiation. Glia 54: 578-590.

Chapter III

Extensive remyelination after chronic toxic demyelination in the central nervous system

Maren Lindner[1,2], Jantje Fokuhl[1], Franziska Linsmeier[1], Corinna Trebst[1], Martin Stangel[1,2*]

[1]Department of Neurology, Medical School Hannover, [2]Center for Systems Neuroscience, Hannover, Germany

in preparation

Abstract

Most multiple sclerosis lesions fail to remyelinate after chronic demyelinating episodes resulting in neurologic disability which is mainly caused by axonal loss. In the current study, chronic demyelination was investigated by using the cuprizone model, a toxic demyelination model. C57BL/6 mice were administered a 0.2 % cuprizone diet up to 16 weeks to induce chronic demyelination. For comparison, another mice group was maintained only for 6 weeks on cuprizone to model acute demyelination. Both groups were analysed regarding the remyelination process after withdrawal of the toxin. The rate of remyelination after chronic demyelination was slower compared to the acute demyelination. Although the number of oligodendrocyte precursor cells was reduced during chronic demyelination extensive remyelination occurred after withdrawal of cuprizone and was nearly complete after 12 weeks. There was only minor but significant axonal damage as judged by APP staining. Axonal damage correlated with macrophage/microglia accumulation. These data suggest that sole demyelination is not sufficient to induce major axonal damage and that even after a prolonged interval of demyelination the natural environment in the CNS is capable to lead to extensive remyelination and thus preventing further damage.

Introduction

Axonal loss is considered an early and persistent event in the progression of MS pathology which correlates with the extent of inflammation (Ferguson et al., 1997; Kuhlmann et al., 2002). Damaged axons are the main reason for neurological deficits in multiple sclerosis patients (Trapp et al., 1999). Since demyelination predisposes axons to additional damage, one of the main functions of myelin is to maintain the integrity of the axons and protect them from subsequent injury. Within demyelinated lesions secondary injury may result from the toxic effects of glutamate, a direct attack of cytotoxic T cells, autoreactive antibodies (Owens, 2003), or from a failure of local neurotrophic support caused by the absence of myelinating oligodendrocytes (Rodriguez, 2003; Bjartmar et al., 2003). Therefore, one avenue of MS research focuses on neuroprotective strategies via enhancement of remyelination in order to prevent axonal damage (Bjartmar and Trapp, 2001).

Induction of toxic demyelination by feeding the copper chelator cuprizone is a widely used model to explore the pathophysiology of remyelination (Matsushima and Morell, 2001). After complete demyelination in the CNS spontaneous remyelination occurs (Hiremath et al., 1998; Lindner et al., 2007). However, the impact of chronic demyelination regarding the repair capacity has not been intensively investigated (Ludwin, 1980; Ludwin, 1994; Mason et al., 2001; Mason et al., 2004; Armstrong et al., 2006). Furthermore, the consequences of chronic demyelination in regard to axon pathology in the absence of severe inflammation are not well understood.

We therefore investigated, whether the pure absence of myelin is sufficient to promote severe axonal damage in C57BL/6 mice. Moreover, we were interested whether the remyelination potential is reduced due to depletion of oligodendrocyte precursor cells after chronic cuprizone exposure.

Materials and Methods

Cuprizone treatment and tissue processing

C57BL/6 mice were obtained from Charles River (Sulzfeld, Germany). All experiments were performed according to the national animal laws and approved by the local government authority. Male mice (8 weeks old) were fed *ad libitum* 0.2% (w/w) cuprizone (bis-cyclohexanone oxaldihydrazone, Sigma-Aldrich Inc., St.Louis, MO) mixed into a ground standard rodent chow. To induce acute demyelination mice were kept on a cuprizone diet for 6 weeks and afterwards maintained on a normal diet for another 6 weeks. Chronic demyelination was induced by feeding cuprizone for 12 weeks, followed by a 12 week recovery phase. In addition, some mice were kept for 14 or 16 week on cuprizone, followed by a 4 week recovery phase. Anaesthetised mice (n = 5 to 6) were perfused with 4% paraformaldehyde (PFA) by cardiac puncture, brains were removed and paraffin embedded.

Histology and Immunohistochemistry

7µm serial paraffin sections between bregma -0.94 and bregma -1.8 (according to mouse atlas by Paxinos and Franklin (Paxinos and Franklin, 2001)) were analysed. Sections were stained for myelin with Luxol- fast blue-periodic acid Schiff base (LFB-PAS). For immunohistochemistry, paraffin embedded sections were de-waxed, rehydrated and microwaved for 5 min in 10 mM citrate buffer (pH 6.0). Sections were quenched with H_2O_2, blocked for 1 h in PBS containing 3% normal goat serum, 0.1% Triton X-100, and then incubated overnight with primary antibody. The following primary antibodies were used: for myelin proteins PLP (mouse IgG, 1:500 Serotec, Düsseldorf, Germany), MBP (mouse IgG, 1:1000 Sternberger Monoclonals Inc.,Berkeley, USA) and MOG (mouse IgG, 1:2 hybridoma supernatant, generous gift by C. Linington), for astrocytes GFAP (mouse IgG, 1:200, Chemicon, Hamphire, UK), for microglia/monocytes Mac-3 (rat IgG, 1:50, BD Pharmingen, Heidelberg, Germany) and the lectin RCA-1 (biotinylated, 1:1000 Vector Laboratories,

Burlingame, UK), for oligodendrocyte precursor cells NG2 (rabbit polyclonal, 1:200, Chemicon, Hamphire, UK). Axonal damage was detected by APP staining (mouse monoclonal IgG, 1:800 Chemicon). After washing, sections were further incubated with biotinylated secondary antibody (Vector Laboratories, Burlingame, UK) for one h, followed by peroxidase-coupled avidin-biotin complex (ABC Kit, Vector Laboratories). Reactivity was visualized with diamino-3,3'benzidine (DAB, Dako Cytomation, Hamburg, Germany).

Extent of de- and remyelination

LFB and myelin protein (PLP, MBP, MOG) stained section were scored in a blinded manner by three independent observers using a scale from 0 (normal myelin) to 3 (complete demyelination) as described previously (Lindner et al., 2007).

Quantification of cells

Immunopositive cells with identified nucleus (counterstaining with hematoxilin) were counted at the midline left and right of the midline within the corpus callosum at least within an area of 0.125 mm^2 using a magnification of 40x (Leica DMLB, Wetzlar, Germany). Counted cells (cells/mm^2) are presented as mean with standard error of the mean (SEM) from 5 to 6 mice for each time point.

Statistical Analysis

To determine significant differences among stages of the de- and remyelination process data were analysed with StatView (Abacus, UK) using one-way analysis of variance (ANOVA) with a post-hoc Tukey's multiple comparison test or linear regression analysis. A p value <0.05 was considered as statistically significant.

Results

Remyelination after chronic demyelination is extensive at a reduced rate

The de- and remyelination process during acute (Fig. 1A) and chronic (Fig. 1B) cuprizone exposure was monitored by scoring of LFB and myelin protein stained sections as described previously (Lindner et al., 2007). Withdrawal of the toxin resulted in spontaneous remyelination, which was almost complete at the end of the recovery phase. Surprisingly, this holds true for both the acute (6 weeks on cuprizone + 6 weeks recovery) as well as the chronic (12 weeks on cuprizone + 12 weeks recovery) demyelination setting. Although remyelination was extensive even after chronic cuprizone treatment, the rate was considerably reduced. In comparison to acute demyelination, the speed of remyelination was reduced approximately by a factor of two. The difference after 6 and 12 weeks of cuprizone exposure was statistically significant in the LFB (Fig. 2A) and MOG (Fig. 2B) scoring. The extension of cuprizone treatment up to 16 weeks did not show a reduction in the remyelination potential compared to the 12 week cuprizone exposure (data not shown). Thus, the potential for extensive remyelination was maintained, but slower after chronic demyelination (12 weeks cuprizone treatment) as compared to short term demyelination (6 weeks cuprizone treatment).

Interestingly, MBP stainings revealed that there was partial remyelination beginning after 4 weeks of cuprizone treatment despite continuous application of cuprizone. This could be observed until week 8 (Fig. 1B). To a lesser degree this was also seen for PLP, but not for MOG, suggesting that this remyelination effort did not yield functional myelin.

The number of oligodendrocyte precursor cells is depleted during chronic demyelination

During acute cuprizone exposure the number of OPC (Fig. 3A) increased in response to demyelination and decreased after 2 weeks on normal diet to baseline level (data not shown), whereas a continued cuprizone exposure lead to a depletion of OPC (Fig. 3B, 4A). The oligodendrocyte density was lowest after 12 weeks of demyelination. The OPC dynamics

were remarkably different after acute and chronic demyelination (Fig. 4B). The progressive loss of NG2+ progenitors after chronic demyelination could only be reversed after 12 weeks on normal diet (Fig. 4A).

Astrogliosis during acute and chronic demyelination is similar

The accumulation of astrocytes in the corpus callosum was first observed after the fourth week of cuprizone application and maintained the same high level until the end of the recovery phase. The number of astrocytes was similar in both experimental settings (data not shown). After a 12 week cuprizone exposure (Fig. 3D) the processes of astrocytes were less intense stained, possibly characterizing a less activated state, compared to the intensely stained processes after week 6 (Fig.3C).

Macrophage/microglia accumulation is persistent during chronic demyelination

Macrophages/microglia were identified by RCA-1 and mac-3 staining. Because both stainings yielded similar results only the data for mac-3 are presented here. Only few macrophages/microglia were observed in the corpus callosum of control mice. During 6 weeks of cuprizone exposure (Fig. 5A) macrophage/microglia accumulation peaked at week 6 (Fig. 3E) followed by a rapid clearance after withdrawal from the diet. When mice were fed cuprizone for 12 weeks (Fig. 3F), macrophage/microglia accumulation peaked at week 6 (Fig. 5B) and then decreased to persist on a lower level as long as cuprizone was administered. During the recovery phase macrophages/microglia still could be detected at a low level until the end of the observation period (Fig. 5B).

Axonal damage is not increased during chronic demyelination

Axonal damage was monitored by APP staining. There were only few APP positive axons. However, the numbers were significantly higher at week 4 and week 6 compared to control

animals (Fig. 6A). Prolongation of the demyelination phase (12 weeks on cuprizone) did not increase the number of APP positive axons (Fig. 6B). In contrast, the number was decreasing after week 6 but significantly elevated compared to control animals until week 10 (Fig. 6B). Most APP positive axons could be observed at week 6 (Fig. 3G), whereas a small amount was seen after 12 weeks on cuprizone (Fig. 3H). Continued cuprizone exposure up to 16 weeks did not result in a different number of APP positive axons compared to 12 weeks of treatment.

Axonal damage correlates with accumulation of macrophages/microglia

Although the axonal damage detected is only minimal the counted number of APP positive axons coincided with the presence of macrophages/microglia. Macrophage/microglia accumulation peaked at week 6 where also numbers of APP positive cells were highest. Regression analysis revealed a strong correlation ($R = 0.973$, $p<0.001$) during the acute de- and remyelination and during chronic de- and remyelination ($R=0.896$, $p<0.001$).

Discussion

In chronic MS lesions remyelination frequently fails despite the presence of premyelinating oligodendrocytes (Chang et al., 2002; Wolswijk, 1997). However, demyelinated axons retain their potential to be myelinated throughout life (Setzu et al., 2004), thus other factors might contribute to remyelination failure, e.g. an unfavourable milieu for oligodendrocyte differentiation. We have therefore investigated the course and extent of chronic de- and remyelination in the cuprizone model.

Here, we showed that extensive remyelination occurs after chronic demyelination despite severe depletion of OPC. Several investigators reported either no remyelination (Mason et al., 2004) or impaired remyelination (Armstrong et al., 2006) after chronic cuprizone treatment. Both studies allowed regeneration only for a short period (maximum of 6 weeks). In contrast, we followed remyelination up to 12 weeks demonstrating that remyelination is slowed down after prolonged demyelination using cuprizone but nevertheless extensive. Furthermore, Armstrong et al. (Armstrong et al., 2006) used MOG immunohistochemistry as a marker for remyelination that is known to be expressed only in the late phase of remyelination in contrast to MBP and PLP that are re-expressed early during remyelination (Lindner et al., 2007). Using theses markers we could demonstrate here that remyelination is initiated early and continues in the following weeks. Interestingly, MBP was partially re-expressed already after 6 weeks of demyelination while the animals were still fed cuprizone, suggesting that remyelination may be initiated while demyelination is still ongoing. However, this myelin seems to be damaged immediately by the continuous application of the toxin since there is no re-expression of the late myelin marker MOG at this time and subtle remyelination is quickly demyelinated. These observations are in line with previous studies using 0.2% cuprizone in C57BL/6 mice (Matsushima and Morell, 2001).

Although the remyelination was extensive after chronic demyelination the rate of the process was impaired. This coincided with a significantly reduced numbers of NG2 positive OPC after chronic demyelination. This suggest that the impaired remyelination may be caused by the depletion of OPC rather than by the age dependency of the remyelination process (Shields et al., 1999; Sim et al., 2002; Zhao et al., 2006).

In our study axonal damage was only mild throughout the whole observation period of chronic demyelination. These results are in contrast to inflammatory experimental models of demyelination like EAE (Onuki et al., 2001) or MS lesions (Ferguson et al., 1997; Kuhlmann et al., 2002) where the numbers of damaged axons was increased by a multitude compared to our results. However, in both EAE and MS, a severe macrophage response coincident with acute axonal damage. Despite the small comparatively axonal damage such a correlation was also observed in our study with a peak of both APP positive axons and mac-3 positive macrophages/microglia after 6 weeks of cuprizone diet. Similar results after a short period of demyelination were also described by Merkler et al. (Merkler et al., 2005), where little or no axonal damage was observed after 6 weeks of cuprizone treatment of young adult mice. An electron microscopic study demonstrated only a change in axon calibre (Mason et al., 2001). However, aged (6-7 months old) mice exhibited a more pronounced axonal damage associated with a higher response of macrophages/microglia and astrocytes (Irvine and Blakemore, 2006). This data suggest that microglia/macrophage accumulation plays a key role in the pathomechanisms leading to axonal damage in the cuprizone model. This further suggest that demyelination on its own has little impact on axonal damage and additional neurotoxic signals are required to induce permanent axonal impairment. In turn this may point to the importance to control the inflammatory reaction in diseases like MS to prevent additional axonal damage.

Acknowledgements

We thank Ilona Cierpka-Leja for excellent technical assistance and Dr. Thomas Skripuletz for helpful comments on the manuscript. This work was supported by internal funds of the MHH (HiLF) and the DFG (SFB 566).

Fig.1A

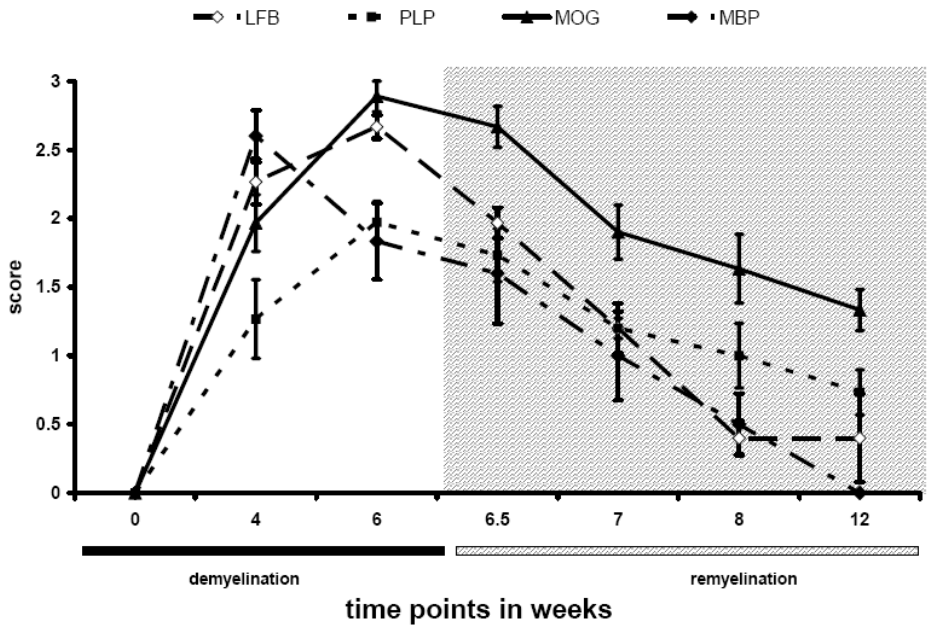

Fig.1B

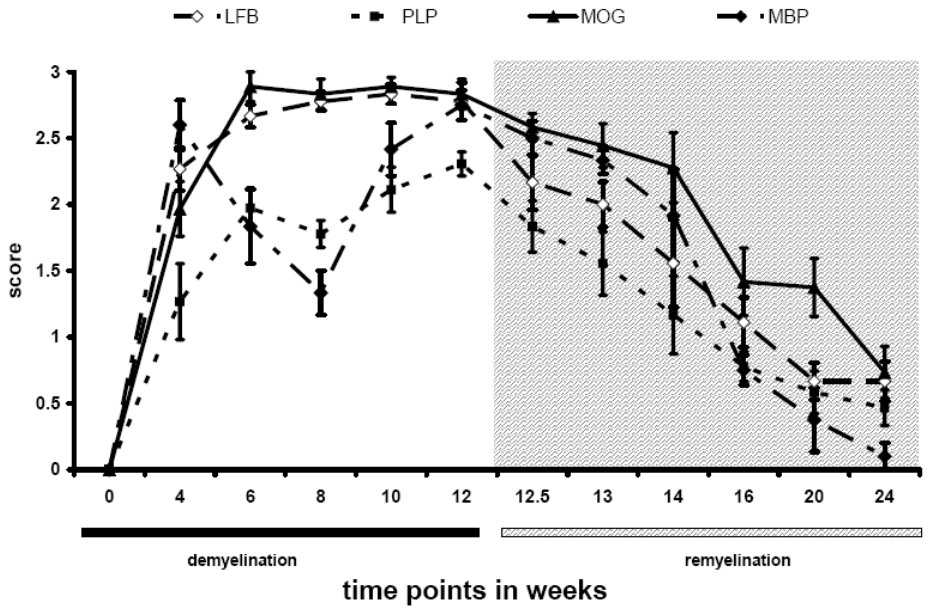

Fig. 1

Course of de- and remyelination using staining for Luxol-fast blue, PLP, MOG and MBP during acute demyelination (**A**) and chronic demyelination (**B**). Acute demyelination was induced by feeding the mice a cuprizone diet for 6 weeks followed by another 6 weeks recovery phase, during chronic demyelination the cuprizone feeding was extended to 12 weeks, recovery phase was also twice as long (12 weeks). Stained sections (n = 5 to 6) were scored by three independent observers. A score of 0 represents normal myelin and a score of 3 complete demyelination. Error bars represent standard error of the mean (SEM).

Fig.2A

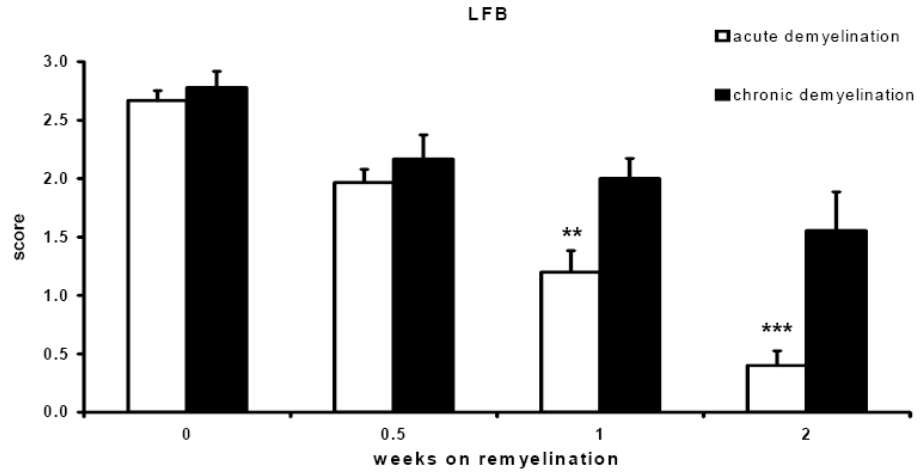

Fig.2B

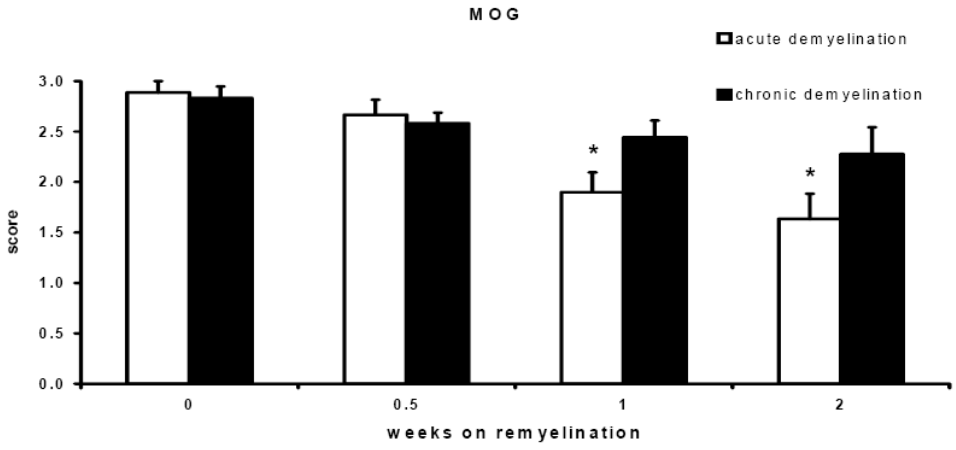

Fig. 2

Comparison of remyelination after acute and chronic demyelination quantified by scoring of LFB (**A**) and MOG (**B**). n = 5 to 6. Error bars represent standard error of the mean (SEM). Statistically significant differences are indicated by asterisk (*p<0.05, **p<0.01, ***p<0.001).

Fig.3

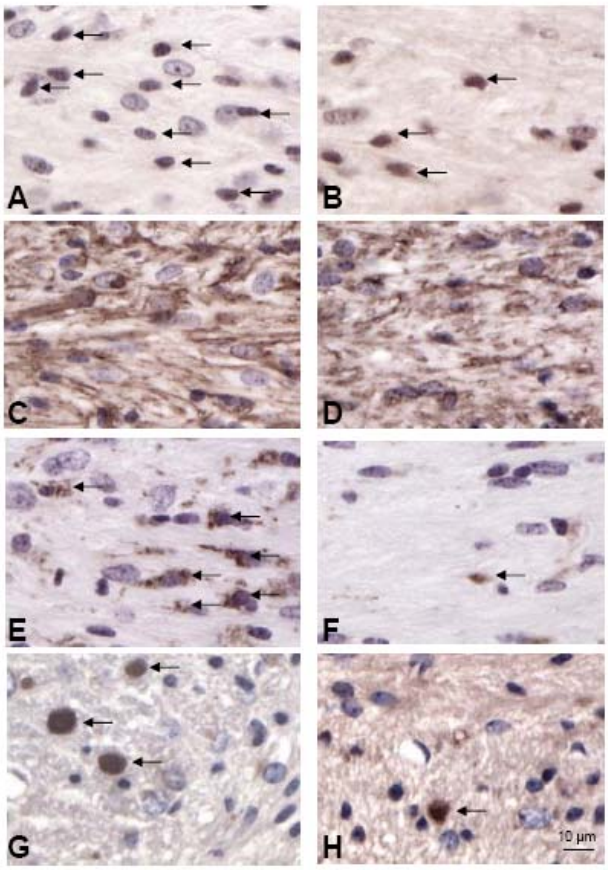

Fig. 3

Comparison of immunohistochemical stainings after 6 (**A, C, E, G**) and 12 weeks (**B, D, F**, **H**) of cuprizone treatment. **A, B** oligodendrocyte precursor cells (NG2; **C, D** Astrogliosis (GFAP staining); **E, F** Microglial accumulation (Mac-3 staining; **G, H** APP positive axons. Bar represents 10µm

Fig.4A

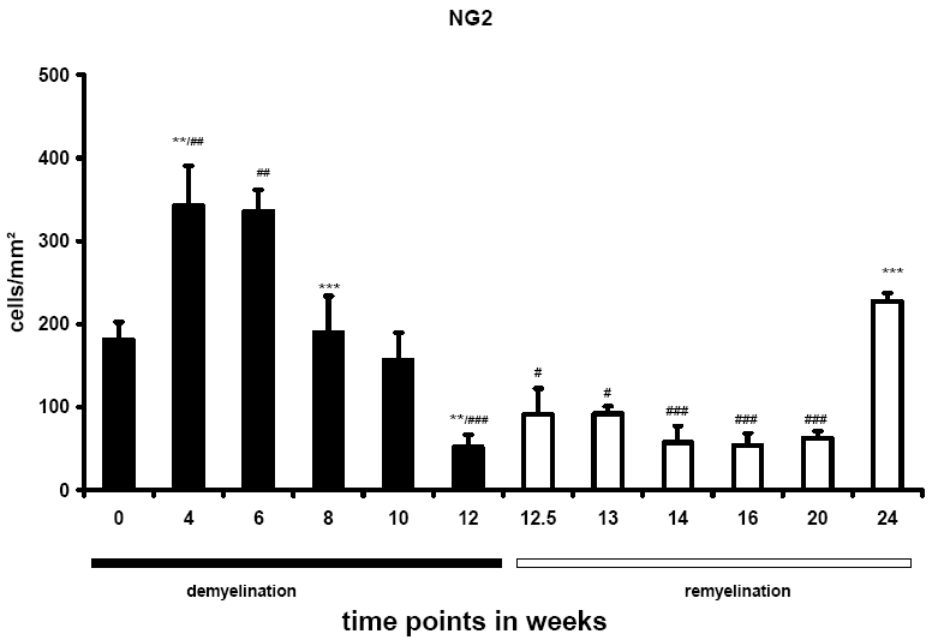

Fig.4B

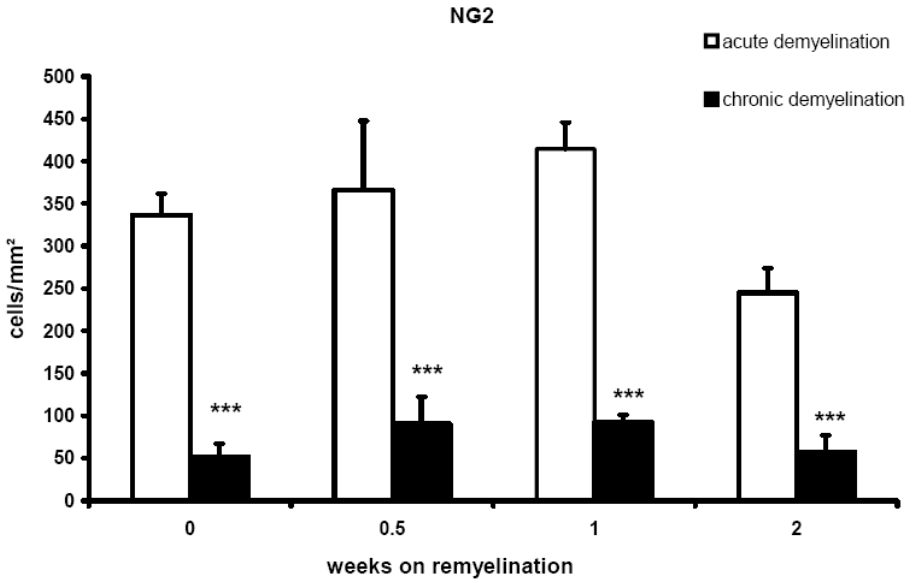

Fig. 4

Quantification of NG2 positive cells during chronic demyelination (**A**) in the corpus callosum. (n = 5 to 6). Error bars represent standard error of the mean (SEM). Statistically significant differences are indicated by asterisk or rhombs (*#p<0.05, **##p<0.01, ***###p<0.001), * vs. previous time point, # vs. control

(**B**) OPC are depleted after chronic demyelination compared to acute demyelination. Error bars represents standard error of the mean (SEM). Significant effects are indicated by asterisk (*p<0.05, **p<0.01, ***p<0.001).

Fig.5A

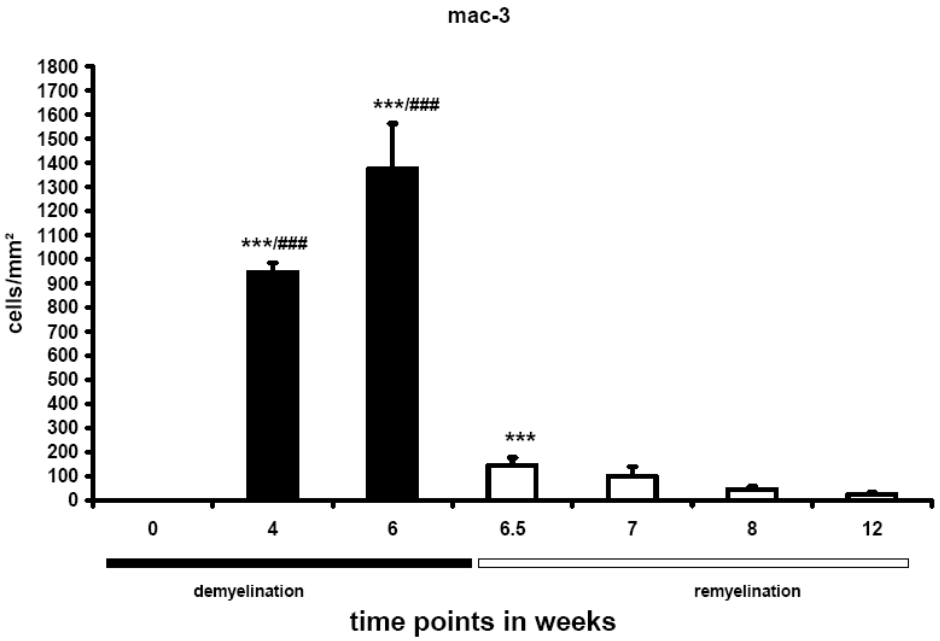

Fig.5B

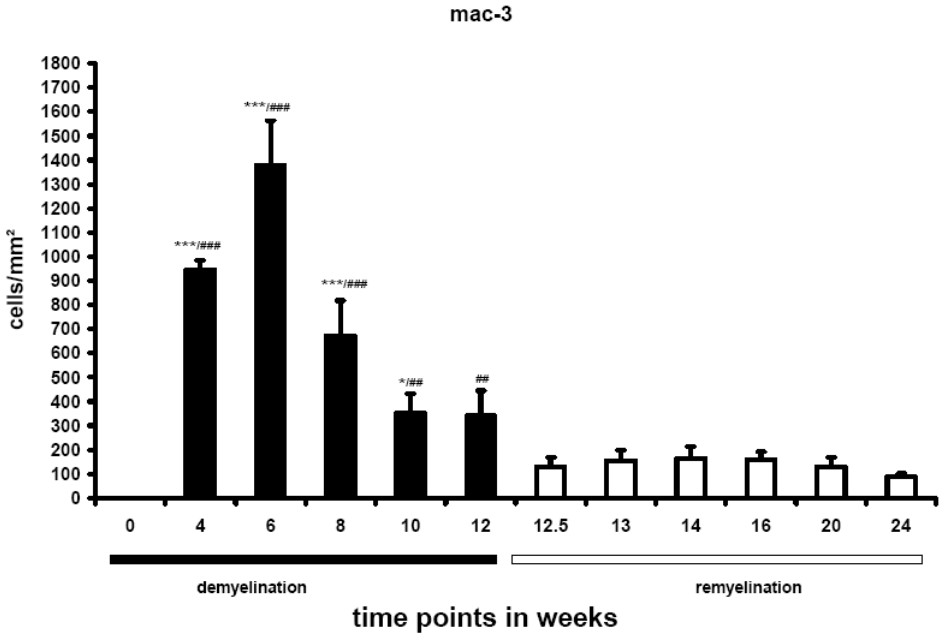

Fig. 5

Quantification of microglia (Mac-3) during acute (**A**) and chronic (**B**) demyelination in the corpus callosum. (n = 5 to 6). Error bars represent standard error of the mean (SEM). Statistically significant differences are indicated by asterisk or rhombs (*#p<0.05, **##p<0.01, ***###p<0.001), * vs. previous time point, # vs. control

Fig.6A

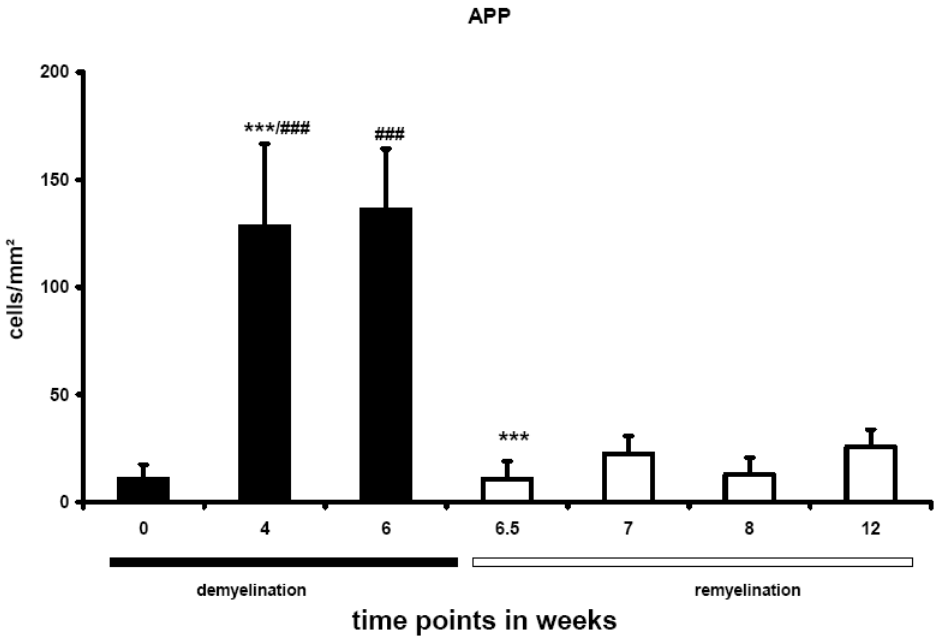

Fig.6B

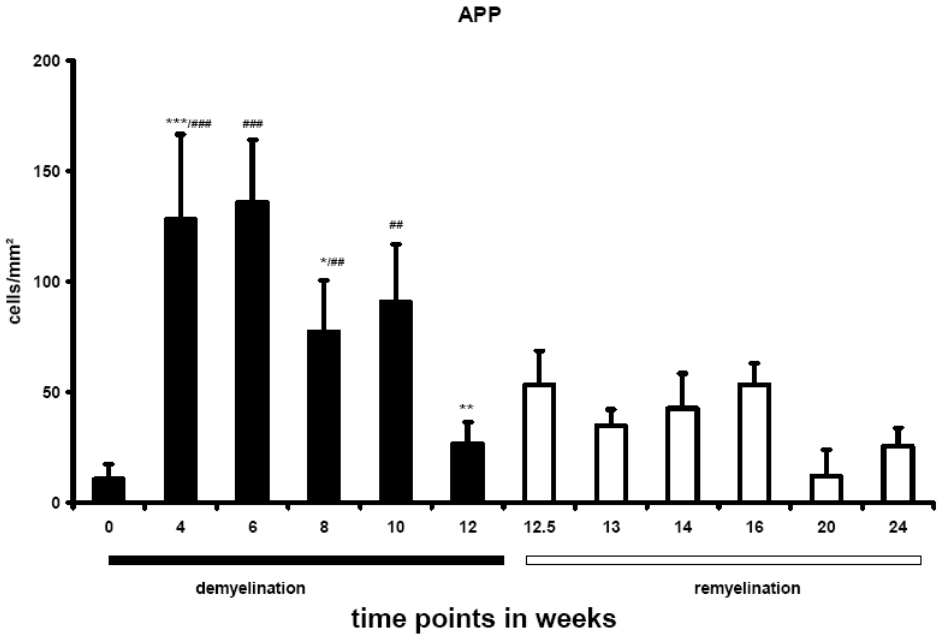

Fig. 6

Quantification of APP positive axons during acute (**A**) and chronic (**B**) demyelination in the corpus callosum. (n = 5 to 6). Error bars represent standard error of the mean (SEM). Statistically significant differences are indicated by asterisk or rhombs (*#p<0.05, **##p<0.01, ***###p<0.001), * vs. previous time point, # vs. control

References

1. Armstrong RC, Le TQ, Flint NC, Vana AC, Zhou YX (2006) Endogenous cell repair of chronic demyelination. J Neuropathol Exp Neurol 65: 245-256.

2. Bjartmar C, Trapp BD (2001) Axonal and neuronal degeneration in multiple sclerosis: mechanisms and functional consequences. Curr Opin Neurol 14: 271-278.

3. Bjartmar C, Wujek JR, Trapp BD (2003) Axonal loss in the pathology of MS: consequences for understanding the progressive phase of the disease. J Neurol Sci 206: 165-171.

4. Chang A, Tourtellotte WW, Rudick R, Trapp BD (2002) Premyelinating oligodendrocytes in chronic lesions of multiple sclerosis. N Engl J Med 346: 165-173.

5. Ferguson B, Matyszak MK, Esiri MM, Perry VH (1997) Axonal damage in acute multiple sclerosis lesions. Brain 120: 393-399.

6. Hiremath MM, Saito Y, Knapp GW, Ting JP, Suzuki K, Matsushima GK (1998) Microglial/macrophage accumulation during cuprizone-induced demyelination in C57BL/6 mice. J Neuroimmunol 92: 38-49.

7. Irvine KA, Blakemore WF (2006) Age increases axon loss associated with primary demyelination in cuprizone-induced demyelination in C57BL/6 mice. J Neuroimmunol 175: 69-76.

8. Kuhlmann T, Lingfeld G, Bitsch A, Schuchardt J, Bruck W (2002) Acute axonal damage in multiple sclerosis is most extensive in early disease stages and decreases over time. Brain 125: 2202-2212.

9. Lindner M, Heine S, Haastert K, Garde N, Fokuhl J, Linsmeier F, Grothe C, Baumgaertner W, Stangel M (2007) Sequential myelin protein expression during remyelination reveals fast and efficient repair after central nervous system demyelination. Neuropathol Appl Neurobiol in press

10. Ludwin SK (1980) Chronic demyelination inhibits remyelination in the central nervous system. An analysis of contributing factors. Lab Invest 43: 382-387.

11. Ludwin SK (1994) Central nervous system remyelination: studies in chronically damaged tissue. Ann Neurol 36 Suppl:S143-5.: S143-S145.

12. Mason JL, Langaman C, Morell P, Suzuki K, Matsushima GK (2001) Episodic demyelination and subsequent remyelination within the murine central nervous system: changes in axonal calibre. Neuropathol Appl Neurobiol 27: 50-58.

13. Mason JL, Toews A, Hostettler JD, Morell P, Suzuki K, Goldman JE, Matsushima GK (2004) Oligodendrocytes and progenitors become progressively depleted within chronically demyelinated lesions. Am J Pathol 164: 1673-1682.

14. Matsushima GK, Morell P (2001) The neurotoxicant, cuprizone, as a model to study demyelination and remyelination in the central nervous system. Brain Pathol 11: 107-116.

15. Merkler D, Boretius S, Stadelmann C, Ernsting T, Michaelis T, Frahm J, Bruck W (2005) Multicontrast MRI of remyelination in the central nervous system. NMR Biomed 18: 395-403.

16. Onuki M, Ayers MM, Bernard CC, Orian JM (2001) Axonal degeneration is an early pathological feature in autoimmune-mediated demyelination in mice. Microsc Res Tech 52: 731-739.

17. Owens T (2003) The enigma of multiple sclerosis: inflammation and neurodegeneration cause heterogeneous dysfunction and damage. Curr Opin Neurol 16: 259-265.

18. Paxinos G, Franklin KBJ (2001) The Mouse Brain in Stereotaxic Coordinates. Academic Press, New York.

19. Rodriguez M (2003) A function of myelin is to protect axons from subsequent injury: implications for deficits in multiple sclerosis. Brain 126: 751-752.

20. Setzu A, Ffrench-Constant C, Franklin RJ (2004) CNS axons retain their competence for myelination throughout life. Glia 45: 307-311.

21. Shields SA, Gilson JM, Blakemore WF, Franklin RJ (1999) Remyelination occurs as extensively but more slowly in old rats compared to young rats following gliotoxin-induced CNS demyelination. Glia 28: 77-83.

22. Sim FJ, Zhao C, Penderis J, Franklin RJ (2002) The age-related decrease in CNS remyelination efficiency is attributable to an impairment of both oligodendrocyte progenitor recruitment and differentiation. J Neurosci 22: 2451-2459.

23. Trapp BD, Ransohoff R, Rudick R (1999) Axonal pathology in multiple sclerosis: relationship to neurologic disability. Curr Opin Neurol 12: 295-302.

24. Wolswijk G (1997) Oligodendrocyte precursor cells in chronic multiple sclerosis lesions. Mult Scler 3: 168-169.

25. Zhao C, Li WW, Franklin RJ (2006) Differences in the early inflammatory responses to toxin-induced demyelination are associated with the age-related decline in CNS remyelination. Neurobiol Aging 27: 1298-1307.

Chapter IV

Cortical demyelination can be induced in mice using the cuprizone model and is strain dependent

Thomas Skripuletz[1*], **Maren Lindner[1*,2]**, Alexandra Kotsiari[1], Niklas Garde[1], Jantje Fokuhl[1], Franziska Linsmeier[1], Corinna Trebst[1], and Martin Stangel[1,2].

[1] Department of Neurology, Medical School of Hannover, Germany, [2] Center for Systems Neuroscience, Hannover, Germany

[*] both authors contributed equally

in preparation

Abstract

The model of toxic demyelination in the CNS using cuprizone is commonly used to explore the pathobiology of remyelination in the corpus callosum. However, in human demylinating diseases like multiple sclerosis recent evidence shows that beside white matter damage there is also a considerable amount of cortical demyelination. We have thus investigated cortical demyelination in the cuprizone model. To induce demyelination, C57BL/6 mice were challenged with 6 weeks of 0.2% cuprizone feeding followed by a 6 week recovery phase with a cuprizone-free diet. Beside the expected demyelination in the corpus callosum the cortical area of young adult C57BL/6 mice was completely demyelinated after 6 weeks of cuprizone feeding. After withdrawl of the cuprizone the cortex underwent complete remyelination similar to the corpus callosum. When mice were fed cuprizone for a prolonged time of 12 weeks, cortical remyelination was significantly delayed. Since strain differences are described we have also investigated the effects of cuprizone on cortical demyelination in balb/cJ mice. Here cortical demyelination was only partial and incomplete. Cortical microglia accumulation was markedly increased in the balb/cJ mice, whereas microglia were absent in C57BL/6 mice. In summary, we found that cuprizone feeding is an excellent model to study cortical de- and remyelination including contributing genetic factors represented by strain differences.

Introduction

Multiple sclerosis (MS) is a chronic inflammatory disease of the central nervous system (CNS), which leads to focal plaques of the CNS white matter and axonal loss (Lucchinetti et al, 2001). However, in recent years studies have shown that lesions also arise within grey matter structures, particularly the cortex (Kidd et al, 1999). Cerebral and cerebellar cortical lesions may be characterized by complete demyelination with relative preservation of neurons, axons and synapses (Kutzelnigg et al, 2007). Cortical demyelination and diffuse white matter damage are particularly prominent in primary and secondary progressive MS, but are rare in the acute or relapsing form (Kutzelnigg et al, 2005). In contrast, classical active inflammatory plaques predominantly occur in patients with acute or relapsing MS, while focal white matter lesions in patients with progressive MS are either inactive or show slow expansion at the edges. Using active sensitization with MOG cortical demyelination could be induced only in certain rat strains, while all analyzed rat strains developed extensive white matter demyelination (Storch et al, 2006).

Although new aspects of underlying pathomechanisms of demyelination in MS are being discovered continuously, the complex pathophysiological interactions still are far from being completely understood. Therefore rodent models like the cuprizone-induced toxic demyelination have become helpful in exploring the underlying mechanisms. However, all models only partly mimic the processes of multiple sclerosis with every model having its advantages and disadvantages. Cuprizone intoxication is a commonly used model to study experimental remyelination, with the corpus callosum and the superior cerebellar peduncles being the most frequently investigated white matter tracts (Matsushima and Morell, 2001, Blakemore, 1974). In this model young adult mice are fed with the copper chelator cuprizone (bis-cyclohexanone oxaldihydrazone), which leads to a reproducible CNS demyelination within weeks (Blakemore, 1973). After removal of the toxin spontaneous remyelination

occurs (Armstrong et al, 2006). However, cortical demyelination has not yet been investigated in this model. Here we describe that cortical demyelination is a prominent feature in this model and characterise the pathological process in detail.

Material and methods

Animals and experiments

C57BL/6 male mice were obtained from Charles River (Sulzfeld, Germany). balb/cJ male mice were purchased from Jackson Labs (Bar Harbor, ME, USA). Animals underwent routine cage maintenance once a week and were microbiologically monitored according to Federation of European Laboratory Animal Science Associations recommendations (Rehbinder et al, 1996). Food and water were available ad libitum. All research and animal care procedures were approved by the Review Board for the Care of Animal Subjects of the district government (Lower Saxony, Germany) and performed according to international guidelines on the use of laboratory animals.

Demyelination was induced by feeding 8-week-old male C57BL/6 mice a diet containing 0.2% cuprizone (bis-cyclohexanone oxaldihydrazone, Sigma-Aldrich Inc., St.Louis, MO, USA) mixed into a ground standard rodent chow. Cuprizone was maintained for 6 weeks, thereafter mice were put on a normal chow for another 6 weeks. At different time points (0=control, 4, 6, 6.5, 7, 8, and 12 weeks), aiming a group size of six, animals were perfused with 4% paraformaldehyde (PFA) in phosphate buffer via left cardiac ventricle as previously described (Lindner et al, *in press*). The brains were removed, postfixed in 4% PFA and paraffin embedded. For light microscopy, 7 µm serial paraffin sections were cut and dried at 37°C overnight.

For chronic demyelination the cuprizone diet was maintained for 12 weeks thereafter mice were put on a normal chow for another 12 weeks. Animals were ivestigated at different time points (0=control, 4, 6, 8, 10, 12, 12.5, 13, 14, 16, 20, 24) aiming a group size of six.

To explore strain dependency further experiments using 8-week-old balb/cJ mice were performed. Demyelination was induced by feeding 0,2% cuprizone. Aiming a group size of five different time-points (0, 3, 6, 7, 8, 12) were investigated.

Histology and Immunohistochemistry

Histology and immunohistochemistry were performed as previously described (Lindner et al, *in press*). Briefly, 7µm serial paraffin sections between bregma -0.94 and bregma -1.8 (according to mouse atlas by Paxinos and Franklin (2001)) were analyzed. Sections were stained for myelin with Luxol-fast blue periodic acid-Schiff base (LFB-PAS). For immunohistochemistry, paraffin embedded sections were de-waxed, rehydrated and microwaved for 5 min in 10 mM citrate buffer (pH 6.0). Sections were quenched with H_2O_2, blocked for 1 h in PBS containing 3% normal goat serum, 0.1% Triton X-100, and then incubated overnight with primary antibody. The following primary antibodies were used: for myelin proteins PLP (mouse IgG, Serotec, Düsseldorf, Germany) and MBP (mouse IgG, Sternberger Monoclonals Inc., Berkeley, USA), for microglia mac-3 (rat IgG, BD Pharmingen, Heidelberg, Germany), for astrocytes GFAP (mouse IgG, Chemic, UK). After washing, sections were further incubated with biotinylated secondary antibody (Vector Laboratories, Burlingame, UK) for one h, followed by peroxidase-coupled avidin-biotin complex (ABC Kit, Vector Laboratories). Reactivity was visualized with diamino-3,3'benzidine (DAB, Dako Cytomation, Hamburg, Germany).

Determination of cortical de- and remyelination

For cortical de- and remyelination myelin protein-stained sections for PLP and MBP were scored by three blinded observer using a scale from 0 (complete demyelination) to 4 (normal myelin). Using a light microscope all sections were scanned for the complete cortex (figure 1C). Camera images of a part of the cortex for each score-degree were drawn (figure 1D-I).

In addition, cortical myelin was always compared to the most frequently studied corpus callosum myelin. For this, stained sections were scored in a blinded manner by three observer

and graded on a scale from 0 (complete demyelination) to 3 (normal myelin) as described previously (Lindner et al, *in press*).

Statistical analysis

Statistical analysis was performed using one-way analysis of variance (ANOVA) with the factor “time/week” followed by the Fisher-PLSD-test for post hoc comparison if appropriate. All data are given as arithmetic means ± standard error of the mean (SEM). *P* values of the different ANOVAs are given in RESULTS, while group comparisons derived from post hoc analysis are provided in the figures. In the latter case, significant effects are indicated by asterisks or rhombs ($*^{\#}P < 0.05$; $**^{\#\#}P < 0.01$; $***^{\#\#\#}P < 0.001$).

Results

Cortical de- and remyelination is prominent in the cuprizone model

To investigate whether mice show cortical myelin damage after cuprizone treatment, brain sections were immunohistochemically stained for the myelin proteins PLP and MBP. A marked demyelination after exposure of C57BL/6 mice to 0.2% cuprizone was evident as determined by a significant loss of myelin already after 4 weeks compared to control animals (Fig. 2A, $p<0.001$). After 6 weeks of cuprizone treatment no cortical myelin was detectable. After removal of cuprizone after 6 weeks a time dependent increase of remyelination was observed. Normal myelin structures were seen already 6 weeks after withdrawal of the toxin in all animals. Since there was no significant difference between the analyzed PLP and MBP stained sections, only PLP results are shown. The sensitivity of the LFB staining was not sufficient to uncover cortical myelination.

Cortical remyelination depends on the duration of cuprizone treatment

When C57BL/6 mice were maintained on a cuprizone diet beyond 6 weeks, cortical demyelination persisted (Fig. 2B). First signs of remyelination could be observed after 8 and 10 weeks of cuprizone treatment, which were not significant. Significant remyelination in the cortex began only after withdrawal of the toxin at week 12. Thereupon a time dependent increase of remyelination was seen ($p<0.001$). Cortical remyelination was significantly delayed in the chronic 12 week cuprizone feeding (Fig. 3, $p<0.001$) as compared to the acute demyelination for 6 weeks. Time to reappearance of normal myelin was approximately twice as long.

De- and remyelination in the cortex is similar to changes in the corpus callosum

To further characterize the model for cortical de- and remyelination we compared for each timepoint the changes of the cortical myelin structure with the well characterized processes in the corpus callosum. As seen in figure 4 in the acute demyelination model (A) as well as in the chronic demyelination model (B) complete cortical demyelination can be induced (acute model: lowest value at week 6: score 0 ± 0, chronic model: lowest value at week 12: score 0 ± 0). This demyelination was even more prominent than in the corpus callosum where a severe but not complete demyelination was observed. Nonetheless, the time course of de- and remyelination was nearly identical in both short- and long-term demyelination.

Extent of cortical demyelination in mice is strain dependent

Since strain dependency could play a role in cortical demyelination we performed further investigations in balb/cJ mice, which were fed with 0.2% cuprizone for 6 weeks. Control balb/cJ animals showed a similar myelin structure before cuprizone treatment compared to C57BL/6 mice (figure 1J-L). Loss of myelin was not seen before 6 weeks of cuprizone feeding. Furthermore there was only incomplete demyelination when compared with C57BL/6 mice. A band-like residual myelin structure remained in the middle of the cortex (figure 1K). The time to build up a normal myelin structure was similar to the results of C57BL/6 mice in the acute model (data not shown).

Cortical microglia response in de- and remyelination is strain dependent

Accumulation of microglia/monocytes was investigated by mac-3 staining in both mice strains. In contrast to the corpus callosum only a few microglia were seen in the cortex after 6 weeks of cuprizone diet in the C57BL/6 strain (figure 1M-O). At all other time points of investigation microglia were absent and only sporadically seen in the cortex. In the balb/cJ strain cortical microglia accumulation began after 3 weeks of cuprizone diet and peaked in a pronounced manner after 6 weeks of cuprizone (figure 1P-S). After withdrawal of the toxin

the number of cortical microglia decreased and microglia were only sporadically seen at week 12.

Cortical astrocyte response during de- and remyelination

There was a marked increase in GFAP positive astrocytes in the cortex already after 4 weeks of cuprizone treatment in C57BL/6 mice (figure 5A-B). Furthermore the bodies of the astrocytes were hypertrophic and the processes were thick. The decrease of astrogliosis in the cortex began slowly after withdrawal of the toxin. Thereupon a time dependent decline was seen, but astrocytes were still present at week 16 in the chronic demyelination model and at week 8 in the acute demyelination model (data not shown). At the last investigated time points (week 24 in the chronic model, week 12 in the acute model) only few astrocytes were still seen in the cortex. Since there was no significant difference between the mice strains, only the brain sections of C57BL/6 mice are shown.

Discussion

Here we show for the first time that feeding of the neurotoxicant cuprizone represents an appropriate model to study cortical de- and remyelination processes. In this new model of cortical damage the C57BL/6 mouse strain provides a well-suited genetic background.

Although it has long been recognised that de- and remyelination can occur in the corpus callosum and in the superior cerebellar peduncles (Blakemore 1974, Matsushima and Morell, 2001) the extent and effectiveness of cortical damage has not been determined to date. The present study has shown that in young adult male C57BL/6 mice both demyelination as well as the consecutive remyelination in the cortex are almost complete. Exposure of mice to dietary cuprizone for 6 weeks induced loss of cortical myelin relative to controls. When animals were allowed to recover on a regular diet, the myelin loss was completely compensated within another 6 weeks. If exposure to cuprizone was extended to 12 weeks, demyelination persisted. Only after removal of cuprizone from the diet remyelination started. Interestingly the time for recovery was delayed by a factor of apptoximately two compared to the acute demyelination.

When we compared the changes of cortical myelin to those in the corpus callosum, de- and remyelination processes always occurred in the same temporal pattern. Surprisingly, demyelination in the cortex was complete after week 6 and more pronounced compared to the changes in the corpus callosum. This may suggest that cortical myelin changes are even more sensitive in the cuprizone model.

Since the LFB staining offers excellent results investigating myelin changes in the corpus callosum after cuprizone treatment it is a widely and the most often used myelin staining method. However, its sensitivity is not sufficient to uncover cortical myelination which may explain why cortical changes were not described to date using this method. Therefore for analysis of cortical de- and remyelination immunohistochemical staining methods should be preferred.

Additionally in contrast to C57BL/6 mice, balb/cJ mice challenged with 0.2% cuprizone exhibited less cortical demyelination. It is well known that the extent of cuprizone induced damage to corpus callosum myelin largely depends on the cuprizone dose, the age and the strain of mice (Stidworthy et al, 2003, Hiremath et al, 1998). This seems to hold true also for the cortical changes described here.

Microglia were absent or only sporadically seen in the cortex of C57BL/6 mice. As previously described most of the microglia were seen in the area of the corpus callosum (Hiremath et al, 1998). In contrast, balb/cJ mice showed a marked cortical microglia recruitment after cuprizone treatment which was associated with a less pronounced cortical demyelination. These observations indicate different pathomechanisms between the investigated mice strains leading to different cortical myelin damage possibly via different microglia responses. Storch et al (2006) could demonstrate that the incidence and extent of cortical demyelination in rat EAE is regulated by genetic influences from the MHC I and II isotypes and alleles. Cortical demyelination could be induced only in certain rat strains, while all analyzed rat strains developed extensive white matter demyelination. These rat strains showed minimal macrophage recruitment in active lesions. Since the C57BL/6 mice and the balb/cJ mice have different MHC haplotypes it may be an influencing factor for the strain dependent demyelination after cuprizone treatment.

Analysis of astrocytes showed a marked increase in cortical astrogliosis after cuprizone treatment in both mice strains. After withdrawal of the toxin a time dependent slow decrease of the astrogliosis occured. The role of this astrocytosis is currently not clear. It can only be speculated if this represents an unspecific activation or if these astrocytes actively interfere with the de- or remyelination. Further experiments need to clarify a possible role of astrocytes in the cortical myelination changes after cuprizone diet.

In recent years, the presence of cortical lesions has come into the focus of MS research (Kutzelnigg et al, 2005, Kidd et al, 1999, Bo et al, 2003a). The pathologic mechanisms

leading to cortical demyelination and the functional clinical consequences of the cortical lesions have not yet been completely understood. Cortical lesions may lead to sensory and motor deficits, as well as to cognitive impairment, which is found in MS patients (Rao et al, 1991). Kutzelnigg et al (2005) could show that cortical demyelination and diffuse white matter damage are prominent in primary and secondary progressive MS, but are sparse in the acute or relapsing form. Active cortical lesions in progressive MS show only very mild lymphocytic infiltrates in the lesion parenchyma (Kutzelnigg et al, 2005, Bo et al, 2003b). The lack of efficacy of immunosuppressive or immunomodulatory therapies in patients with progressive MS could be indicative that neurodegeneration in such patients occurs independently of inflammation (Noseworthy et al, 2000, Leary et al, 2003). Since the pathomechanisms of cortical demyelination and possible repair processes have not yet been studied in detail the cuprizone model may help to understand the molecular mechanisms in the future and serve as an complementary model to fill gaps not represented by other animal models of cortical demyelination (Merkler et al, 2006).

The cuprizone model offers the advantage of consistent, anatomically reproducible and well detectable de- and remyelination processes, which are easy to score (Blakemore 1974, Mason et al, 2001, Lindner et al, in press). In contrast to the model of autoimmune encephalomyelitis (Fabis et al, 2007) in the cuprizone model there is no breakdown of the blood-brain barrier (Bakker and Ludwin, 1987, Kondo et al, 1987). This may explain why T cells are rare during cuprizone induced demyelination (Matsushima and Morell, 2001). In this context, the cuprizone model may help to investigate events, which are more directly related to de- and remyelination mechanisms bypassing possible interferences of the immune system.

In conclusion, the present work demonstrates that cuprizone feeding is an excellent model to study cortical pathology during de- and remyelination. Further experiments can be designed to clarify the pathophysiology and the functional consequences of cortical demyelination.

Acknowledgments

The excellent technical assistance of I. Cierpka-Leja is gratefully acknowledged. This work has been supported by German Research Foundation Grant SFB566 (project A11) and internal funds of the MHH (HiLF).

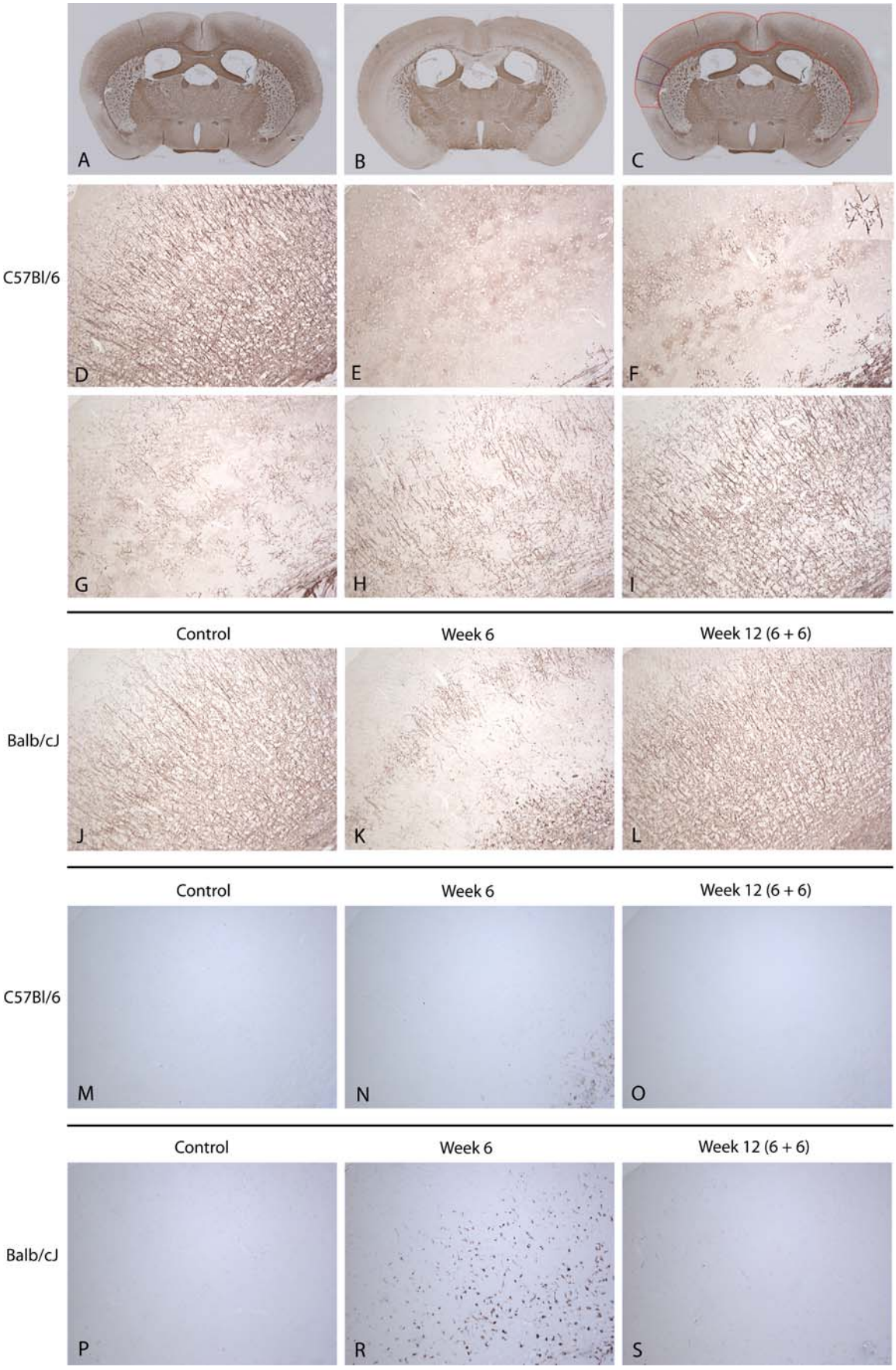
A
B
C
C57Bl/6
D
E
F
G
H
I
Control
Week 6
Week 12 (6 + 6)
Balb/cJ
J
K
L
Control
Week 6
Week 12 (6 + 6)
C57Bl/6
M
N
O
Control
Week 6
Week 12 (6 + 6)
Balb/cJ
P
R
S

Figure 1

Fig. 1. For determination of cortical de- and remyelination brain sections were immunohistochemically stained for PLP (A-I C57BL/6 mice, J-L balb/cJ mice). In figure A brains of control animals are shown, while figure B represents complete demyelination after 6 weeks of cuprizone diet. All brain sections were scanned for the complete cortex which is marked with a red line in figure C. The blue line marked area of the cortex in figure C represents the demonstrated cortex-area of which camera images were drawn.

For each score-degree images were drawn of the brain sections of C57BL/6 mice (D-I). In figure D a normal myelination-structure in the cerebral cortex of control animals is shown (score 4), while figure E represents complete cortical demyelination (score 0). First indicators of beginning remyelination are several separately "radiating" myelin-structures as shown in figure F (score 1). In the course of further remyelination a beginning crosslinking between the several myelination areas could be identified (figure G; score 2). In figure H there is almost complete remyelination in the cortex but several demyelinated areas indicate a continued cortical pathology (score 3). Figure I represents complete remyelination after demyelination.

In figures J-L brain sections of balb/cJ mice which were immunohistochemically stained for PLP are shown. Mice were fed cuprizone for 6 weeks followed by 6 weeks of a cuprizone-free diet. In figure J a normal myelination pattern in the cerebral cortex is shown. As seen in figure K after 6 weeks of cuprizone feeding a band-like residual myelin pattern remained in the middle of the cortex showing that cortical demyelination was still incomplete. After 6 weeks of cuprizone-free diet cortical myelination looked complete again (L).

For determination of cortical microglia/monocytes brain sections of control animals (M C57BL/6 mice, P balb/cJ mice), animals after 6 weeks of cuprizone treatment (N C57BL/6 mice, R balb/cJ mice), and animals after 6 weeks of cuprizone free-diet (O C57BL/6 mice, S balb/cJ mice) are shown. As seen in figure N after 6 weeks cuprizone diet in C57BL/6 mice microglia were seen in the area of the corpus callosum, but were almost absent in the cortex. In contrast a marked microglia accumulation occurs in balb/cJ mice after 6 weeks of cuprizone treatment.

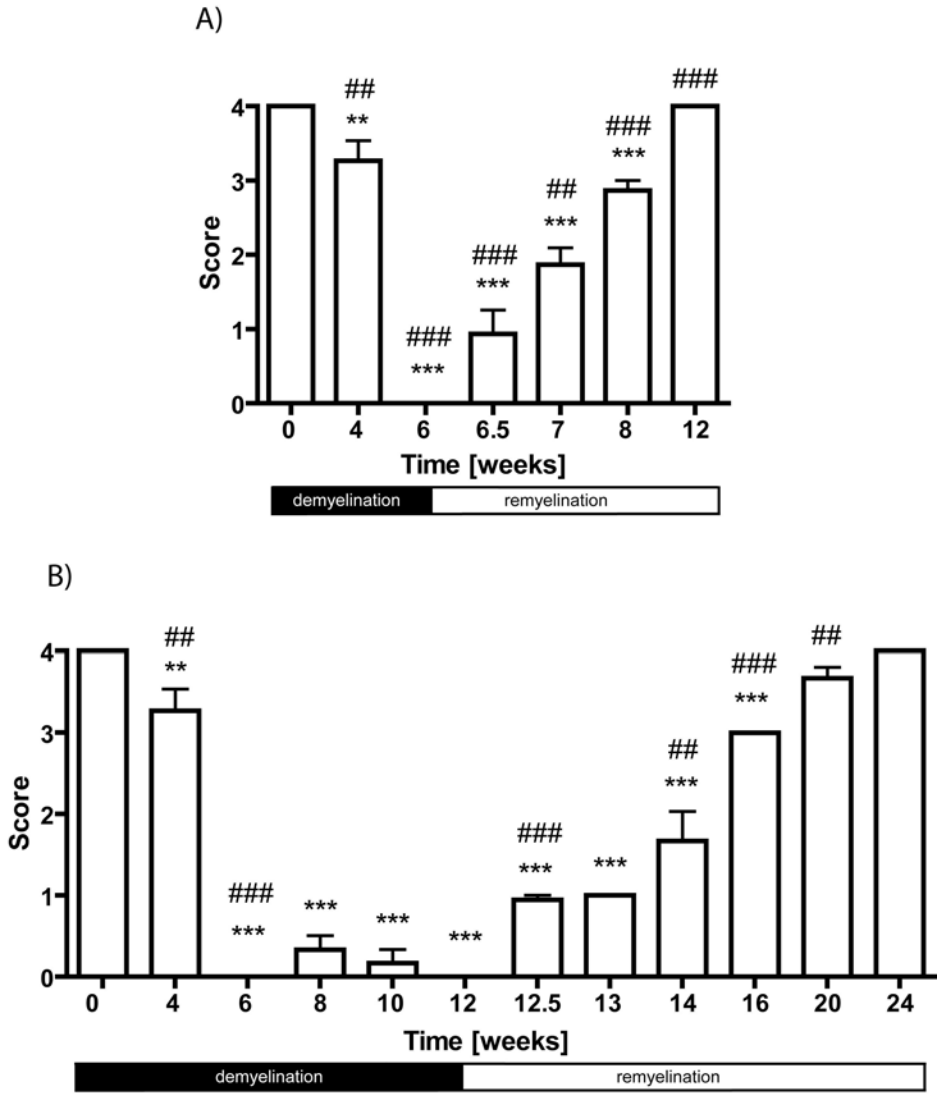

Figure 2

Fig. 2. Time course of acute (A) and chronic (B) cortical de- and remyelination induced by 0.2% cuprizone in C57BL/6 mice. The extent of cortical de- and remyelination was assessed by scoring PLP stained sections. A score of 4 represents complete myelination, while a score of 0 represents complete demyelination (compare to fig. 1). Significant effects vs. controls are indicated by asteriks $*p < 0.05$, $**p < 0.01$, and $***p < 0.001$, significant effects vs. the preceding timepoint are indicated by rhombs $\#p < 0.05$, $\#\#p < 0.01$, and $\#\#\#p < 0.001$.

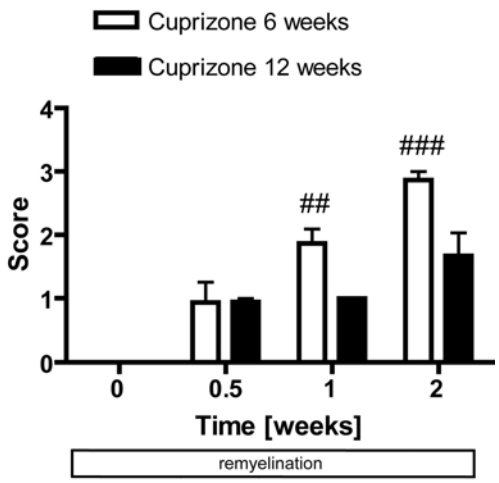

Figure 3

Fig. 3. Comparison of the time course of acute (6 weeks cuprizone) and chronic (12 weeks cuprizone) cortical remyelination. Timepoint 0 demonstrates the end of cuprizone treatment and the onset of cuprizone-free diet. Complete myelination is represented by a score of 4, while complete demyelination is represented by a score of 0. Significant post hoc effects between groups (acute vs. chronic) are indicated by rhombs #$p < 0.05$, ##$p < 0.01$, and ###$p < 0.001$.

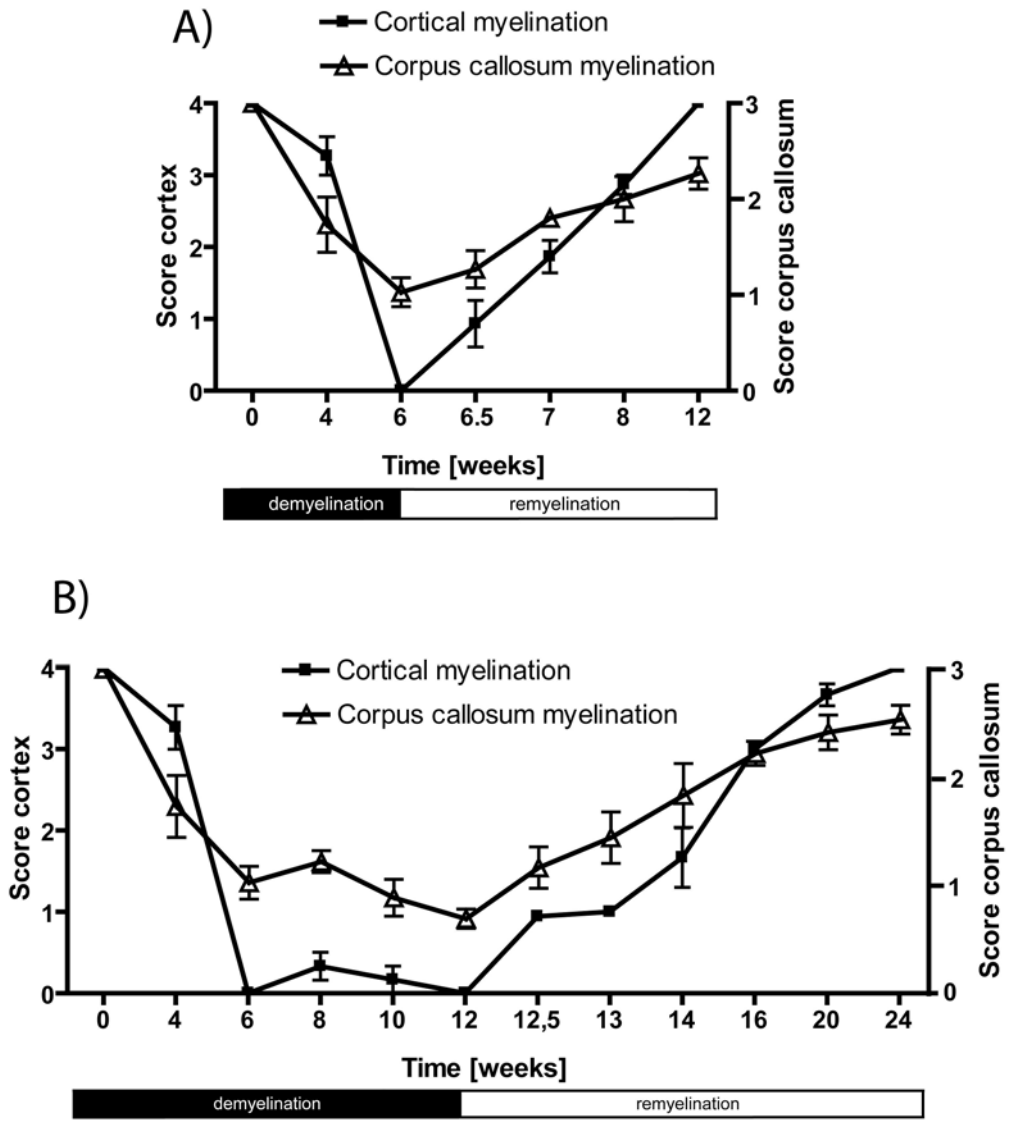

Figure 4

Fig. 4. Comparison of the course of de- and remyelination in the cortex as well as in the more commonly investigated corpus callosum in the acute (A) and chronic (B) cuprizone model. For cortical myelination changes: a score of 4 represents complete myelination, while a score of 0 represents complete demyelination. For myelination changes in the corpus callosum: a score of 3 represents complete myelination, while a score of 0 represents complete demyelination.

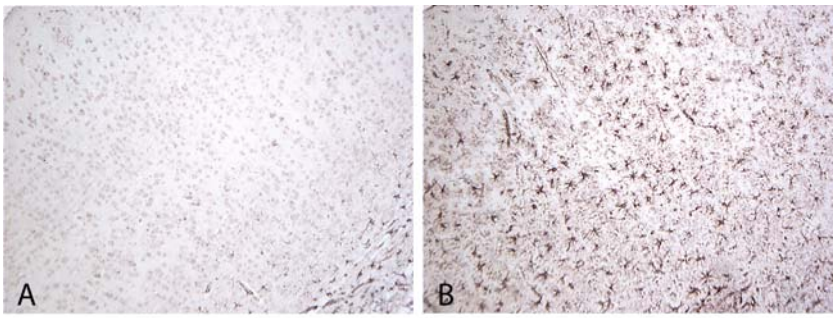

Figure 5

Fig. 5. Brain sections of C57BL/6 mice which were immunohistochemically stained for GFAP. In figure A only some occasional GFAP positive astrocytes are seen in the cortex. As seen in figure B after 4 weeks of cuprizone feeding a marked cortical astrogliosis with hypertrophied bodies and thick processes were seen.

References

Armstrong RC, Le TQ, Flint NC, Vana AC, Zhou YX: Endogenous Cell Repair of Chronic Demyelination. J Neuropathol Exp Neurol 2006, 65:245–256

Bakker DA, Ludwin SK: Blood-brain barrier permeability during Cuprizone-induced demyelination. Implications for the pathogenesis of immune-mediated demyelinating diseases. J Neurol Sci 1987, 78:125-37

Blakemore WF: Remyelination of the superior cerebellar peduncle in the mouse following demyelination induced by feeding cuprizone. J Neurol Sci 1973, 20:73-83

Blakemore WF**:** Remyelination of the superior cerebellar peduncle in old mice following demyelination induced by cuprizone. J Neurol Sci 1974, 22:121-126

Bo L, Vedeler CA, Nyland HI, Trapp BD, Mork SJ: Subpial demyelination in the cerebral cortex of multiple sclerosis patients. J Neuropathol Exp Neurol 2003a, 62:723-32

Bo L, Vedeler CA, Nyland H, Trapp BD, Mork SJ: Intracortical multiple sclerosis lesions are not associated with increased lymphocyte infiltration. Mult Scler 2003b, 9:323-31

Fabis MJ, Scott GS, Kean RB, Koprowski H, Hooper DC: Loss of blood-brain barrier integrity in the spinal cord is common to experimental allergic encephalomyelitis in knockout mouse models. Proc Natl Acad Sci U S A 2007, 104:5656-61

Hiremath MM, Saito Y, Knapp GW, Ting JP, Suzuki K, Matsushima GK: Microglial/macrophage accumulation during cuprizone-induced demyelination in C57BL/6 mice. J Neuroimmunol 1998, 92:38-49

Kidd D, Barkhof F, McConnell R, Algra PR, Allen IV, Revesz T: Cortical lesions in multiple sclerosis. Brain 1999, 122:17-26

Kondo A, Nakano T, Suzuki K: Blood-brain barrier permeability to horseradish peroxidase in twitcher and cuprizone-intoxicated mice. Brain Res 1987, 425:186-90

Kutzelnigg A, Lucchinetti CF, Stadelmann C, Bruck W, Rauschka H, Bergmann M, Schmidbauer M, Parisi JE, Lassmann H: Cortical demyelination and diffuse white matter injury in multiple sclerosis. Brain 2005, 128:2705-12

Kutzelnigg A, Faber-Rod JC, Bauer J, Lucchinetti CF, Sorensen PS, Laursen H, Stadelmann C, Bruck W, Rauschka H, Schmidbauer M, Lassmann H: Widespread demyelination in the cerebellar cortex in multiple sclerosis. Brain Pathol 2007, 17:38-44

Leary SM, Miller DH, Stevenson VL, Brex PA, Chard DT, Thompson AJ: Interferon beta-1a in primary progressive MS: an exploratory, randomized, controlled trial. Neurology 2003, 60:44-51

Lindner M, Heine S, Haastert K, Garde N, Fokuhl J, Linsmeier F, Grothe C, Baumgaertner, Stangel M: Sequential myelin protein expression during remyelination reveals fast and efficient repair after central nervous system demyelination. Neuropathol Appl Neurobiol, *in press*

Lucchinetti C, Bruck W, Noseworthy J: Multiple sclerosis: recent developments in neuropathology, pathogenesis, magnetic resonance imaging studies and treatment. Curr Opin Neurol 2001, 14:259-69

Mason JL, Langaman C, Morell P, Suzuki K, Matsushima GK: Episodic demyelination and subsequent remyelination within the murine central nervous system: changes in axonal calibre Neuropathol Appl Neurobiol 2001, 27:50-8

Matsushima GK, Morell P: The neurotoxicant, cuprizone, as a model to study demyelination and remyelination in the central nervous system. Brain Pathol 2001, 11:107-116

Merkler D, Ernsting T, Kerschensteiner M, Bruck W, Stadelmann C: A new focal EAE model of cortical demyelination: multiple sclerosis-like lesions with rapid resolution of inflammation and extensive remyelination. Brain 2006, 129:972-83

Noseworthy JH, Lucchinetti C, Rodriguez M, Weinshenker BG: Multiple sclerosis. N Engl J Med 2000, 343:938-52

Paxinos G, Franklin KBJ: The Mouse Brain in Stereotaxic Coordinates. Academic Press, New York, 2001

Rao SM, Leo GJ, Bernardin L, Unverzagt F: Cognitive dysfunction in multiple sclerosis. I. Frequency, patterns, and prediction. Neurology 1991, 41:685-91

Rehbinder C, Baneux P, Forbes D, van Herck H, Nicklas W, Rugaya Z, Winkler G: FELASA recommendations for the health monitoring of mouse, rat, hamster, gerbil, guinea pig and rabbit experimental units. Report of the Federation of European Laboratory Animal Science Associations(FELASA) Working Group on Animal Health accepted by the FELASA Board of Management, November 1995. Lab Anim 1996, 30:193–208

Stidworthy MF, Genoud S, Suter U, Mantei N, Franklin RJ: Quantifying the early stages of remyelination following cuprizone-induced demyelination. Brain Pathol 2003, 13:329-39

Storch MK, Bauer J, Linington C, Olsson T, Weissert R, Lassmann H: Cortical demyelination can be modeled in specific rat models of autoimmune encephalomyelitis and is major histocompatability complex (MHC) haplotype-related. J Neuropathol Exp Neurol 2006, 65:1137-42

Chapter V

Epileptic seizures and hippocampal damage after cuprizone-induced demyelination in mice

Katrin Hoffmann[1], **Maren Lindner[2]**, Ina Gröticke, Martin Stangel[2,3], Wolfgang Löscher[1,3]

[1]Department of Pharmacology, Toxicology, and Pharmacy, University of Veterinary Medicine, Hannover, Germany, [2] Department of Neurology, Medical School Hannover, Germany, and [3]Center for Systems Neuroscience, Hannover, Germany

Experimental Neurology *submitted*

Abstract

Epileptic seizures are known to occur in different animal models of demyelination and have also been described in demyelinating diseases of the central nervous system (CNS) such as multiple sclerosis. The exact mechanisms why myelin deficiency can lead to seizures are not known, but may involve axonal pathology and resultant alterations in neuronal excitability. The cause of seizures occurring in rodent demyelination models is unknown. In the present study, we used EEG/video monitoring to record seizures occurring during chronic demyelination of C57BL/6 mice fed for 12 weeks with 0.2% cuprizone. Furthermore, in the search for a morphological correlate of the seizures, the hippocampal formation was histologically examined. Epileptiform spikes resembling interictal spikes known from chronic epilepsy were recorded in all cuprizone-treated mice, but not in controls. Generalized tonic-clonic seizures were observed in most animals upon stress-inducing stimuli, whereas a spontaneous seizure was only observed in 1 of 15 mice evaluated in this regard. Apart from the known demyelination of the corpus callosum, massive demyelination was found in the hippocampal formation. This was associated with neuronal alterations, including a loss of neurons in the hilus of the dentate gyrus. In view of the role of the dentate gyrus in epileptogenesis, such hilus damage could be causally involved in the paroxysmal alterations observed after prolonged treatment with cuprizone. The present data suggest a potential role of the hippocampal formation for seizures occurring as a consequence of neuronal damage secondary to CNS demyelination.

Introduction

Epileptic seizures occur in demyelinating diseases of the central nervous system (CNS) such as multiple sclerosis (MS) with a prevalence of about three to six times that in the general adult population, indicating an association between MS and seizures by an unknown mechanism (Poser and Brinar, 2003). Axonal damage early in the course of MS (Trapp et al., 1998; Kuhlmann et al., 2002) and cortical lesions in progressive forms of MS (Kutzelnigg et al., 2005) may contribute to the development of epileptic seizures, but their frequency would suggest an even higher prevalence in MS patients.

Epileptic seizures are long known to occur in different mouse and rat mutants with myelin diseases (Seyfried et al., 1986; Rosenbluth, 1990; Griffiths, 1996; Bradl et al., 1999; Bloom et al., 2002) and in the cuprizone model of toxic demyelination (Kesterson and Carlton, 1970). However, to our knowledge, the type(s), frequency, and potential progression of these seizures have not been characterized.

In recent years, demyelination of the corpus callosum by the copper chelator cuprizone has gained acceptance as a mouse model for the study of de- and re-myelination in the CNS (Matsushima and Morell, 2001). Feeding cuprizone to young adult mice leads to a reproducible demyelination of the corpus callosum and the superior cerebellar peduncle within weeks (Blakemore, 1973) with nearly complete remyelination after withdrawal of the cuprizone from the diet (Ludwin, 1980). Although the exact mechanisms why the cuprizone-induced copper deficit primarily affects oligodendroglia are not yet known, disturbance of energy metabolism is assumed to be the major cause of demyelination (Matsushima and Morell, 2001).

The extent of remyelination is largely dependent on the cuprizone dose and the mouse strain used. Early work established and investigated the cuprizone model in Swiss mice (Carlton, 1967; Blakemore, 1972; Ludwin, 1980), while newer studies focus on C57BL/6 mice (Hiremath et al., 1998). While demyelination is usually induced by 6 weeks of cuprizone

feeding, it is possible to study chronic demyelination by feeding C57BL/6 mice a dose of 0.2 % cuprizone in the diet for 12 weeks (Mason et al., 2001; Mason et al., 2004).

The occurrence of seizures in the cuprizone model has only been described in Swiss mice treated with high doses of cuprizone (0.3% and above) in the diet (Kesterson and Carlton, 1970 and 1972). In the present study, we describe and characterize epileptic seizures occurring during chronic demyelination of C57BL/6 mice fed with 0.2% cuprizone for 12 weeks. In the search for a morphological correlate of the seizures, the hippocampal formation was histologically examined.

Materials and Methods

Cuprizone treatment

Starting at 8 weeks of age, male C57BL/6 mice (Charles River Laboratories, Sulzfeld, Germany) were fed *ad libitum* 0.2% (w/w) cuprizone (Sigma-Aldrich Inc., St.Louis, MO) milled into mouse chow for 6-12 weeks to induce chronic demyelination. Thereafter, in one experiment, remyelination was allowed to proceed for 5 weeks. Group size was 7-15 mice. Control mice were maintained on a normal pellet chow. All behavioral alterations observed in the mice were noted. Lethal rate was less than 4%. Mice were housed under controlled conditions (ambient temperature 24-25°C, humidity 50-60%, lights on from 6:00 am to 6:00 pm). All experiments were done in compliance with the European Communities Council Directive of 24 November 1986 (86/609/EEC). All efforts were made to minimize animal suffering and to reduce the number of animals used.

Implantation of EEG electrodes and monitoring of seizures

This was essentially done as described by us previously (Altrock et al., 2003). In short, for electrode implantation, mice were anesthetized with chloral hydrate (500 mg/kg i.p.) and additionally treated with the opioid analgesic buprenorphine (0.1 mg/kg). The animals were placed into a stereotaxic frame according to the method of Paxinos and Franklin (2001). The skull surface was exposed and two small stainless steel screw electrodes of 1.6 mm diameter were screwed into the skull above the parietal cortices under sterile conditions. The stereotaxic coordinates relative to bregma according to the atlas of Paxinos and Franklin (2001) were: lateral 2 mm; posterior 2 mm. A third screw was placed 1 mm lateral and 1 mm anterior relative to bregma and served as indifferent reference-electrode. To form the screw electrodes, a 0.1-mm Teflon-insulated stainless steel wire with a standard microelectronic

connector was soldered to the head of the screws. The electrode assembly was combined to form a female connector and was anchored to the skull with dental acrylic cement. After surgery, the animals were allowed to recover for a period of 1 week.

Monitoring of the spontaneous seizures was performed by a combined video- and EEG-detection system. For the EEG-recording, mice were connected via a flexible cable to an 8-channel amplifier (CyberAmp, Axon Instruments Inc., Foster City, CA) which was connected to an analogue-digital converter (PowerLab/800s, ADInstruments Ltd., Hastings, East Sussex, UK). The data were recorded and analyzed with the Chart4 for windows software (ADInstruments Ltd., Hastings, East Sussex, UK). The sampling rate was 200 Hz. A high pass filter for 0.1 Hz and a low pass filter of 60 Hz was used. Simultaneously to the EEG-recording, the mice were videomonitored with light-sensitive black-white cameras (CCD-Kamera-Modul; Conrad Elektronik, Hannover, Germany). For detection of spontaneous seizures, the EEG-recordings were visually analyzed for characteristic paroxysmal (epileptiform) activity. To evaluate the behavioral correlation to paroxysmal activity in the EEG, the corresponding video-recording was viewed.

In a first, preliminary experiment, one group of 7 animals that had been treated with cuprizone for 12 weeks and 4 untreated controls were monitored with video-recordings for 18 h (12 h during the dark period, 6 h during the light period). Simultaneously, 4 of these cuprizone-treated mice and the 4 untreated controls were monitored with EEG-recordings throughout the 18 h. Based on the data from this preliminary experiment (see Results), another group of 8 cuprizone-treated animals was monitored with video- and EEG-recordings for 9 days, 24 hours a day. Recordings started on the day of termination of a 12-week period of treatment with cuprizone. The last 3 days of the 9 days of video- and EEG-recordings, the animals were fed with 0.2% cuprizone-diet ad libitum to reveal potential acute effects of the treatment. For comparison, one group of 8 untreated control-animals was monitored consecutively for 9 days. Animals were housed during recordings under controlled conditions (ambient temperature 24-

25°C, humidity 50-60%, lights on from 6:00 am to 6:00 pm); video recordings during the dark phase were carried out using infrared light.

In addition to video/EEG monitoring, the normal behavior of the mice was observed by an experienced investigator in the absence or presence of various stress-inducing stimuli known to precipitate seizures in susceptible rodents, such as handling, audiogenic stimuli, or visual stimuli.

Histology and immunohistochemistry

Five groups of mice were used for histology and immunohistochemistry. Group 1: controls (n = 6); group 2: mice (n = 6) that were treated for 6 weeks with cuprizone and were immediately killed at termination of treatment; group 3: mice (n = 5) that were treated for 12 weeks with cuprizone and were immediately killed at termination of treatment; group 4: mice (n = 5) that were treated for 12 weeks with cuprizone, followed by seizure monitoring in the absence of cuprizone treatment, and then killed 5 weeks after termination of the 12-week cuprizone treatment period; and group 5: one mouse that was treated in the same way as group 4, but exhibited frequent spontaneous generalized tonic-clonic seizures associated by paroxysmal alterations in the EEG (see Results).

Animals were deeply anesthetized and perfused with 4% paraformaldehyde (PFA) in phosphate buffer by cardiac puncture via the left ventricle. Brains were removed and postfixed in 4% PFA and paraffin embedded. Four sections of 7 µm per animal (bregma -1.7, -1.94, -2.18, -2.46 according to mouse atlas by Paxinos and Franklin [2001]) were stained with hematoxylin and eosin (H&E) or 1% thionin at pH 4.0 for 20 min.

For immunohistochemistry, paraffin sections were de-waxed, rehydrated, and microwaved for 5 min in 10 mM (pH 6.0) citrate buffer. Sections were quenched with H_2O_2, blocked for 1 h in phosphate-buffered saline containing 3% normal goat serum, 0.1% Triton X-100, and then incubated overnight with primary antibody for proteolipid protein (PLP; 1:500; Serotec,

Düsseldorf, Germany), the major myelin protein of the CNS. After washing, sections were further incubated with biotinylated secondary antibody (Vector Lab, Burlingame, UK) for one hour, followed by peroxidase-coupled avidin-biotin complex (ABC Kit, Vector Lab). Reactivity was visualized with diamino-3,3'benzidine (DAB; Dako Cytomation, Hamburg, Germany), nuclei were counterstained with hematoxylin.

PLP-stained sections were visually examined for demyelination in the corpus callosum, hippocampus, and adjacent areas. H&E and thionin-stained sections were visually examined for neuronal damage in the hippocampus. In addition, polymorphic neurons (i.e., mossy cells and interneurons) were counted in the dentate hilus of the hippocampal formation. Counts involved only cells larger than 8 µm, smaller ones being considered as glial cells. Apart from size, neurons were clearly identifiable on morphological grounds. Neuronal loss was quantified in the hilus of the right hemispere in 3 adjacent sections (-1.7, -1.94 and -2.18 mm according to bregma). The hilus was defined as the inner border of the granule cell layer and two straight lines connecting the tips of the granule cell layer and the proximal end of the CA3c region. The area of each hilus counted was measured with the KS400 software (Carl Zeiss, Germany). In addition to calculating average numbers of neurons in the hilus, neuronal densities (neurons per unit area) were calculated. The investigator was blinded to the treatment of the respective animal. The significance of differences between groups was calculated by one-way analysis of variance (ANOVA), followed by the Dunnett's test. A $P<0.05$ was considered significant. Counting of hilar neurons was repeated, including measuring the area and diameter of all cells that were considered neurons. Furthermore, for comparison, cell counts were performed in a group of 8 mice that were killed one week after a status epilepticus (SE) induced by pilocarpine. For induction of SE, pilocarpine was repeatedly administered at 100 mg/kg i.p. every 20 min until induction of a self-sustaining SE with continuous seizure activity. SE was terminated after 90 min by diazepam (10 mg/kg i.p.). In order to avoid peripheral cholinergic effects, methylscopolamine (1 mg/kg) was

administered 30 min before the first application of pilocarpine. In a separate group of pilocarpine-treated mice that was not killed one week after pilocarpine, the cortical EEG was recorded for comparison with cuprizone-treated mice.

Additional sections of cuprizone- and pilocarpine-treated mice were stained by Fluoro-Jade C, a sensitive and specific fluorescent marker of neuronal degeneration (Schmued et al., 2005). Fluoro-Jade C is highly resistant to fading and is compatible with virtually all histological processing and staining protocols, including paraffin-embedded tissue sections (Schmued et al., 2005). For staining with Fluoro-Jade C, sections were deparaffinized through two 10 min changes of xylene and then rehydrated through a graded ethanol series. Once in distilled water, the sections were transferred to 0.06% potassium permanganate solution for 10 min. Following a 1-2 min water rinse, the slides were then transferred to a 0.0001% solution of Fluoro-Jade C (Chemicon International Inc.; Hamshire, UK) dissolved in 0.1% acetic acid as described by Schmued et al. (2005). The slides were then rinsed through three changes of distilled water for 1 min per change. Excess water was drained onto a paper towel, and then the slides were air dried over night. The dried slides were cleared in xylene for at least 1 min and then coverslipped with DPX (Fluka; Seelze, Germany).

Results

Behavioral observations during the demyelination and remyelination periods

Body weight of cuprizone treated mice was reduced by 30% as compared to control animals (data not shown). During the toxin treatment, mice exhibited roughed fur, reduced reaction velocity and some balance disturbance becoming prominent at around 6 weeks of cuprizone treatment.

Starting after 9 weeks of cuprizone treatment, we frequently observed seizures that persisted throughout the demyelination and the following remyelination period of 5 weeks during feeding with normal diet. These seizures were observed in nearly all treated mice when the cage was opened or when mice were lifted by their tail. Seizures lasted 5 to 10 sec, with tonic-clonic movement of the limbs, loss of balance, and facial myoclonus. No spontaneous occurrence of seizures, i.e., in the absence of handling or other disturbances, was observed.

Continuous video/EEG monitoring of seizures

In order to characterize the epileptic seizures in more detail and determine whether cuprizone-treated mice exhibit seizures also spontaneously, i.e., in the absence of handling or other disturbances, one group of 7 animals that had been treated with cuprizone for 12 weeks and 4 untreated controls were monitored with video- or video- and EEG-recordings for 18 h (see Methods section for detailed description). No spontaneous seizures were observed during EEG/video recording in the absence of any disturbing stimuli, but all EEG-monitored cuprizone-treated mice exhibited short but frequent spike discharges in the EEG (Fig. 1C), which were not observed in controls (Fig, 1A). When switching on the light in the observation room, one cuprizone-treated mouse exhibited a generalized tonic-clonic seizure (resembling the seizures observed before in the absence of EEG recordings) that was not associated by any

EEG alterations.

These preliminary findings prompted us to perform an experiment in mice with a longer period of EEG/video recording. In this experiment, 8 cuprizone-treated mice and 8 controls with cortical electrodes were continuously video/EEG monitored for 24 h/day over 9 consecutive days. The monitoring was started immediately after termination of treatment with cuprizone for 12 weeks.

Spontaneous seizures were only recorded in one of eight cuprizone-treated mice (12.5%). These seizures were characterized by discharges with high-amplitude in the EEG (Fig. 1B), which were sometimes associated with generalized tonic-clonic seizures and loss of righting reflexes. The paroxysmal alterations in the EEG had a duration of 2-10 sec and occurred one to four times per hour. They were recorded both during the light and dark periods.

All of the cuprizone-treated mice exhibited short but frequent spike discharges in the EEG (Fig. 1C), which were not associated with any obvious behavioral abnormalties. Such discharges, resembling interictal spikes, were never observed in normal mice (Fig. 1A). For direct comparison with the cuprizone-treated mice, we recorded the cortical EEG of mice about 4 months after a pilocarpine-induced SE. As shown in Fig. 1E, we observed interictal spikes after pilocarpine that were indistinguishable from the paroxysmal EEG alterations observed in cuprizone-treated mice. In pilocarpine-treated mice, these interictal spikes were observed before the first spontaneous seizures as well as in between spontaneous recurrent seizures.

In all cuprizone-treated mice, clinical seizures could be induced by different types of startle-inducing stimulations, including handling, opening of the cage lid, or flashes of light during the period of EEG/video monitoring. These seizures were generalized tonic-clonic with loss of righting reflexes and had a duration of 5-10 sec. However, these seizures were not associated with any obvious paroxysmal alterations in the cortical EEG (Fig. 1D).

Following 12 weeks of treatment with cuprizone, the different types of seizures described

above were both observed in the absence and presence of treatment with cuprizone. In other words, these seizures could be observed with the same frequency and characteristics during the 6 days of treatment-free recordings and subsequently during the 3 days with cuprizone-treament (for details see Methods).

Histology

Immunostaining for PLP confirmed that prolonged treatment with cuprizone led to a marked demyelination in the corpus callosum (Fig. 2b,c). Following termination of 12 weeks of treatment with cuprizone, remyelination was observed after 5 weeks of treatment with cuprizone-free diet in those mice that had been used for the video/EEG recordings, i.e., groups 4 and 5 (Fig. 2d).

Unexpectedly, marked demyelination was also observed in the hippocampal formation. After 6 weeks of cuprizone-treatment, the dorsal hippocampal formation was nearly free of PLP-positive structures, which was especially remarkable in contrast to the intensely-stained adjacent tissue like the fimbria of the hippocampus and the thalamic formation (Fig. 3b). The clear-cut myelin-positive structures of the stratum lacunosum of the molecular layer in the hippocampal formation as seen in control animals (Fig. 3c) were absent in cuprizone-treated mice (Fig. 3d). Similarly, lack of myelin staining was observed in the inner molecular layer, i.e., the mossy cell termination zone, of cuprizone-treated mice (Fig. 3d,f, Fig. 4d,g,e,h). Furthermore demyelination was especially prominent in layers around the pyramidal cells of the CA2-region (Fig. 3g,h) and in the polymorphic layer of the dentate gyrus (Fig. 3e,f). After 12 weeks of treatment with cuprizone (Fig. 4d-f), the loss of myelin in the dorsal hippocampal formation was as extensive as after 6 weeks of treatment. After both 6 and 12 weeks of treatment, marked demyelination was also observed in the ventral hippocampal formation (not shown). Similar to the corpus callosum, partial remyelination was observed in the hippocampus after 5 weeks following a 12-week period of treatment with cuprizone (Fig. 4g-

i).

The demyelination in the hippocampus was associated with neuronal alterations. Thus, a high incidence of “dark neurons”, i.e., neurons having a dark blue color of the perikaryal and dendritic cytoplasm with the H&E stain, was observed in the CA1 (Fig. 5e,g) and CA3 pyramidal cell layers (not shown), in the granular cell layer of the dentate gyrus (Fig. 5f,h) and in neurons of the hilus of the dentate gyrus (Fig.5f,h) of cuprizone-treated mice. Such dark neurons were observed in all mice after 12 weeks of cuprizone treatment (Fig. 5e-h), but not in any of the controls (Fig. 5a,b), which were processed together with the cuprizone-treated mice, or any animal of group 2, i.e., after 6 weeks of treatment with cuprizone (Fig. 5c,d). The number of dark neurons was higher in group 4 (Fig. 5g,h; 5 weeks after termination of 12 weeks treatment with cuprizone) than in group 3 (Fig. 5e,f; directly after 12 weeks of treatment with cuprizone), indicating that a presumed pathological process progressed in the absence of cuprizone.

In order to obtain unequivocal evidence of neurodegeneration, we used the fluorescent marker Fluoro-Jade C, which is extremely specific for degenerating neurons (Schmued et al., 2005). As shown in Fig. 6, no staining was seen in controls (Fig. 6a,b), whereas Fluoro-Jade stained neurons were observed in the dentate granule cell layer of group 3 (Fig. 6d) and in the granule cell layer and CA1 pyramidal cell layer of group 4 (Fig. 6e,f). Examination of various other brain regions indicated that intense Fluoro-Jade staining was unique to the hippocampal formation of cuprizone-treated mice, with only sporadic staining of single neurons in cortex and hypothalamic regions (not illustrated). For comparison, we also stained brain sections of mice that were killed one week after 90 min of SE induced by pilocarpine. As shown in Fig. 6g,h, Fluoro-Jade staining was similar to that seen in cuprizone-treated mice of group 4, with labelled cells in the dentate granule cell layer and CA1.

In neither cuprizone-treated nor pilocarpine-treated mice, Fluoro-Jade C stained neurons in the dentate hilus, although such hilus neurons are known to be particularly sensitive to

pilocarpine-induced SE. Therefore, we counted the number and density of neurons in the hilus of the different groups (Fig. 7). The hilus area was not affected by treatment with cuprizone or pilocarpine (Fig. 7A). Furthermore, no loss of neurons was observed after 6 or 12 weeks of cuprizone treatment, i.e., in groups 2 and 3 (Fig. 7B). However, both density (neurons per unit area) and total number of neurons in the hilus were significantly reduced in group 4, i.e., 5 weeks after 12 weeks treatment with cuprizone (Fig. 7B,C). The lowest density and number of hilus neurons was observed in group 5, i.e., the animal with frequent spontaneous tonic-clonic seizures after cuprizone. A similar extent of neuronal loss was also observed after pilocarpine-induced SE (Fig. 7B,C).

In order to correct for potential changes in cell size that could artifactually lead to decreased cell counts without any change in underlying cell number, we repeated the cell counts performed in the hilus of cuprizone-treated mice at high magnification and measured the area and diameter of all cells that were clearly identifiable as neurons on morphological grounds. Average cell area was 188 ± 14 μm^2 (mean ± SD) and cell diameter calculated via cell area was 15.4 ± 0.6 µm (mean ± SD) without any significant difference between controls or cuprizone-treated mice. The results of cell counting in the hilus (not illustrated) confirmed the results of the first counting shown in Fig. 7.

Apart from these neuronal changes in the hippocampal formation, marked dilatation of ventricles leading to deformations of the hippocampal formation was observed after 12 weeks of treatment with cuprizone (Fig. 8). A comparable dilatation of ventricles was also observed in chronic epileptic mice several weeks after pilocarpine-induced SE (not illustrated).

Discussion

To our knowledge, this is the first study using video/EEG recordings to evaluate in detail the occurrence and characteristics of seizures in mice chronically demyelinated by the copper chelator cuprizone. Following 12 weeks of treatment with 0.2% cuprizone, which was associated with severe demyelination in the corpus callosum as previously described (Mason et al., 2001), all mice examined with EEG recordings (n = 12) exhibited frequent epileptiform discharges, resembling interictal spikes known from patients with partial epilepsy (Staley et al., 2005). These short discharges were not associated with any behavioral alterations. Interictal spikes are periodic, brief bursts of neuronal activity that are observed in the electroencephalogram of patients and rodents with acquired epilepsy and are widely accepted diagnostically as a sign of epilepsy (Staley et al., 2005). They are sustained by synchronous paroxysmal membrane depolarization generated by assemblies of hyperexcitable neurons (de Curtis and Avanzini, 2001). In animal models of acquired epilepsy, interictal spikes appear before the first spontaneous seizures and in the interictal period between spontaneous recurrent seizures, and such spikes are sufficient to induce long-term changes in synaptic connections between neurons (Staley et al., 2005). It is widely believed that interictal spiking sets a condition that preludes to the onset of an ictal discharge (Staley et al., 2005). In line with this hypothesis, overt generalized tonic-clonic seizures could be precipitated in almost all cuprizone-treated mice by stress- or startle-inducing sensory stimuli, resembling seizure precipitation in mouse models of reflex epilepsy in which seizures are precipitated by sensory stimuli (Löscher, 1984; Naquet and Valin, 1998; Löscher, 1999). However, in cuprizone-treated mice, such reflex seizures were not associated with paroxysmal EEG alterations in cortical EEG recordings. Furthermore, such reflex seizures were only observed after at least 9 weeks of treatment with 0.2% cuprizone. In humans, startle-induced seizures are reflex seizures precipitated by a sudden, surprising stimulus, usually auditory (Xue and Ritaccio,

2006). Similar to the findings with cortical EEG electrodes in cuprizone-treated mice, startle-induced seizures are not always associated with clear paroxysmal alterations in the scalp EEG (Mothersill et al., 2000). For further evaluation of whether reflex seizures in cuprizone-treated mice are associated with paroxysmal EEG alterations, we plan to perform depth recordings from subcortical areas, including the hippocampus, at a higher sampling rate. In contrast to the high incidence of reflex seizures in cuprizone-treated mice, spontaneous seizures were only observed in one of 15 mice (6.6%) after 12 weeks of treatment with cuprizone. These generalized tonic-clonic seizures were associated with paroxysmal alterations in the cortical EEG and could thus be clearly differentiated from the startle-induced reflex seizures.

Because in recent years, cuprizone intoxication has generally been considered to be largely oligodendrocyte specific, cuprizone is widely used as a model of de- and remyelination in the CNS (Matsushima and Morell, 2001). The massive demyelination with spontaneous remyelination particularly in the corpus callosum renders this model particularly useful to study the consequences of demyelination and the mechanisms of remyelination as a model for human diseases like MS (Matsushima and Morell, 2001; Skundric, 2005). As mentioned in the Introduction, similar to the cuprizone model, seizures also occur in other rodent models of CNS demyelination, including models of experimental allergic encephalomyelitis (EAE), and have also been described in human MS. MS is a chronic disabling disease of the CNS, pathologically characterized by the presence of areas of demyelination, T-cell predominant perivascular inflammation in the brain white matter, axonal damage, and astrogliosis (Waxman, 2000; Frohman et al., 2006). The corpus callosum is a region that is especially sensitive to demyelination in MS, possibly due to its intimate neuroanatomic relationship to the lateral ventricular roofs and its relationship to small penetrating vessels (Waxman, 2000). The clinical symptoms of MS are numerous and can include epileptic seizures, sometimes as the first observable symptom (Waxman, 2000). Based on some 30 clinical studies of adult patients who had epileptic seizures and MS, the prevalence of epileptic seizures in patients

with MS is 2.3% on average (range 0.5-10.8) and thus about three to six times that in the general adult population (Poser and Brinar, 2003). This suggests a causal relationship between MS and seizures by a mechanism that is not fully understood but may involve cortical and subcortical lesions, including lesions in the hippocampus, that provide a potential anatomic basis for the occurrence of MS-induced seizures (Trapp et al., 1998; Kuhlmann et al., 2002; Poser and Brinar, 2003; Kutzelnigg et al., 2005; Vercellino et al., 2005). All types of seizures have been reported in association with MS, but partial onset secondary generalized tonic-clonic seizures appear to be particularly frequent (Poser and Brinar, 2003). Interestingly, although rare, temporal lobe epilepsy (TLE) with complex partial seizures and interictal spikes in the EEG may occur as a unique manifestation of MS (Gambardella et al., 2003).

Almost all of the numerous previous studies on the cuprizone model concentrated on the corpus callosum because of is known role in CNS diseases such as MS (cf., Matsushima and Morell, 2001). Because of the important role of the hippocampal formation in epilepsy (Chang and Lowenstein, 2003), we were interested whether seizures in the cuprizone model are associated with alterations in the hippocampus or dentate gyrus. Unexpectedly, we found a massive demyelination in the hippocampal formation after only 6 weeks of feeding with 0.2% cuprizone, whereas adjacent brain regions were not affected. To our knowledge, such massive demyelination of the hippocampal formation has not been previously described in the cuprizone model. Recently, Zatta et al. (2005) described a nearly total disappearance of myelinated fibres in the entorhinal cortex as well as the afferent and efferent fibre tracts upon chronic cuprizone treatment in mice. Since demyelination may lead to axonal pathology and thus neuronal damage (Stidworthy et al., 2003), this prompted us to examine neuronal alterations in the hippocampal formation.

In mice that were treated for 12 weeks with cuprizone treatment, dark neurons were observed in the CA1 and CA3 pyramidal cell layer of the hippocampus and in the granular cell layer and hilus of the dentate gyrus. Since such dark neurons were not observed in any of the

control mice that were processed together with the cuprizone-treated animals or mice fed with cuprizone for only 6 weeks, they are unlikely to represent an artifact but more likely represent dying or degenerated cells as described from experimentally induced status epilepticus, hypoglycemia and ischemia (Jortner, 2006). However, because the presence of dark neurons should not be interpreted as unequivocal evidence of degenerating neurons (Jortner, 2006), we stained additional sections by Fluoro-Jade C, which is a relatively novel and highly specific fluorescent marker for the identification of neuronal degeneration (Schmued et al., 2005). Fluoro-Jade C positive cells were observed in the CA1 and dentate granule cell layer of mice that were treated for 12 weeks with cuprizone. Similar findings were obtained one week after a pilocarpine-induced SE. In neither pilocarpine nor cuprizone treated mice, Fluoro-Jade C stained neurons in the dentate hilus, although hilus neurons are known to degenerate after a pilocarpine-induced SE in mice (Borges et al., 2003). However, by using Fluoro-Jade staining or hilar cell counting, it has been shown that damage of hilus neurons develops within 24-48 h after a pilocarpine-induced SE in mice (Borges et al., 2003; Hagihara et al., 2005), so that one week after SE may be too late to visualize neuronal degeneration in the dentate hilus by Fluoro-Jade. Similarly, we may have missed the optimal time for Fluoro-Jade staining to detect hilar neurodegeneration in the cuprizone model. Therefore , we counted neurons in the dentate hilus after treatment with cuprizone or pilocarpine. Immediately after 6 or 12 weeks of treatment with cuprizone, no loss of neurons was observed. However, 5 weeks following termination of a 12-week period of treatment with cuprizone, we found a significant loss of neurons in the dentate hilus compared to controls. A similar loss of hilar neurons was observed in the pilocarpine model.

Loss of neurons in the hilus is a characteristic finding in most rodent models of TLE, including the pilocarpine model, in which mice develop spontaneous recurrent seizures after a latency period following the SE (Leite et al., 2002). Furthermore, in patients with TLE and other types of partial epilepsy, the most consistent cell loss occurs in the hilus of the dentate

gyrus (Sloviter, 1994; Lowenstein, 2001; Nadler, 2003). Hilar cell loss observed in TLE patients and models of acquired partial epilepsy involves both excitatory mossy cells and inhibitory peptide-containing interneurons. There are two controversial scenarios of how this hilar cell loss may result in hyperexcitability of dentate granule cells, which could be causal for increased seizure susceptibility or the development of spontaneous seizures. One prominent theory of epileptogenesis is based on the assumption that loss of mossy cells results in reduction of afferent excitatory drive onto insult-resistant inhibitory basket cells, rendering them "dormant" and granule cells hyperexcitable (Sloviter, 1987; Sloviter, 1991). Alternatively, loss of inhibitory interneurons in the hilus may lead to a loss of inhibitory synaptic input to granule cells that could contribute to the abnormal recurrent excitation of granule cells found in epileptic rats (Kobayashi and Buckmaster, 2003; Ratzliff et al., 2004). As in acquired epilepsy, degeneration of hilar neurons could be causally involved in the occurrence of seizures in the cuprizone model. If cuprizone is affecting hilar neurons directly, it is probably affecting hilar mossy cells selectively because mossy cells are myelinated and interneurons are not (Amaral, 1978). This assumption is substantiated by the lack of myelin staining observed in the inner molecular layer, i.e., the mossy cell termination zone, of cuprizone-treated mice. Thus, one likely mechanistic explanation of seizures in the cuprizone model is that cuprizone is demyelinating mossy cells, which then die as a consequence, resulting in hyperexcitability of dentate granule cells. Alternatively, the neuronal pathology could be secondary to the seizures observed in cuprizone-treated mice. This, however, is considered unlikely, because we and others have shown that short seizures as observed in cuprizone-treated mice are not associated with significant cell loss in the dentate hilus (Tuunanen and Pitkänen, 2000; Brandt et al., 2004; Morimoto et al., 2004).

In the present study, paroxysmal EEG discharges, seizures and loss of neurons in the hilus were observed at a time following termination of feeding with cuprizone at which remyelination already started. This may indicate that once demyelination has led to neuronal

pathology, the functional consequences of this pathology cannot be reversed by remyelination. Although myelination has previously not been considered central to the pathogenesis of epilepsy, impairment of myelination is associated with certain types of epilepsy, e.g., West syndrome (infantile spasms) in children (Schropp et al., 1994; Muroi et al., 1996). An association between myelin deficiency and seizures is also substantiated by experiments in myelin-deficient mutant mice with tonic seizures, in which treatment with the antiepileptic drug phenobarbital markedly improved survival (Matthieu et al., 1984).

In conclusion, although it is long known that myelin deficiency may be associated with seizures in both laboratory animals and patients, the clinical characteristics and the pathogenesis of such seizures have only been studied rarely, particularly in rodent models of CNS demyelination. Our study suggests that the seizures occurring in the cuprizone model are a consequence of neuronal degeneration in the hippocampal formation that develops as a consequence of the impaired myelination in this region. The present data provide thus another example of the usefulness of the cuprizone model in studying the pathological and functional consequences of demyelination. The study further demonstrates the importance of rapid remyelination to prevent neuronal damage that may lead to irreversible functional defects, which have to be considered for the design of regenerative therapies. Based on our data, we propose to study the hippocampal formation also in other rodent models of demyelination associated with epileptic seizures. Recently, Geurts et al. (2006) reported magnetic resonance spectroscopic evidence for hippocampal damage in patients with progressive MS, which could indicate that this brain region may also be involved as an anatomical substrate of seizures observed in patients with MS.

Acknowledgements

We thank Prof. D. Schmidt (Epilepsy Research Group, Berlin, Germany) for discussion during the preparation of this manuscript. We thank Dr. Claudia Brandt for assistance and discussion during video- and EEG recordings and Ina Gröticke for help with the pilocarpine model. The study was partly supported by internal grants of the Hannover Medical School (HiLF).

Fig. 1

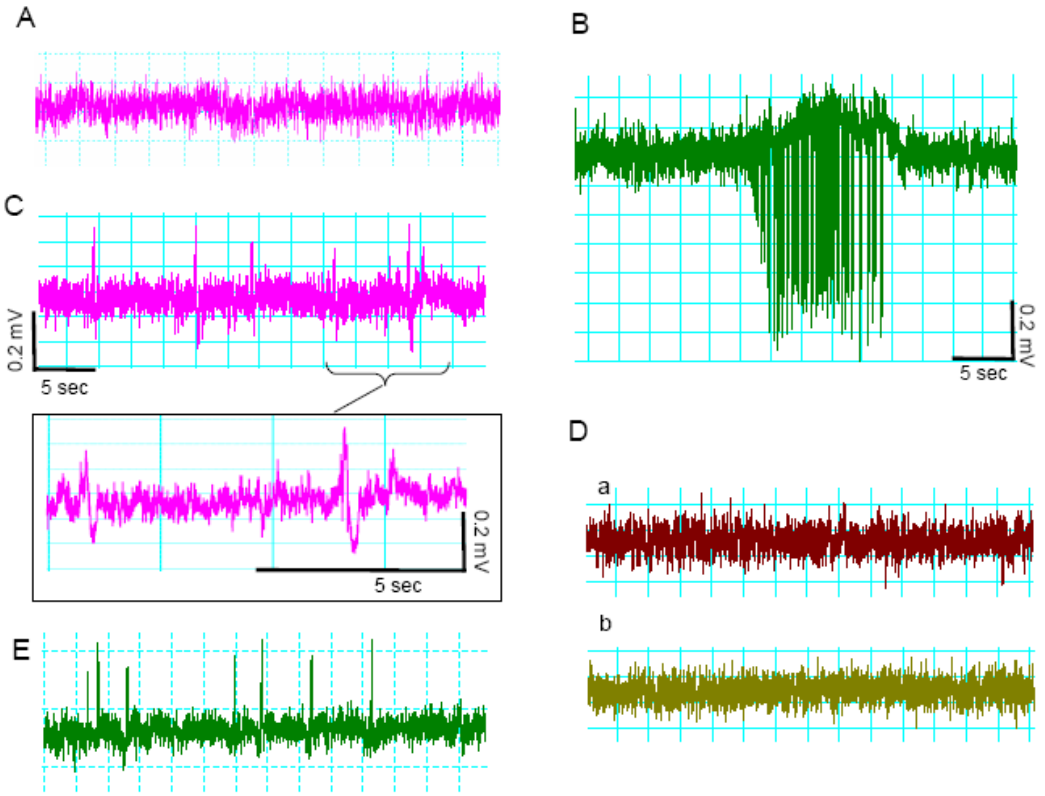

Fig. 1

Cortical EEG recordings from a normal control mouse (A) and mice after treatment with cuprizone (B-D). One of the cuprizone-treated mice exhibited spontaneous generalized tonic-clonic seizures which were associated by high-amplitude discharges in the cortical EEG (B). All cuprizone-treated mice exhibited short but frequent spike discharges in the EEG (C), which were not associated with any obvious behavioral abnormalities and were never observed in normal mice. These spike discharges were indistinguishable from interictal spikes observed in pilocarpine-treated mice in between spontaneous recurrent seizures. For comparison, (E) illustrates such interictal spikes in the cortical EEG from an epileptic mouse about 4 months after a pilocarpine-induced SE. In all cuprizone-treated mice, generalized tonic-clonic seizures could be induced by handling or other types of sensory stimulation; however, these seizures were not associated with paroxysmal alterations in the cortical EEG (D). The upper EEG trace in D ("a") is from a mouse during a handling-induced tonic-clonic seizure. The EEG is not different from that shown in the lower part of D, which is from a cuprizone-treated mice in the absence of any seizure ("b").

Fig. 2

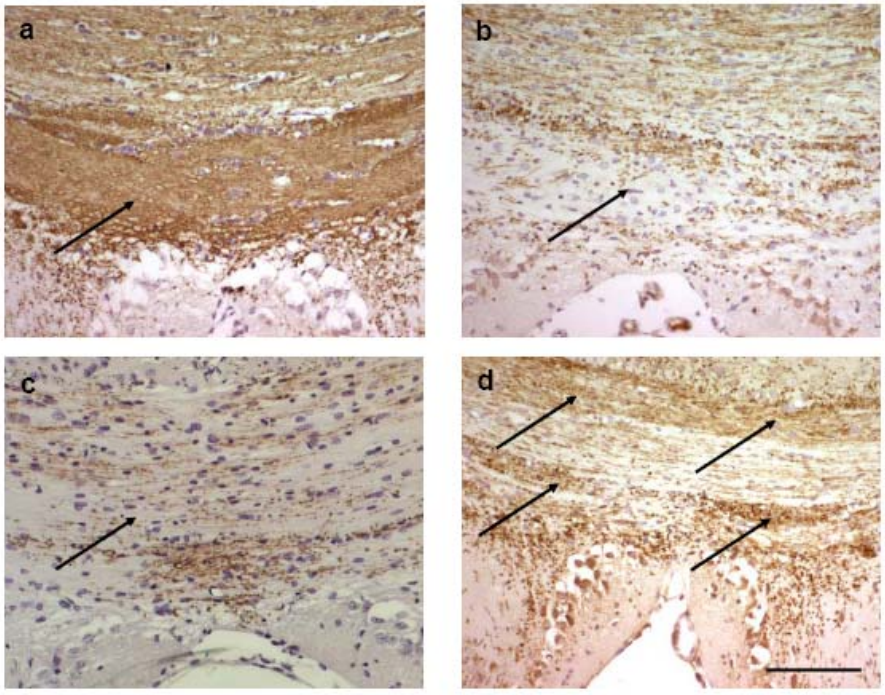

Fig. 2

Expression of the myelin protein PLP (proteolipid protein) in the corpus callosum of representative coronal sections of mouse brain (-1.94 mm according to bregma). In control mice, the corpus callosum represents a band of myelin-positive bundles (a). A marked demyelination could be observed after 6 weeks of cuprizone-treatment (b; group 2). A similar degree of demyelination in the corpus callosum was seen after 12 weeks of treatment in group 3 (c); remyelination occurred 5 weeks after a 12-week period of cuprizone-treatment (d; group 4). Scale bar indicates 100 µm. Arrows show what is being referred to above.

Fig. 3, part 1

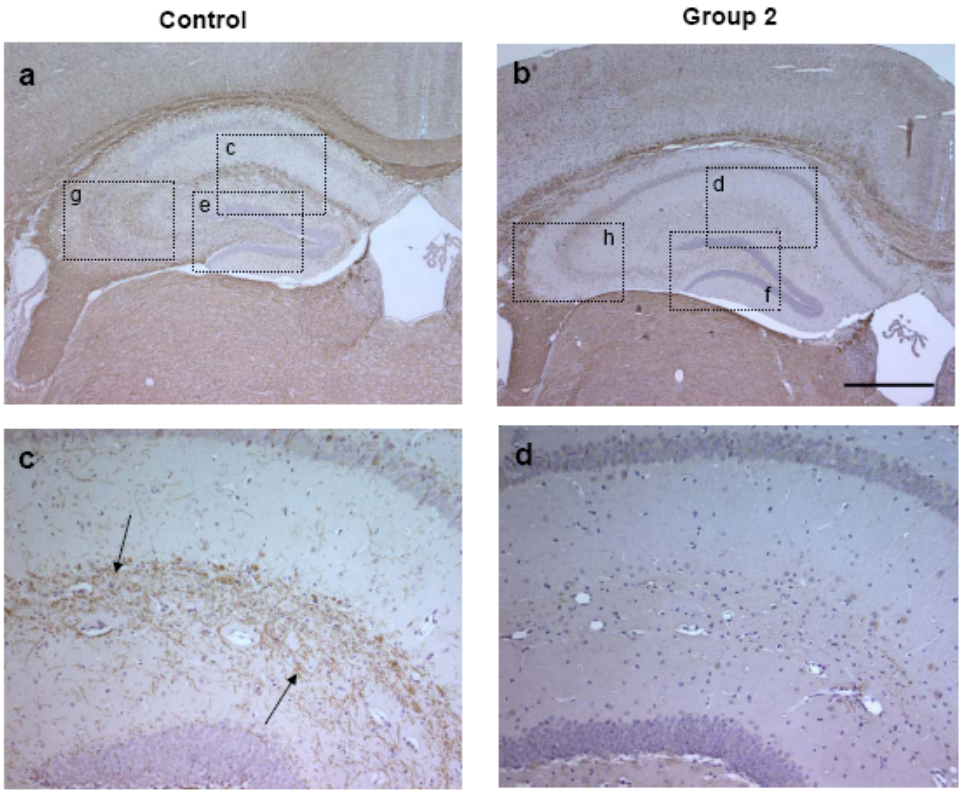

Fig. 3, part 2

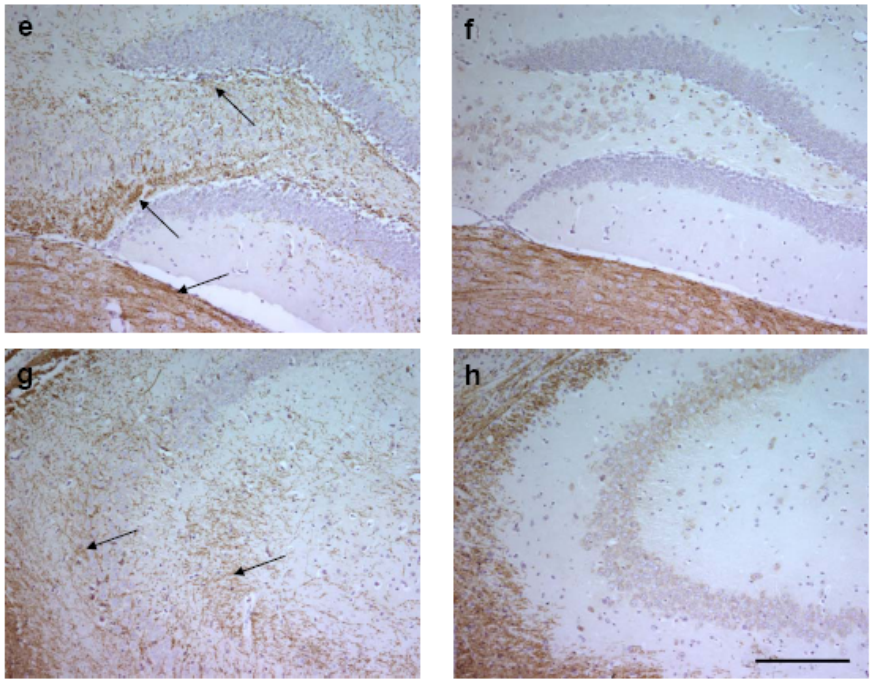

Fig. 3

Expression of the myelin protein PLP (proteolipid protein) in the dorsal hippocampus of representative coronal sections of mouse brain (-1.94 mm according to bregma) in control mice (a, c, e, g) and mice of group 2 after 6 weeks of cuprizone-treatment (b, d, f, h). Note the extensive demyelination of the hippocampus in group 2 (b) compared to control (a) in contrast to the intense myelin-positive structures of the fimbria of the hippocampus and the thalamic formation. The most obvious changes in myelination between control and group 2 could be observed in stratum lacunosum of the molecular layer (c, d), in the layers surrounding the CA2 pyramidal cell layer (g,h) and region of the dentate gyrus, respectively (e,f). Arrows in c, e and g point to myelin-positive structures. Scale bars indicate 500 µm in a and b, and 200 µm in c-h.

Fig. 4, part 1

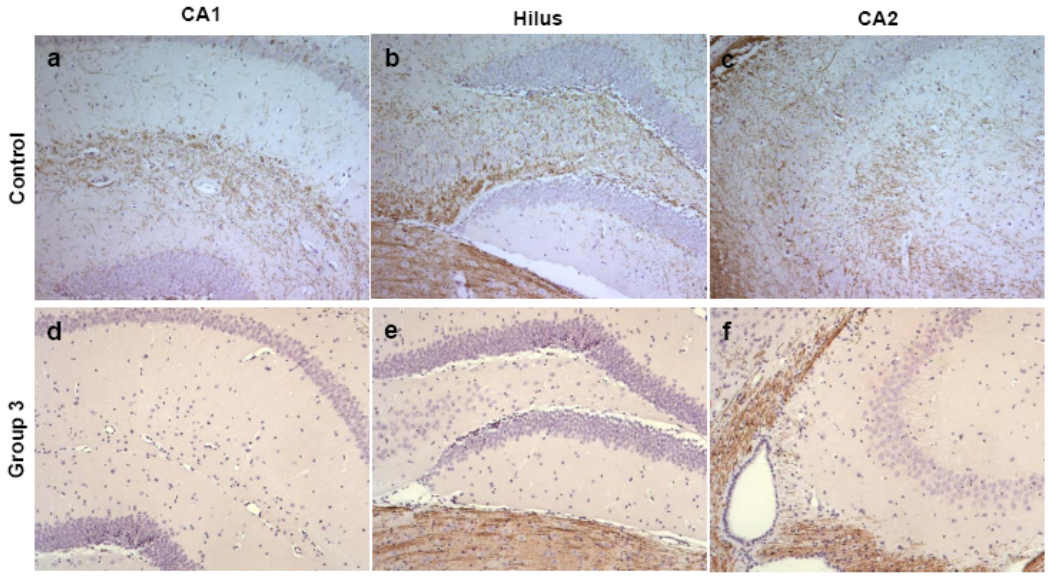

Fig. 4, part 2

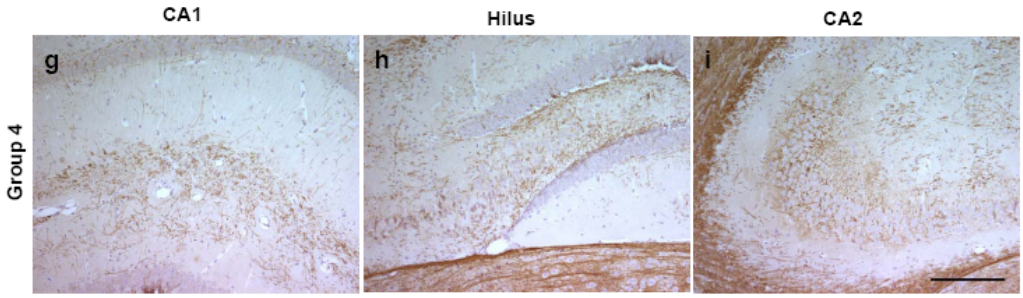

Fig. 4

Expression of the myelin protein PLP (proteolipid protein) in the dorsal hippocampus of representative coronal sections of mouse brain (-1.94 mm according to bregma) in control mice (a-c) and mice of group 3 (d-f; 12 weeks treatment with cuprizone) and group 4 (g-i; 5 weeks after a period of 12 weeks of cuprizone-treatment). The figures from group 4 illustrate the remyelination process in the hippocampal formation. Scale bar indicates 200 µm.

Fig. 5

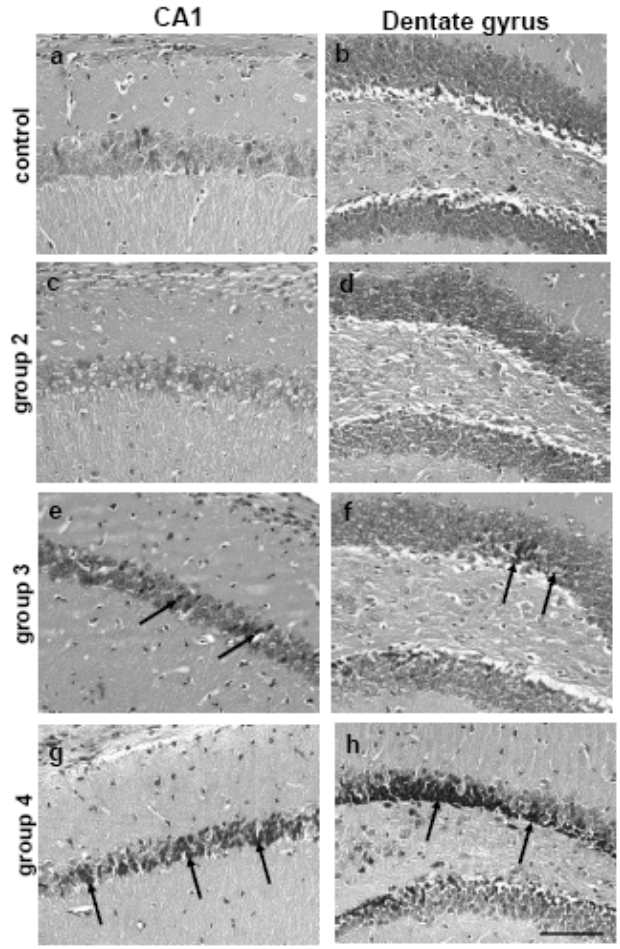

Fig. 5

Occurence of dark neurons in representative hematoxylin-eosin stained coronal sections of mouse brain (-1.94 mm according to bregma) in the CA1 region and dentate gyrus of the dorsal hippocampus. Normal staining was observed in all control mice (a,b) and mice of group 2 after 6 weeks of cuprizone-treatment (c,d). Intensely stained neurons occured in all animals of group 3 after 12 weeks of treatment with cuprizone; these dark neurons could be found in CA1 (e) and CA3 region (not shown) of the pyramidal cell layer and in the granula cell layer and the hilus of the dentate gyrus (f). In group 4, i.e., 5 weeks after termination of a 12-week treatment period with cuprizone, the frequency of dark neurons in CA1 (g) and dentate gyrus (h) was higher than in group 3 (e,f), indicating progression of neurodegeneration in the absence of cuprizone. Scale bar indicates 100 µm.

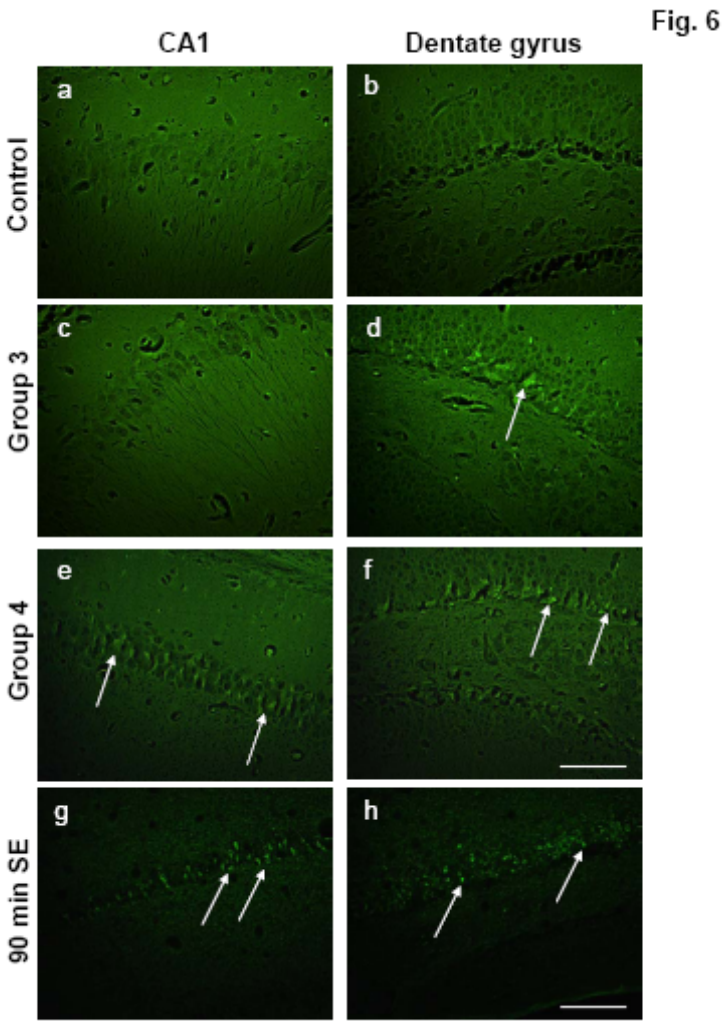

Fig. 6

Comparison of cuprizone and pilocarpine induced neuronal degeneration in hippocampal sections stained with Fluoro-Jade C. In control tissue, neurons were not labelled (a,b), whereas Fluoro-Jade C positive degenerating neurons were seen in all mice of group 3 (c,d; 12 weeks of treatment with cuprizone), group 4 (e,f; 5 weeks after 12 weeks of treatment) and group 5 (not illustrated). In group 3, labelled neurons were only seen in the granule cell layer of the dentate gyrus, whereas additional labelling of CA1 pyramidal cells was observed in group 4. Similarly, pilocarpine-treated mice exhibited Fluoro-Jade C positive cells in CA1 and dentate granule cell layer. Scale bar indicates 100 µm. Arrows point to Fluoro-Jade C positive cells.

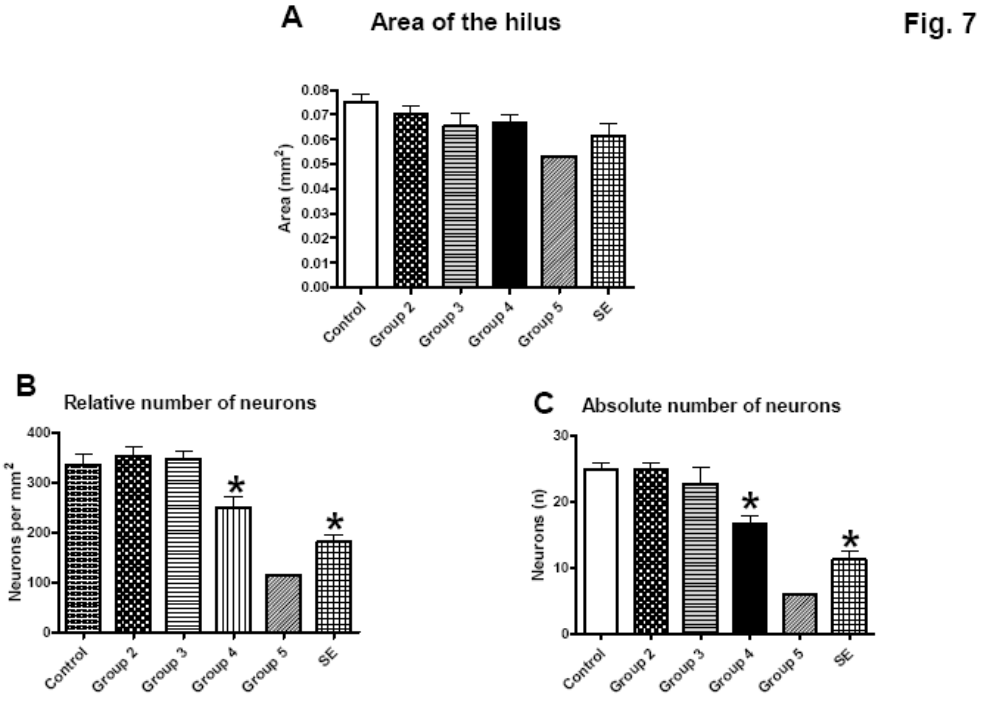

Fig. 7

Quantitative comparison of area and number of neurons in the hilus of control mice (n=6) and mice of group 2 (n=6; 6 weeks of treatment with cuprizone), group 3 (n=5; 12 weeks of treatment), group 4 (n = 5; 5 weeks after 12 weeks of treatment) and group 5 (n=1; 5 weeks after 12 weeks of treatment). For comparison, data from 8 mice that were killed one week after a pilocarpine-induced status epilepticus (SE) are shown. Data from 3 sections were averaged per mouse, and data are shown as means ± SEM except for group 5. Statistical comparison of groups by ANOVA did not indicate a significant inter-group difference in the area of the hilus (A). In contrast, groups differed significantly ($P< 0.01$) with respect to neuronal density (neurons per unit area; B) and total number of neurons in the hilus (C). Post hoc analysis indicated that group 4 and the SE group had a reduced density of neurons (B) and less neurons in the hilus (C) compared to controls ($P<0.05$; indicated by an asterisk).

Fig. 8

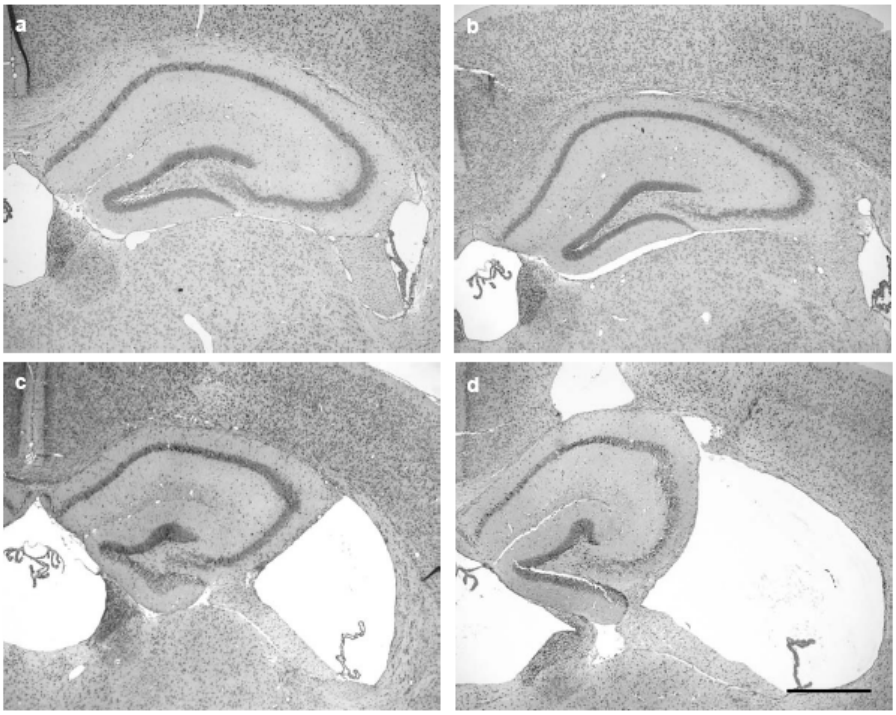

Fig. 8

Representative thionin-stained sections of mouse brain (-1.94 mm according to bregma) of control mice (a) and mice of group 2 (b), group 4 (c) and group 5 (d). Note the massively dilated lateral ventricle and dorsal part of the 3rd ventricle in group 4 and 5 (c,d), which led to a marked deformation of the hippocampus, compared to control (a). Dilatation of ventricles was also observed in group 3 (not illustrated), whereas no obvious dilatation was apparent in animals of group 2 (b). Note that although the hilus area of the mouse of group 4 shown in "c" appears small, the average hilus area of the whole group did not differ significantly from controls (Fig. 7A). Scale bar indicates 500 µm.

References

Altrock WD, tom Dieck S, Sokolov M, Meyer AC, Sigler A, Brakebusch C, Fassler R, Richter K, Boeckers TM, Potschka H, Brandt C, Löscher W, Grimberg D, Dresbach T, Hempelmann A, Hassan H, Balschun D, Frey JU, Brandstatter JH, Garner CC, Rosenmund C, Gundelfinger ED (2003) Functional inactivation of a fraction of excitatory synapses in mice deficient for the active zone protein bassoon. Neuron 37: 787-800.

Amaral DG (1978) A Golgi study of cell types in the hilar region of the hippocampus in the rat. J Comp Neurol 182: 851-914.

Blakemore WF (1972) Observations on oligodendrocyte degeneration, the resolution of status spongiosus and remyelination in cuprizone intoxication in mice. J Neurocytol 1: 413-426.

Blakemore WF (1973) Demyelination of the superior cerebellar peduncle in the mouse induced by cuprizone. J Neurol Sci 20: 63-72.

Bloom CM, Anch AM, Dyche JS (2002) Behavioral effects of chronic melatonin and pregnenolone injections in a myelin mutant rat (taiep). J Gen Psychol 129: 226-237.

Borges K, Gearing M, McDermott DL, Smith AB, Almonte AG, Wainer BH, Dingledine R (2003) Neuronal and glial pathological changes during epileptogenesis in the mouse pilocarpine model. Exp Neurol 182: 21-34.

Bradl M, Bauer J, Inomata T, Zielasek J, Nave KA, Toyka K, Lassmann H, Wekerle H (1999) Transgenic Lewis rats overexpressing the proteolipid protein gene: myelin degeneration and its effect on T cell-mediated experimental autoimmune encephalomyelitis. Acta Neuropathol (Berl) 97: 595-606.

Brandt C, Ebert U, Löscher W (2004) Epilepsy induced by extended amygdala-kindling in rats: lack of clear association between development of spontaneous seizures and neuronal damage. Epilepsy Res 62: 135-156.

Carlton WW (1967) Studies on the induction of hydrocephalus and spongy degeneration by cuprizone feeding and attempts to antidote the toxicity. Life Sci 6: 11-19.

Chang BS, Lowenstein DH (2003) Epilepsy. N Engl J Med 349: 1257-1266.

De Curtis M, Avanzini G (2001) Interictal spikes in focal epileptogenesis. Prog Neurobiol 63: 541-567.

Frohman EM, Racke MK, Raine CS (2006) Multiple sclerosis--the plaque and its pathogenesis. N Engl J Med 354: 942-955.

Gambardella A, Valentino P, Labate A, Sibilia G, Ruscica F, Colosimo E, Nistico R, Messina D, Zappia M, Quattrone A (2003) Temporal lobe epilepsy as a unique manifestation of multiple sclerosis. Can J Neurol Sci 30: 228-232.

Geurts JJ, Reuling IE, Vrenken H, Uitdehaag BM, Polman CH, Castelijns JA, Barkhof F, Pouwels PJ (2006) MR spectroscopic evidence for thalamic and hippocampal, but not cortical, damage in multiple sclerosis. Magn Reson Med 55: 478-483.

Griffiths IR (1996) Myelin mutants: model systems for the study of normal and abnormal myelination. Bioessays 18: 789-797.

Hagihara H, Hara M, Tsunekawa K, Nakagawa Y, Sawada M, Nakano K (2005) Tonic-clonic seizures induce division of neuronal progenitor cells with concomitant changes in expression of neurotrophic factors in the brain of pilocarpine-treated mice. Brain Res Mol Brain Res 139: 258-266.

Hiremath MM, Saito Y, Knapp GW, Ting JP, Suzuki K, Matsushima GK (1998) Microglial/macrophage accumulation during cuprizone-induced demyelination in C57BL/6 mice. J Neuroimmunol 92: 38-49.

Jardim LB, Pires RF, Martins CE, Vargas CR, Vizioli J, Kliemann FA, Giugliani R (1994) Pyridoxine-dependent seizures associated with white matter abnormalities. Neuropediatrics 25: 259-261.

Jortner BS (2006) The return of the dark neuron. A histological artifact complicating contemporary neurotoxicologic evaluation. Neurotoxicology 27: 628-634.

Kesterson JW, Carlton WW (1970) Aqueductal stenosis as the cause of hydrocephalus in mice fed the substituted hydrazine, cuprizone. Exp Mol Pathol 13: 281-294.

Kesterson JW, Carlton WW (1972) Cuprizone toxicosis in mice--attempts to antidote the toxicity. Toxicol Appl Pharmacol 22: 6-13.

Kobayashi M, Buckmaster PS (2003) Reduced inhibition of dentate granule cells in a model of temporal lobe epilepsy. J Neurosci 23: 2440-52.

Kuhlmann T, Lingfeld G, Bitsch A, Schuchardt J, Bruck W (2002) Acute axonal damage in multiple sclerosis is most extensive in early disease stages and decreases over time. Brain 125: 2202-2212.

Kutzelnigg A, Lucchinetti CF, Stadelmann C, Bruck W, Rauschka H, Bergmann M, Schmidbauer M, Parisi JE, Lassmann H (2005) Cortical demyelination and diffuse white matter injury in multiple sclerosis. Brain 128: 2705-2712.

Leite JP, Garcia-Cairasco N, Cavalheiro EA (2002) New insights from the use of pilocarpine and kainate models. Epilepsy Res 50: 93-103.

Lheureux P, Penaloza A, Gris M (2005) Pyridoxine in clinical toxicology: a review. Eur J Emerg Med 12: 78-85.

Lowenstein DH (2001) Structural reorganization of hippocampal networks caused by seizure activity. Int Rev Neurobiol 45: 209-236.

Löscher W (1984) Genetic animal models of epilepsy as a unique resource for the evaluation of anticonvulsant drugs. A review. Methods Findings Experiment Clin Pharmacol 6: 531-547.

Löscher W (1989) GABA and the epilepsies. Experimental and clinical considerations. In: GABA. Basic research and clinical applications (Bowery NG, Nisticò G, eds), pp 260-300. Rome: Pythagora Press.

Löscher W (1999) Animal models of epilepsy and epileptic seizures. In: Antiepileptic drugs. Handbook of experimental pharmacology (Eadie MJ, Vajda F, eds), pp 19-62. Berlin: Springer.

Ludwin SK (1980) Chronic demyelination inhibits remyelination in the central nervous system. An analysis of contributing factors. Lab Invest 43: 382-387.

Mason JL, Langaman C, Morell P, Suzuki K, Matsushima GK (2001) Episodic demyelination and subsequent remyelination within the murine central nervous system: changes in axonal calibre. Neuropathol Appl Neurobiol 27: 50-58.

Mason JL, Toews A, Hostettler JD, Morell P, Suzuki K, Goldman JE, Matsushima GK (2004) Oligodendrocytes and progenitors become progressively depleted within chronically demyelinated lesions. Am J Pathol 164: 1673-1682.

Matsushima GK, Morell P (2001) The neurotoxicant, cuprizone, as a model to study demyelination and remyelination in the central nervous system. Brain Pathol 11: 107-116.

Matthieu JM, Eggenberger P, Almazan G, Ginalski-Winkelmann H (1984) Anticonvulsive treatment of myelin-deficient (mld) mice improves survival and confirms the delayed increase of myelin basic protein. Neurochem Pathol 2: 115-121.

Morimoto K, Fahnestock M, Racine RJ (2004) Kindling and status epilepticus models of epilepsy: rewiring the brain. Prog Neurobiol 73: 1-60.

Mothersill IW, Hilfiker P, Kramer G (2000) Twenty years of ictal EEG-EMG. Epilepsia 41 Suppl 3: S19-S23.

Muroi J, Okuno T, Kuno C, Yorifuji T, Shimizu K, Matsumura M, Takahashi Y, Okuno T, Matsuo M (1996) An MRI study of the myelination pattern in West syndrome. Brain Dev 18: 179-184.

Nadler JV (2003) The recurrent mossy fiber pathway of the epileptic brain. Neurochem Res 28: 1649-1658.

Naquet RG, Valin A (1998) Experimental models of reflex epilepsy. Adv Neurol 75: 15-28.

Paxinos G, Franklin, K.B.J. (2001) The Mouse Brain in Stereotaxic Coordinates. New York: Academic Press.

Poser CM, Brinar VV (2003) Epilepsy and multiple sclerosis. Epilepsy Behav 4: 6-12.

Ratzliff AH, Howard AL, Santhakumar V, Osapay I, Soltesz I (2004) Rapid deletion of mossy cells does not result in a hyperexcitable dentate gyrus: implications for epileptogenesis. J Neurosci 24: 2259-2269.

Rosenbluth J (1990) Axolemmal abnormalities in myelin mutants. Ann N Y Acad Sci 605: 194-214.

Schmued LC, Stowers CC, Scallet AC, Xu L (2005) Fluoro-Jade C results in ultra high resolution and contrast labeling of degenerating neurons. Brain Res 1035: 24-31.

Schropp C, Staudt M, Staudt F, Bise K, Obletter N, Breit A, Weinmann HM (1994) Delayed myelination in children with West syndrome: an MRI-study. Neuropediatrics 25: 116-120.

Seyfried TN, Glaser GH, Yu RK, Palayoor ST (1986) Inherited convulsive disorders in mice. Adv Neurol 44: 115-133.

Skundric DS (2005) Experimental models of relapsing-remitting multiple sclerosis: current concepts and perspective. Curr Neurovasc Res 2: 349-362.

Sloviter RS (1987) Decreased hippocampal inhibition and a selective loss of interneurons in experimental epilepsy. Science 235: 73-76.

Sloviter RS (1991) Permanently altered hippocampal structure, excitability, and inhibition after experimental status epilepticus in the rat: the "dormant basket cell" hypothesis and its possible relevance to temporal lobe epilepsy. Hippocampus 1: 41-66.

Sloviter RS (1994) The functional organization of the hippocampal dentate gyrus and its relevance to the pathogenesis of temporal lobe epilepsy. Ann Neurol 35: 640-654.

Staley K, Hellier JL, Dudek FE (2005) Do interictal spikes drive epileptogenesis? Neuroscientist 11: 272-276.

Stidworthy MF, Genoud S, Suter U, Mantei N, Franklin RJ (2003) Quantifying the early stages of remyelination following cuprizone-induced demyelination. Brain Pathol 13: 329-339.

Trapp BD, Peterson J, Ransohoff RM, Rudick R, Mork S, Bo L (1998) Axonal transection in the lesions of multiple sclerosis. N Engl J Med 338: 278-285.

Tuunanen J, Pitkänen A (2000) Do seizures cause neuronal damage in rat amygdala kindling? Epilepsy Res 39: 171-6.

Vercellino M, Plano F, Votta B, Mutani R, Giordana MT, Cavalla P (2005) Grey matter pathology in multiple sclerosis. J Neuropathol Exp Neurol 64: 1101-1107.

Waxman SG (2000) Multiple sclerosis as a neuronal disease. Arch Neurol 57: 22-24.

Xue LY, Ritaccio AL (2006) Reflex seizures and reflex epilepsy. Am J Electroneurodiagnostic Technol 46: 39-48.

Zatta P, Raso M, Zambenedetti P, Wittkowski W, Messori L, Piccioli F, Mauri PL, Beltramini M (2005) Copper and zinc dismetabolism in the mouse brain upon chronic cuprizone treatment. Cell Mol Life Sci 62: 1502-1513.

4 Discussion

The present work investigated the de- and remyelination process in the cuprizone model. In the first part a fast and reliable quantification method to describe the various stages of the de- and remyelination process was established (Lindner et al., 2007). In this study we examined the myelin protein expression after demyelination. We used a combination of immunohistochemical stainings for different myelin proteins; myelin basic protein (MBP), phospholipid protein (PLP), 2',3-cyclic nucleotide 3' phosphodiesterase (CNPase), myelin oligodendrocyte glycoprotein (MOG) and Luxol-fast blue (LFB) myelin staining. The stained sections were evaluated by a scoring system. We found that MBP, PLP and CNPase are re-expressed within 4 days after removal of the toxin, whereas MOG could be first detected as early as 2 weeks on recovery phase. Thus, remyelination is a fast process triggered within days after withdrawal of cuprizone. Additionally, the myelin protein stained section were analysed by AnalySIS software and compared with the scoring results. We could demonstrate that a scoring system is more advantageous than using a computer based method. We verified the quality of the scoring system by correlating the data with electron microscopy (EM) results. We showed that in contrast to previous studies (Mason et al., 2001) LFB correlated well with EM results. In addition, the combination of an early re-expressed protein (like MBP or PLP) with a late re-expressed myelin protein (MOG) reflects best remyelination yielding additional information about the integrity of the newly build myelin sheath. Therefore, this fast and reliable method was used for all further experiments.

We next investigated the influence of the chemokine receptor CXCR2 during the de- and remyelination. CXCR2 is functionally expressed on oligodendrocyte precursor cells (OPC) (Nguyen and Stangel, 2001; Robinson et al., 1998; Tsai et al., 2002) and can also be found on oligodendrocytes in MS lesions (Omari et al., 2005; Omari et al., 2006), suggesting a role of CXCR2 on OPC during proliferation, migration and differentiation. We found constitutive

expression of CXCR2 on precursor and mature oligodendrocytes during de- and remyelination. Interestingly, double staining showed that microglia/monocytes upregulate CXCR2 expression during demyelination. Hence, the regulation of CXCR2 expression in oligodendrocytes is other than in microglia/monocytes. These findings are in line with a previous study of CNS injury (Valles et al., 2006), where differential regulation of CXCR2 on microglia/monocytes was observed. However, our study in CXCR2-/- mice revealed no difference in the myelination pattern compared to control mice. This contrast a previous study (Tsai et al., 2002), where the migration behaviour of OPC was different at P7 within the spinal cord. In our study we investigated only the corpus callosum and did not detect a difference in the number of NG2 positive cells, thus the migration behaviour of OPC was not altered during physiological myelination. Moreover, the remyelination after cuprizone-induced demyelination was not influenced by the absence of CXCR2. CXCR2-/- mice showed no difference in the process of remyelination as assessed by scoring of LFB, PLP and MOG. In addition, the number of OPC and microglia/monocytes was not altered in CXCR2-/- mice compared to wildtype littermates. Thus, the absence of CXCR2 altered neither the physiological myelination nor the de- and remyelination process of the cuprizone model. This suggests that CXCR2 signalling does not play a major role in the recruitment of OPC or microglia/monocyte during toxin induced demyelination. Its function seems to be compensated in vivo probably by other chemokine receptors e.g. the chemokine receptor CXCR4 (Maysami et al., 2006). This study again demonstrated the redundancy and complexity of the chemokine system (Baggiolini, 1998; Mantovani, 1999). It is not clear whether our findings are also relevant in the human chemokine system and whether CXCR2 has a unique function in MS patients.

The influence of chronic demyelination in regard to the remyelination potential has not been extensively studied in the past (Mason et al., 2004; Armstrong et al., 2006). Here we could show that despite severe OPC depletion an extensive remyelination is possible even after

chronic cuprizone treatment for up to 16 weeks. This contrasts previous studies which showed no (Mason et al., 2004) or insufficient (Armstrong et al., 2006) remyelination after chronic cuprizone treatment. This may arise from the short remyelination period (only 4 weeks) (Mason et al., 2004) and the used method to quantify remyelination (staining of the late re-expressed MOG) (Armstrong et al., 2006), which can lead to an underestimation of the newly built myelin. In our study we used immunohistochemistry of an early and late re-expressed myelin protein to describe the various stages of remyelination, as mentioned earlier. However, the rate of the remyelination was impaired compared to acute demyelination (6 weeks on cuprizone). This may result from a depletion of OPC. Furthermore we could demonstrate that the pure absence of the myelin sheath is not sufficient to induce severe axonal damage as it is described in EAE studies (Onuki et al., 2001) or in MS lesions (Kuhlmann et al., 2002; Ferguson et al., 1997). Hence, the observed axonal damage is only minimal and correlates strongly with the occurrence of microglia/monocytes. This supports the hypothesis that microglia are involved in cytotoxic effects that can damage axons.

Surprisingly, demyelination was not only seen at the corpus callosum, but also within the cortex. The involvement of cortical demyelination in MS is nowadays an extensively studied field (Kutzelnigg and Lassmann, 2005; Kutzelnigg et al., 2005). Although the cuprizone model is used since decades this feature has been overlooked. This may rise from the fact that most of the investigators have only employed LFB staining as a quantification method and this histological staining is not sensitive enough to detect cortical changes. In our study we used immunohistochemistry of the myelin proteins PLP and MBP to describe the cortical de- and remyelination, which was similar to the de- and remyelination stages observed at the corpus callosum. We characterized this previously not described feature of the cuprizone model and showed that the degree of demyelination within the cortex seems to be strain dependent. C57BL/6 mice exhibit a severe demyelination of the cortex whereas balb/c mice showed less demyelination. Interestingly, microglia/monocytes were absent within the cortex,

whereas at the corpus callosum there was an extensive microglial accumulation. This holds true for C57BL/6 mice, whereas in balb/c mice microglia/monocytes accumulate abundantly in the cortex during demyelination. Thus, the mechanisms of oligodendrocyte death and involvement of microglia/monocytes appear to be different in the corpus callosum and the cortex. In conclusion, the cuprizone model is an ideal model to study cortical demyelination, the different mechanisms of demyelination in the cortex and in the corpus callosum and the role of microglia/monocytes within the system.

Epileptic seizures are known to occur in different animal models of demyelination and have also been described in MS patients (Poser and Brinar, 2003; Griffiths, 1996). We described and characterized epileptic seizures occurring during chronic demyelination in detail. This feature has not been described in recent chronic demyelination studies (Mason et al., 2001; Mason et al., 2004; Armstrong et al., 2006) but has been mentioned in the very early cuprizone experiments (Ludwin, 1978; Kesterson and Carlton, 1972; Kesterson and Carlton, 1970). Most animals exhibited epileptic seizures upon stress-induced stimuli after chronic demyelination. In addition massive demyelination of the hippocampal formation and the associated neuronal alteration was shown here for the first time. Our data suggest that the seizures occurring in the cuprizone model are a consequence of neuronal degeneration in the hippocampal formation.

These new findings further characterised the cuprizone model and revealed new aspects of demyelination that will allow the study of the mechanisms und functional consequences of demyelination.

References Discussion

1. Armstrong RC, Le TQ, Flint NC, Vana AC, Zhou YX (2006) Endogenous cell repair of chronic demyelination. J Neuropathol Exp Neurol 65: 245-256.

2. Baggiolini M (1998) Chemokines and leukocyte traffic. Nature 392: 565-568.

3. Ferguson B, Matyszak MK, Esiri MM, Perry VH (1997) Axonal damage in acute multiple sclerosis lesions. Brain 120: 393-399.

4. Griffiths IR (1996) Myelin mutants: model systems for the study of normal and abnormal myelination. Bioessays 18: 789-797.

5. Kesterson JW, Carlton WW (1970) Aqueductal stenosis as the cause of hydrocephalus in mice fed the substituted hydrazine, cuprizone. Exp Mol Pathol 13: 281-294.

6. Kesterson JW, Carlton WW (1972) Cuprizone toxicosis in mice--attempts to antidote the toxicity. Toxicol Appl Pharmacol 22: 6-13.

7. Kuhlmann T, Lingfeld G, Bitsch A, Schuchardt J, Bruck W (2002) Acute axonal damage in multiple sclerosis is most extensive in early disease stages and decreases over time. Brain 125: 2202-2212.

8. Kutzelnigg A, Lassmann H (2005) Cortical lesions and brain atrophy in MS. J Neurol Sci 233: 55-59.

9. Kutzelnigg A, Lucchinetti CF, Stadelmann C, Bruck W, Rauschka H, Bergmann M, Schmidbauer M, Parisi JE, Lassmann H (2005) Cortical demyelination and diffuse white matter injury in multiple sclerosis. Brain 128: 2705-2712.

10. Lindner M, Heine S, Haastert K, Garde N, Fokuhl J, Linsmeier F, Grothe C, Baumgaertner W, Stangel M (2007) Sequential myelin protein expression during remyelination reveals fast and efficient repair after central nervous system demyelination. Neuropathol Appl Neurobiol in press

11. Ludwin SK (1978) Central nervous system demyelination and remyelination in the mouse: an ultrastructural study of cuprizone toxicity. Lab Invest 39: 597-612.

12. Mantovani A (1999) The chemokine system: redundancy for robust outputs. Immunol Today 20: 254-257.

13. Mason JL, Langaman C, Morell P, Suzuki K, Matsushima GK (2001) Episodic demyelination and subsequent remyelination within the murine central nervous system: changes in axonal calibre. Neuropathol Appl Neurobiol 27: 50-58.

14. Mason JL, Toews A, Hostettler JD, Morell P, Suzuki K, Goldman JE, Matsushima GK (2004) Oligodendrocytes and progenitors become progressively depleted within chronically demyelinated lesions. Am J Pathol 164: 1673-1682.

15. Maysami S, Nguyen D, Zobel F, Pitz C, Heine S, Hopfner M, Stangel M (2006) Modulation of rat oligodendrocyte precursor cells by the chemokine CXCL12. Neuroreport 17: 1187-1190.

16. Nguyen D, Stangel M (2001) Expression of the chemokine receptors CXCR1 and CXCR2 in rat oligodendroglial cells. Brain Res Dev Brain Res 128: 77-81.

17. Omari KM, John G, Lango R, Raine CS (2006) Role for CXCR2 and CXCL1 on glia in multiple sclerosis. Glia 53: 24-31.

18. Omari KM, John GR, Sealfon SC, Raine CS (2005) CXC chemokine receptors on human oligodendrocytes: implications for multiple sclerosis. Brain 128: 1003-1015.

19. Onuki M, Ayers MM, Bernard CC, Orian JM (2001) Axonal degeneration is an early pathological feature in autoimmune-mediated demyelination in mice. Microsc Res Tech 52: 731-739.

20. Poser CM, Brinar VV (2003) Epilepsy and multiple sclerosis. Epilepsy Behav 4: 6-12.

21. Robinson S, Tani M, Strieter RM, Ransohoff RM, Miller RH (1998) The chemokine growth-regulated oncogene-alpha promotes spinal cord oligodendrocyte precursor proliferation. J Neurosci 18: 10457-10463.

22. Tsai HH, Frost E, To V, Robinson S, Ffrench-Constant C, Geertman R, Ransohoff RM, Miller RH (2002) The chemokine receptor CXCR2 controls positioning of oligodendrocyte precursors in developing spinal cord by arresting their migration. Cell 110: 373-383.

23. Valles A, Grijpink-Ongering L, de Bree FM, Tuinstra T, Ronken E (2006) Differential regulation of the CXCR2 chemokine network in rat brain trauma: implications for neuroimmune interactions and neuronal survival. Neurobiol Dis 22: 312-322.

5 Summary

The reasons for remyelination failure in multiple sclerosis (MS) lesions are manifold and not completely understood. The present study investigated the remyelination process in a toxic demyelination model, the cuprizone model. Feeding of the copper chelator cuprizone to young adult mice leads to a reproducible demyelination of the corpus callosum. Spontaneous remyelination occurs after withdrawal from the diet. In order to describe the remyelination process and investigate factors which may influence this process we established first a fast and reliable quantification method. Scoring of an early re-expressed myelin protein (like MBP or PLP) and a late re-expressed myelin protein (MOG) was found to correlate well with electron microscopic results even adding additional information. Hence, this time-saving method turned out to be reliable and was used for all further experiments. These experiments could also demonstrate that remyelination is initiated quickly after the toxin is removed and repair processes are switched on within days.

We further studied the role of the chemokine receptor CXCR2 during myelination, de- and remyelination. CXCR2 is believed to influence the behaviour of oligodendrocyte precursor cells (OPC), the myelin producing cells in the central nervous system (CNS). We showed that CXCR2 is constitutively expressed on OPC as well as on mature oligodendrocytes during cuprizone treatment. In addition, double staining demonstrated that microglia/monocyte upregulate the expression of CXCR2 during demyelination. These findings suggest that CXCR2 is differentially regulated on oligodendrocytes and microglia/monocytes. However, physiological myelination in CXCR2 -/- mice was not altered compared to wildtype littermates. Furthermore, the absence of CXCR2 did not influence the de- and remyelination of the cuprizone model. Thus, the impact of CXCR2 signalling is highly compensated for *in vivo* and other chemokine receptors may serve as a substitute for CXCR2. It is still not clear

whether or not CXCR2 plays a role in patients with MS, but our results make it unlikely that this receptor may be a useful therapeutic target.

Additional investigations examined the consequences of prolonged demyelination in this model. Despite severe depletion of OPC after chronic cuprizone exposure (up to 16 weeks), extensive remyelination occurred. Nevertheless, the rate of the observed remyelination process was slowed down compared to acute demyelination (6 weeks on cuprizone diet). Interestingly, the investigated axonal damage was only minimal after acute demyelination and did not increase while cuprizone treatment was continued. The amount of axonal damage correlated best with the microglia/monocyte accumulation, suggesting a role for microglia in the pathomechanisms of axonal loss.

The presence of cortical lesions in MS was mostly neglected in the past and has come more into the focus of current MS research. We described here for the first time cortical demyelination in the cuprizone model. Interestingly, the degree of demyelination within the cortex seems to be strain dependent, since balb/c mice exhibit less demyelination than C57BL/6 mice. Moreover, the mechanisms of oligodendrocyte death appear to be different in the corpus callosum and the cortex. During demyelination microglia/monocytes accumulated extensively in the corpus callosum, whereas microglial accumulation was absent in the cortex. This contrasts observations in balb/c mice, where microglia/monocytes accumulate abundantly in the cortex. These findings underline the importance of the mice strain used in the cuprizone model and suggest a genetic dependence on the underlying molecular mechanisms.

Epileptic seizures are known to occur in different animal models of demyelination. We described and characterized epileptic seizures occurring during chronic demyelination. Upon

stress-inducing stimuli most animals exhibited seizures. Furthermore, we showed for the first time a massive demyelination within the hippocampal formation which was associated with neuronal loss. Our data suggest that the seizures occurring in the cuprizone model are a consequence of neuronal degeneration in the hippocampal formation. Moreover, this study corroborates the usefulness of the cuprizone model in studying the pathological and functional consequences of demyelination.

In conclusion, the present study further characterized the cuprizone model. Several new features including cortical demyelination and hippocampal damage with neuronal loss and epileptic seizures were described. These data provide substantial information about the remyelination process within the cuprizone model and serve as a basis for the further elucidation of the molecular mechanisms of remyelination.

6 Zusammenfassung

Die Gründe für eine unvollständige Remyelinisierung bei der Multiplen Sklerose (MS) sind noch weitgehend ungeklärt. Die vorliegende Studie untersuchte die Remyelinisierung in einem toxischen Demyelinisierungsmodell, dem Cuprizon-Modell. Durch Fütterung des Kupferchelators Cuprizon wird eine gut reproduzierbare Demyelinisierung des Balkens (corpus callosum) herbeigeführt, wobei es nach Absetzen des Toxins zu einer spontanen Remyelinisierung kommt. Um den Prozess der Remyelinisierung zu beschreiben bzw. Faktoren zu untersuchen die diesen beeinflussen können, etablierten wir zuerst eine geeignete Quantifizierungsmethode. Die semi-quantitative Auswertung eines früh exprimierten Myelinproteins (MBP; PLP) in Kombination mit einem spät exprimierten Myelinprotein (MOG) stellte sich als zuverlässige Quantifizierungsmethode heraus.

Im Folgenden untersuchten wir die Rolle des Chemokin Rezeptors CXCR2 während der physiologischen Myelinisierung sowie der De- and Remyelinisierung. Wir konnten zeigen, dass CXCR2 konstitutiv auf Oligodendrozyten exprimiert wird. Darüber hinaus, regulierten Mikroglia/Monozyten die CXCR2 Expression während der Demyelinisierung herauf. Die Regulation der CXCR2 Expression erfolgte unterschiedlich auf den verschiedenen Zelltypen. Untersuchungen in CXCR2 defizienten Mäusen zeigten weder Unterschiede in der Myelinisierung noch einen anderen veränderten Verlauf der De- und Remyelinisierungsphase nach Cuprizongabe. CXCR2 spielt keine entscheidende Rolle bei der Remyelinisierung und dessen Funktion wird kompensiert *in vivo.*

Weitere Versuche sollten den Einfluss einer verlängerten Demyelinisierungsphase klären. Obwohl nach 16-wöchiger Cuprizongabe eine Depletion der Oligodendrozytenvorläuferzellen zu beobachten war, kam es dennoch zu einer weitreichenden Remyelinisierung, die aber langsamer erfolgte als nach kurzer Cuprizongabe (6 Wochen). Die untersuchte axonale Schädigung war nur gering ausgeprägt und steigerte sich nicht unter verlängerter Toxingabe.

Die Anzahl der geschädigten Axone korrelierte gut mit der beobachteten Mikroglia/Monozyten Akkumulation, was die Vermutung zulässt, dass Mikroglia/Monozyten an den Pathomechanismen des axonalen Schadens beteiligt sind.

Die Beteiligung von kortikalen Läsionen am Verlauf der MS rückt zunehmend in den Fokus der MS Forschung. In der vorliegenden Arbeit beschreiben wir zum ersten Mal kortikale Läsionen in Cuprizon-Modell. Der Grad der Demyelinisierung wird vom verwendeten Mausstamm beeinflusst. C57BL/6 Mäuse zeigten nach 6 Wochen Cuprizongabe eine vollständige Demyelinisierung des Kortex, im Gegensatz zu balb/c Mäusen die nur unvollständig demyelinisierten. Darüber hinaus scheinen die Mechanismen die zur Apoptose der Oligodendrozyten führen im Kortex und im Balken unterschiedlich zu sein, da es im Balken während der Demyelinisierung zu einer massiven Mikroglia/Monozyten Akkumulation kam, während diese im Kortex komplett fehlte.

Während verlängerter Cuprizongabe zeigten die Mäuse Stress-induzierte Anfälle, die in der vorliegenden Arbeit näher untersucht wurden. Außerdem konnte eine massive Demyelinisierung des Hippokampus mit einhergehender neuronalen Schädigung gezeigt werden. Unsere Daten lassen vermuten, dass die im Cuprizon-Modell auftretenden Anfälle durch die neuronale Degeneration am Hippokampus ausgelöst werden.

Zusammengefasst, wurde in der vorliegenden Arbeit das Cuprizon-Modell näher charakterisiert und verschiedene neue Aspekte, eingeschlossen kortikale Demyelinisierung sowie Neuronenverlust im Hippokampus, beschrieben. Darüber hinaus unterstreicht die vorliegende Studie, dass sich das Cuprizon-Modell zur Untersuchung der pathologischen und funktionellen Konsequenzen der Demyelinisierung gut eignet. Die vorliegenden Daten geben neuen Aufschluss über den Remyelinisierungsprozess im Cuprizon-Modell und dienen als Basis für eine weiterführende Aufklärung der molekularen Mechanismen der Remyelinisierung.

Curriculum Vitae

Name: Maren Lindner

Date and Place of Birth: 27th October 1977, Berlin, Germany

Nationality: German

Education:

October 2004:	PhD program of Center for Systems Neuroscience Hannover, Project title: The role of oligodendrocyte chemokine receptors during myelination and remyelination
April 2004:	Department of Neurology at group of Martin Stangel, Medical School Hannover, SFB 566/A11: Cytokines and cytokines related pathways
January 2004:	diploma in biotechnology (overall average grade: 1.6) MSc biotechnology Dongseo University Pusan, South Korea
2003:	master thesis “Investigation of the natriuretic peptides and their receptors in transgenic rats” at Max Delbrueck Center for Molecular Medicine in Berlin at the group of Michael Bader
2000/ 2001:	stay abroad in South Korea participant of the Dual-Degree Program between TU-Berlin and Dongseo University (DSU) in Pusan, scholarship from DSU in Pusan
October 1997:	student of biotechnology at Technical University in Berlin
June 1997:	general qualification for university entrance (Abitur) at „Carl von Ossietzky-Gymnasium” in Berlin (2.1)

Publications

Publications:

Langenickel TH, Pagel I, Buttgereit J, Tenner K, **Lindner M**, Dietz R, Willenbrock R, Bader M. Rat corin gene: Molecular cloning and reduced expression in experimental heart failure. Am J Physiol Heart Circ Physiol. 2004 Oct; 287(4):H1516-21.

Langenickel TH, Buttgereit J, Pagel-Langenickel I, **Lindner M**, Monti J, Beuerlein K, Al-Saadi N, Plehm R, Popova E, Tank J, Dietz R, Willenbrock R, Bader M. Cardiac hypertrophy in transgenic rats expressing a dominant-negative mutant of the natriuretic peptide receptor B. Proc Natl Acad Sci U S A. 2006 Mar 21;103(12):4735-40.

Trebst C, Brunhorn K, **Lindner M**, Windhagen A, Stangel M. Expression of chemokine receptors on peripheral blood mononuclear cells of patients with immune-mediated neuropathies treated with intravenous immunoglobulin.
Eur J Neurol. 2006 Dec;13(12):1359-63.

Lindner M, Heine S, Haastert K, Garde N, Fokuhl J, Linsmeier F, Grothe C, Baumgaertner W, Stangel M. Sequential myelin protein expression during remyelination reveals fast and efficient repair after central nervous system demyelination.
Neuropathol Appl Neurobiol *in press*

Hoffman K, **Lindner M**, Groeticke I, Stangel M, Loescher W. Epileptic seizures and hippocampal damage after cuprizone-induced demyelination in mice.
Exp Neurol *submitted*

Heine S, Trebst C, Lienenklaus S, **Lindner M**, Baumgaertner W, Weiss S, Stangel M. Lack of Interferon-beta leads to accelerated remyelination in a toxic model of central nervous system demyelination.
Acta Neuropathol *under revision*

Lindner M, Trebst C, Heine S, Koutsoudaki PN, Stangel M. The chemokine receptor CXCR2 is expressed on oligodendrocyte precursor cells in vivo but is not required for successful remyelination after cuprizone-induced demyelination
In preparation

Publications

Lindner M, Fokuhl J, Linsmeier F, Trebst C, Stangel M. Extensive remyelination after chronic toxic demyelination of the central nervous system
In preparation

Lindner M*, Skripuletz T*, Kotsiari A, Garde N, Fokuhl J, Linsmeier F, Trebst C, Stangel M. Cortical demyelination can be induced in mice using the cuprizone model and is strain dependent
In preparation
*equal contributions as first authors

Poster presentations:

Myelin protein expression during remyelination: new insights into repair mechanisms
Lindner M.[1] , Heine S.[1], Garde N.[1], Baumgärtner W.[2], Stangel M.[1]
[1]Dept. of Neurology, Medical School Hannover, Hannover, Germany; [2]Dept. of Pathology, Veterinary School Hannover, Hannover, Germany
FENS Forum, Vienna, 2006

Role of the chemokine receptor CXCR2 during remyelination
Maren Lindner[1,2], Sandra Heine[1], Martin Stangel[1,2]
[1]Dept. of Neurology, Medical School Hannover, Hannover, Germany and [2]Center for Systems Neuroscience, Hannover, Germany
7th Meeting of the German Neuroscience Society, Göttingen, 2007

Chronic demyelination is not sufficient to induce acute axonal damage
Maren Lindner[1,2], Franziska Linsmeier[1], Sandra Heine[1], Jantje Fokuhl[1], Martin Stangel[1,2]
[1]Dept. of Neurology, Medical School Hannover, Hannover, Germany and [2]Center for Systems Neuroscience, Hannover, Germany
VIII European Meeting on Glial Cells in Health and Disease, London, 2007

Acknowledgements

First I want to thank my supervisor Prof. Martin Stangel for his continued support and scientific advice.

Special thanks to my co-supervisors Prof. Rita Gerardy-Schahn and Prof. Wolfgang Baumgärtner for support and scientific comments.

Thanks to Ilona Cierpka-Leja for excellent technical assistance, Sandra Heine for aid with the animal experiments and Kerstin Rohn for invaluable help with electron microcopy.

Thanks to the medical students: Franziska Linsmeier for investigating the axonal damage and Jantje Fokuhl for analysis of the microglia/monocytes. Thanks to Niklas Garde for performing some myelin stainings.

Special thank to all other members of the Stangel group for fruitful scientific discussions and pleasurable working conditions, especially Alexandra Kotsiari, Darius Moharregh-Khiabani, Paraskevi Koutsoudaki and Corinna Trebst. Thanks to Thomas Skripuletz for the analysis of the cortical lesions and writing the manuscript.

Thanks to all the people who were helpful in the background especially Karin Fricke, Susann Bausneik and Andreas Niesel.

Thanks to all PhD students of the year 2004 from the Center for Systems Neuroscience for just having a good time.

Special thanks to my family, especially Erik, for encouragement and motivation.